ADAPTATION TO ENVIRONMENTAL STRESSES IN *CANDIDA GLABRATA*

A Dissertation

by

MIAN HUANG

Submitted to the Office of Graduate and Professional Studies of
Texas A&M University
in partial fulfillment of the requirements for the degree of

DOCTOR OF PHILOSOPHY

Chair of Committee,	Katy Kao
Committee Members,	Arul Jayaraman
	Hung-Jen Wu
	Xiaorong Lin
Head of Department,	M. Nazmul Karim

May 2017

Major Subject: Chemical Engineering

ABSTRACT

Candida glabrata (*C. glabrata*) is an emerging opportunistic human fungal pathogen with an increasing incidence as the cause of both mucosal and systemic infections. In addition, the fungus is the most commonly used microorganism for pyruvate production and is considered to be a potential producer of other fine chemicals and biofuels. Thus, this yeast has potential importance in both the medical and biotechnology fields. The inherent high tolerance of *C. glabrata* and its' ability to readily adapt to various environmental stressors play key roles in its success as an opportunistic pathogen and potential as an industrial producer. However, the current knowledge on the underlying molecular mechanisms of *C. glabtata* adaptation to environmental stressors is limited. A deeper understanding of how *C. glabrata* adapts to environmental challenges can potentially expand our ability to combat infections involving this organism and to our toolkit for engineering better production hosts. In this dissertation, we focused on *C. glabrata* adaptation to two environmental stressors, hyperthermal and hydrogen peroxide. Using the strategy of adaptive laboratory evolution combined with next generation sequencing and transcriptome analyses, we begin to uncover the important genetic determinants conferring tolerance to these stressors. We showed for the first time that several genes (*e.g.* CAGL0B02739g and CAGL0E01243g) play important roles in cellular tolerance to selected environmental stresses (heat and H_2O_2) in *C. glabrata*; proposed potential mechanisms based on the transcriptome analyses and functions of their orthologs in the model yeast *S. cerevisiae*;

and found that the adaptation to thermal stress in this fungus led to the acquisition of cross-tolerance to a wide range of other environmental stresses, including hydrogen peroxide, acids, and several organic solvents. Mutations in an important component of the fungal MAPK signaling cascades were shown to be responsible for the observed cross-tolerance, suggesting their critical roles in the cross-talk between different signaling pathways for cells to survive hostile environmental conditions.

DEDICATION

To my wife and my parents

ACKNOWLEDGEMENTS

I would like to thank my committee chair, Dr. Kao, for her guidance and support throughout the course of this research and also to each member of my committee for their kind guidance and helpful advice on my research.

In addition, my friends and colleagues make me have a great time at Texas A&M University and I appreciate what they did for me. I also want to extend my gratitude to the National Science Foundation, the Texas Engineering Experimental Station and the National Institutes of Health, which provided the financial support.

Finally, thanks to my wife, Mengyun Feng, my mother, Dan Lu, and father, Yejin Huang, for their encouragement and emotional support.

CONTRIBUTORS AND FUNDING SOURCES

Contributors

This work was supervised by a dissertation committee consisting of Professor Katy Kao (advisor), Arul Jayaraman, and Hung-Jen Wu of the Department of chemical engineering, and Professor Xiaorong Lin of the Department of Biology

The adaptive evolution experiments and phenotypic characterizations for section 4 were conducted in part by Orlando Andres Aguilar Patiño and Julian Daniel Torres Vanegas of the Department of chemical engineering of Universidad Industrial de Santander. All the other work for the dissertation was completed by the student under the advisement of Katy Kao of the Department of chemical engineering.

Funding Sources

This work was made possible in part by National Science Foundation under Grant Number MCB-1054276 and Texas Engineering Experiment Station. Its contents are solely the responsibility of the authors and do not necessarily represent the official views of the National Science Foundation and Texas Engineering Experiment Station.

TABLE OF CONTENTS

Page

Page

LIST OF FIGURES

Page

Page

LIST OF TABLES

Page

1. INTRODUCTION

Candida glabrata (*C. glabrata*) is an emerging opportunistic human fungal pathogen; its incidence in Candidiasis, the fourth most common hospital-acquired infections (1), is on the rise according to many epidemiological studies. Among all *Candida spp*. that cause Candidiasis, *C. glabrata* is the second most frequently isolated species, based on a recent global surveillance program (2). Infections caused by *C. glabrata* ranges from the mild superficial infections to life-threatening systemic infections, and the overall mortality rate associated with the systemic infections caused by *C. glabrata* is higher than most of other *Candida spp*., ranging from 40% to 70% (3). In addition, the fungus not only has an intrinsic low susceptibility to many prescribed antifungal agents, such as polyenes and azoles, but it is also able to readily acquire drug resistance in both clinical and laboratory settings (1, 4-7). Thus, *C. glabrata* has become a medically important opportunistic pathogen capable of causing serious public health issues. Inside the host, *C. glabrata* may face various stressors imposed by the host defense, such as being engulfed by phagocytes, which is the first line of host defense against the invasive pathogens, and elevated body temperature due to the febrile response (8). Once engulfed by phagocytes, such as macrophage and neutrophils, *C. glabrata* is trapped within their phagosomes, where multiple antimicrobial mechanisms are recruited to kill or inhibit the growth of the invasive fungus; these host immune defenses include induction of oxidative stress by reactive oxygen species (ROS) and reactive nitrogen species (NOS) and accumulation of many antimicrobial peptides (9,

10). The knowledge of mechanisms underlying the adaptation of the fungus to stresses imposed by host defense is still limited, which hinders the understanding of the pathogenesis of the fungal pathogen and development of novel drugs to expand the current arsenal of limited antifungal agents.

In addition to its medical relevance, *C. glabrata* also has industrial application for pyruvate production commercialized by the Toray Industry as early as in 1992 (11, 12). Recently, *C. glabrata* has attracted many researchers to further enhance its ability to produce pyruvate (13-17) and characterize its potential in production of other chemicals, including α-ketoglutarate, malate, and ethanol (18-22). These studies also suggest that the enhanced tolerance of *C. glabrata* to various environmental stresses might benefit the production of desired chemicals. For example, increasing the osmotic stress resistance has been shown an effective strategy to enhance the pyruvate production (17). Furthermore, strains that are tolerant to weak organic acids (*e.g.* lactic acid) can be used in bioethanol production to reduce the risk of microbial contamination (21), and thermotolerant strains are useful in simultaneous saccharification and fermentation (SSF) processes (22), which requires biocatalysts capable of growing well at higher temperatures. Knowledge of tolerance mechanisms in *C. glabrata* will not only aid in the rational engineering of this strain, but can potentially benefit the rational engineering of the closely related and generally considered as safe (GRAS) yeast *Saccharomyces cerevisiae*.

Despite its importance as a medical and industrial yeast, *C. glabrata* is grossly understudied compared with *S. cerevisiae* and *C. albicans*; and it has only a few verified

ORFs (4.33% of the predicted ORFs in the genome) with even fewer characterized in detail (23). In this dissertation, we will partially map out the adaptive landscapes and evolutionary trajectories of *C. glabrata* during its adaptation to environmental stressors, specifically oxidative and hyperthermal. To achieve this goal, we developed *in vitro* experimental systems to evolve the *C. glabrata* in the presence of the selected stressor. Prior work has shown that microbes (*e.g. Escherichia coli*, *Salmonella typhimurium*, and *Corynebacterium glutamicum* (*C. glutamicum*)) laboratory evolved for tolerance to one stressor also developed cross-tolerance to multiple stresses (18-20). For example, researchers found that the evolved *C. glutamicum* under the thermal stress has acquired cross-tolerance for isobutanol (20). Therefore, we hypothesize that mutants from the stress-challenged populations will exhibit cross tolerance to other environmental stressors. We further hypothesize that there exist multiple evolutionary trajectories during *C. glabrata* adaptive evolution; thus, we will evaluate time-course population samples to assess the evolutionary dynamics of mutations. The resulting knowledge gained from this study will advance our understanding of the adaptation of *C. glabrata* to environmental stressors of medical and industrial relevance.

2. BACKGROUND AND LITERATURE REVIEW*

2.1. Candidiasis

Most of yeast species from the *Candida* genus are environmental microbes that are widely distributed in nature and many of them could also colonize different niches of the human body as commensal constituents of the normal human microflora. However, under certain alterations in the host environments, some of the *Candida spp*. may become pathogenic agents. These fungal species are opportunistic pathogens; while they rarely trigger infections in healthy people, they can cause serious infections when the host immune system is locally or systemically impaired. The infections caused by Candida species are collectively called Candidiasis, which is further divided into three categories: cutaneous (skin and its appendages), mucosal (oropharyngeal, esophageal, and vulvovaginal), and systemic infections (bloodstream infections, and other deep organ infections). Depending on the underlying illness, the prevalence of different category of Candidiasis in patients may vary. For example, systemic infections are more common in cancer patient receiving chemotherapy or transplant patients following immunosuppression therapy, while superficial infections, including cutaneous and mucosal infections, are more frequently seen in patients infected by the human immunodeficiency virus (HIV). Currently, the Candidiasis is ranked 4th in nosocomial

*Part of this section is reprinted with permission of Springer Nature from Springer Nature Metabolic Engineering for Bioprocess Commercialization, "Tolerance of Microbial Biocatalysts to Feedstocks, Products, and Environmental Conditions", 2016, page73-100, by Mian Huang, George Peabody, and Katy C. Kao, copyright 2016 by Springer International Publishing Switzerland.

infections, with frequency of about 8% to 10%. The mortality due to systemic infections of Candidiasis ranges from 15% to 35%, depending on the causative Candida species (1).

Among the species causing Candidiasis, *Candida albicans* (*C. albicans*) is still the most prevalent causative agent. However, the non-albicans Candida (NAC) species play an increasingly important role in Candidiasis, as suggested by several global surveillance programs, such as SENTRY and ARTEMIS (2). These programs generated massive amounts of data on various aspects of the nosocomial infections caused by Candida species over a large temporal and spatial scales to shed light on the temporal and geographic trends in the species distribution as well as the changes in the antifungal susceptibility of the clinical isolates (2). Combined with other studies on the species frequency of clinical isolates, the data obtained from the global programs revealed that the proportion of the NAC species among the clinical isolates of *Candida* species has been increasing over the past four decades, possibly due to the growing size of the vulnerable population (patients with neutropenia, immunosuppression, metabolic dysfunction, and under the anticancer chemotherapy) and the wide use of azoles in the prophylaxis and antifungal treatments. In the period 1970-1990, NAC species accounted for 10%-40% of all systemic Candidiasis, and the proportion has reached 35%-65% by the end of the 1990s (3).

Among the NAC species, *C. glabrata* is one of the most common causative agents of the Candidiasis, and a recent analysis of ARTEMIS program, spanning the time period 1997-2007, showed that the rates of isolation of the *C. glabrata* continued to

increase from 10.2% to 11.7% and ranked the top among all NAC species (2). The analysis of the geographic distribution of the *C. glabrata* revealed that it is more commonly encountered in the isolates from North America (21.1%) than those from the Latin America (7.4%) (2). The overall mortality associated with *C. glabrata* (40%-70%) is not only higher than most of other NAC species, but also higher than the most prevalent *C. albicans* (20%-40%) (3). Although the overall mortality of *C. glabrata* is impressively high, its attributable mortality is lower compared to the *C. albicans* and some other NAC species, which could be explained by the common observations of the occurrence of its invasive infections in the critically ill patients, such as those in the terminal stages of malignant disease, or receiving intensive care. Another factor making the *C. glabrata* a serious concern for public health is its intrinsically low susceptibility to several common antifungal agents, including polyenes (*e.g.* amphotericin B) and azoles (*e.g.* fluconazole) (1). In a study of *in vitro* susceptibility of yeast isolates to amphotericin B, 0.8% of the 266 *C. albicans* isolates exhibited a MIC over 1 μg/ml, whereas 25.5% of 102 *C. glabrata* isolates exhibited the same level of the drug resistance (4). As to the susceptibility to azoles, the ARTEMIS DISK surveillance program showed that the percentage of *C. glabrata* isolates resistant to fluconazole ranges from 14.3% to 22.8% over a 6.5-year period to 2003 compared with a range from 0.8% to 1.5% for resistant *C. albicans* isolates (24). In addition, three recent multicenter surveys observed that MICs of three azole drugs, itraconazole, posaconazole, and voriconazole, inhibiting 50% or 90% of *C. glabrata* isolates were much higher than those for *C. albicans* isolates as well as many other NAC species (25-28). In addition to

the intrinsic low susceptibility to antifungal agents, *C. glabrata* is able to acquire resistance under the selection of drug pressure, which was documented both in clinical isolates and laboratory evolved strains (5-7). However, although *C. glabrata* is an opportunistic pathogen, it rarely causes infections in healthy people and invasive infections caused by this organism generally only occurs in critically ill patients.

2.2. The potential of *C. glabrata* as a producer in biotechnology industry

In addition to its medical relevance, the fungus exhibits many desired physiological characteristics of industrial significance, including excellent tolerance to low pH environment (<2.5), relatively simple requirement for the nutrient supply, tolerance to high temperatures and osmotic stress (29). Its potential as an industrial producer has been extensively characterized for many decades. In 1992, *C. glabrata* was industrialized for production of pyruvate by Toray Industries at a scale of 400 tons per year (11, 12). Recent efforts in the further enhancement of pyruvate production focused on the following aspects: optimization of the fermentation conditions (*e.g.* vitamin concentration and dissolved oxygen concentration) (13, 14), regulation of intracellular cofactors (*e.g.* ATP, $NADH/NAD^+$, $NADPH/NADP^+$) (15, 16) and improvement of environmental stress tolerance (*e.g.* enhancement of tolerance to osmotic stress) (17). Up until now, the best pyruvate-producing strain to our knowledge was generated by traditional mutagenesis combined with selection under the high level of osmotic stress, which produced 94.3 g/L pyruvate with a yield of 0.635 g per gram of glucose and a productivity of 1.15 g L-1 h-1 in a 7 L fermentor from 150 g L-1 glucose (17).

Inspired by its success in pyruvate production, the potential of *C. glabrata* in producing other weak organic acids that were derived from the pyruvate through the TCA cycle was extensively investigated, including the α-ketoglutarate and malic acid. In the pioneering works that used *C. glabrata* to produce the α-ketoglutarate, Liu and coworkers successfully redistributed the carbon flux from the pyruvate to the α-ketoglutarate by manipulation of extracellular cofactor (thiamine, biotin, and calcium) levels, overexpression of pyruvate decarboxylase (PDC), and inhibition of α-ketoglutarate dehydrogenase complex (KGDH) by hydrogen peroxide (18, 19). The highest α-ketoglutarate concentration they achieved was about 43.7 g/L in a 7-L fermentor after 64-hr fermentation. The same research group also examined the potential of *C. glabrata* in the malate production. They found that the carbon flux can be redistributed from the pyruvate to malate by overexpression of pyruvate carboxylase and malate dehydrogenase, which are encoded by *RoPYC* and *RoMDH* respectively, and with the help of the genome-scale metabolic model iNX804, they were able to figure out a bottleneck of the malate production and enhanced the final titer of the malate to 8.5 g L-1 by overexpression of a introduced dicarboxylate permease encoded by *SpMAE1* gene (20).

Fermentation-based biofuel production is one of the major focuses for biotech industries. Given the similar capacity in ethanol production as the *S. cerevisiae* (30) and many other desired characteristics, the use of *C. glabrata* in ethanol production has been extensively investigated. Many mutants with desired properties were obtained by screening, spontaneous mutations, and traditional mutagenesis to make the ethanol

production more cost-effective. In one study, the lactate-tolerant *C. glabrata* strain was obtained by screening and applied to ethanol production in the presence of 1-2% lactate under the anaerobic fermentation condition to solve the issues of bacterial contamination commonly encountered in the industrial production, which exhibited a significantly higher yield and production rate than a *S. cerevisiae* ethanol producer (21). In addition, a respiratory-deficient mutant was obtained by exposure to a mutagen, ethidium bromide, in another study and its ability to produce ethanol was evaluated in the process of the SSF (22). Compared to the *S. cerevisiae*, the respiratory-deficient mutant is not susceptible to the Pasteur effect at high temperature and able to produce the ethanol without reassimilation, achieving an ethanol concentration of 17.0 g L^{-1} within 48 hours at 66.6% of its theoretical yield at 0.35 g L^{-1} h productivity.

2.3. Environmental stress response and tolerance mechanisms in *C. glabrata*

As an important opportunistic pathogen and successful industrial producer, the inherent high tolerance of *C. glabrata* to various environmental stressors, such as high temperature, osmotic and oxidative stress, plays a key role. The underlying mechanisms at the molecular level attracted attention from both the academic and industrial community. Though still limited, recent studies shed some light on the cellular response to various environmental stressors, mostly for those of medical relevance, and the involved biomacromolecules and signaling pathways. Based on these studies, the stress response pathways of *C. glabrata* are found similar to the model yeast *S. cerevisiae* and the difference in the stress-related phenotypes between the two is likely due to adaptation of the transcriptional wiring in *C. glabrata*.

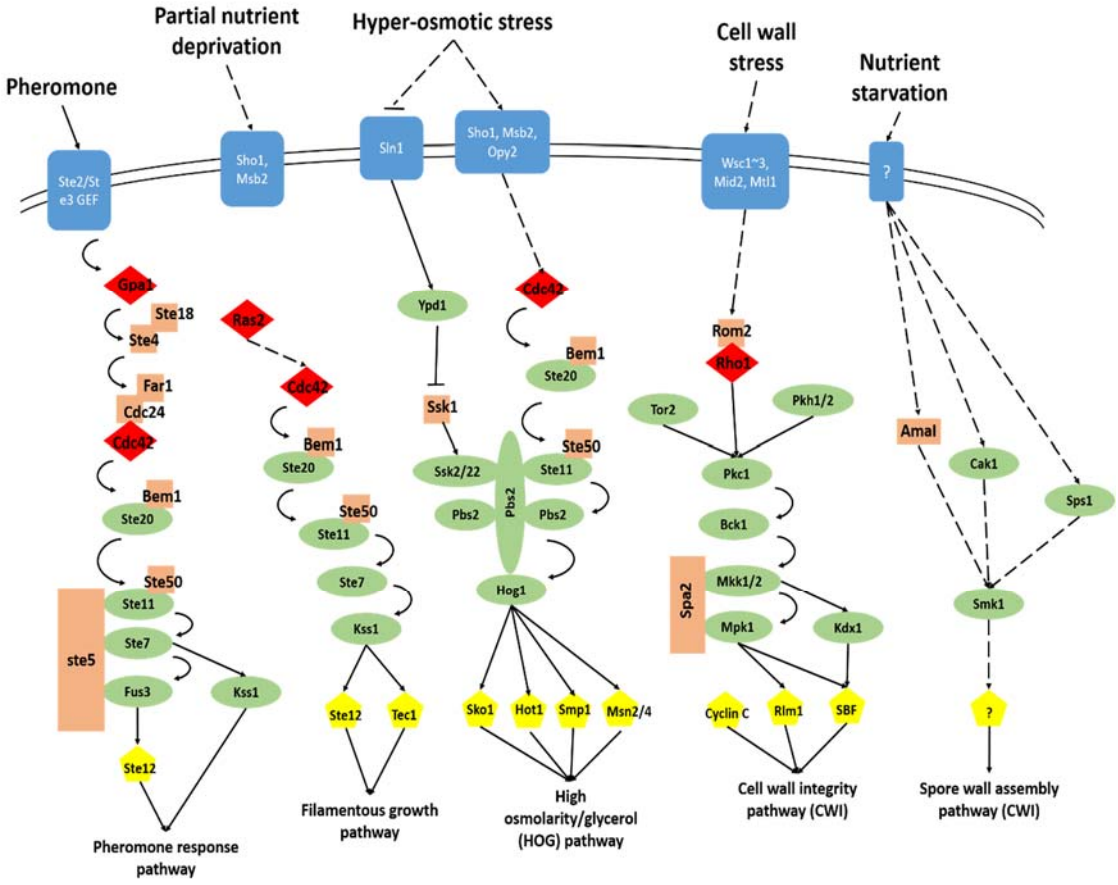

Figure 1. Schematic diagrams of the MAPK signaling pathways in *S. cerevisiae*. The figure is modified from **(**Raymond E. Chen and Jeremy Thorner, 2007) and (Chunyan Jin et al., 2015)(31, 32)**.** Symbols are: protein kinases, ovals (green); GTP-binding proteins, diamonds(red); scaffold, adaptor, and activating proteins, rectangles (orange); cell surface proteins, round rectangles(blue); activation, arrows; inhibition, T-bars; direct action, smooth lines; indirect action (or unknown molecular mechanism), dashed lines; transcription factors, pentagons (yellow); For clarity, the cross-talk between the different signaling pathways are omitted.

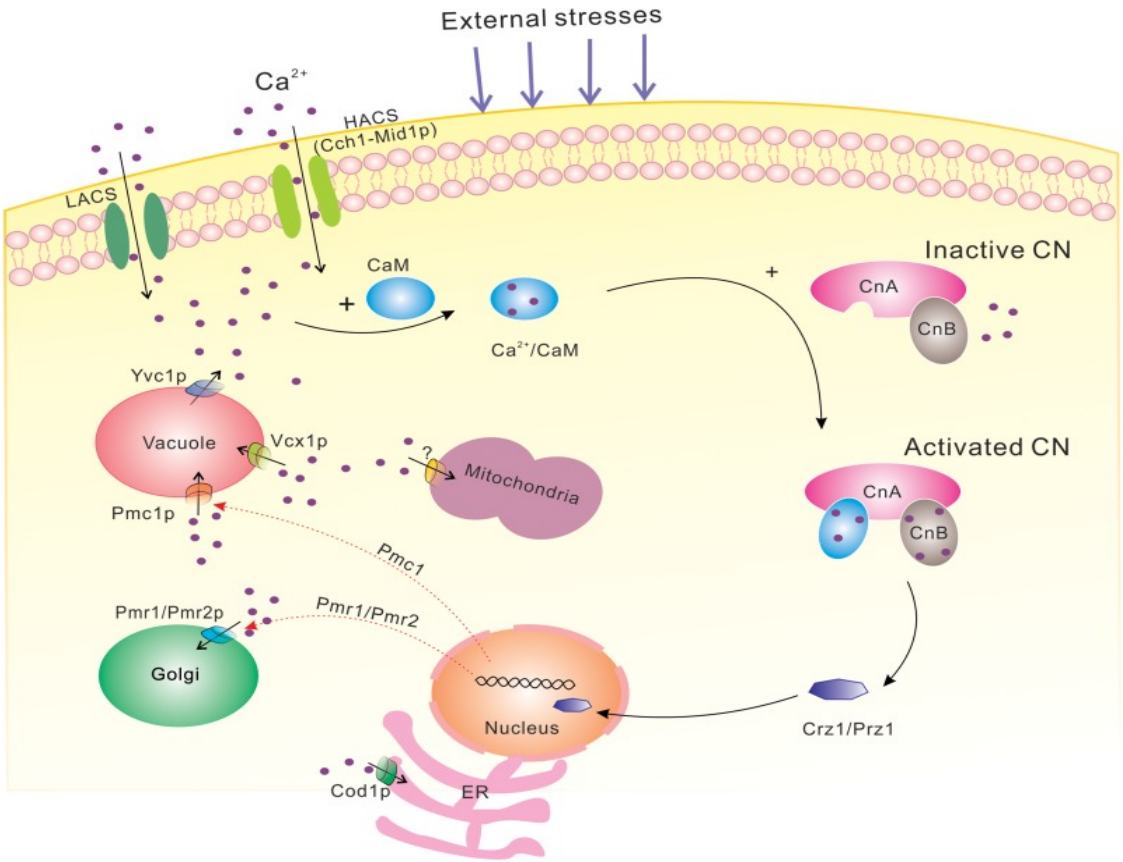

Figure 2. Calcium-calcineurin signaling pathway in yeast. The figure is taken from (Shuyuan Liu et al., 2007)(33). CaM, calmodulin; CN, calcineurin; ER, endoplasmic reticulum; LACS, low-affinity Ca^{2+} influx system; HACS, high-affinity Ca^{2+} influx system.

Several signaling pathways, including high osmolarity glycerol (HOG) pathway, pheromone response pathway, and calcineurin pathway, were shown to play critical roles in the tolerance of *C. glabrata* to various environmental stressors (**figure 1 and figure 2**). The HOG pathway, a mitogen activated protein kinase (MAPK) pathway, and its signaling patterns are well-conserved between *S. cerevisiae* and *C. glabrata* (34). The HOG pathway mediates mainly the cellular response to the osmotic stress and the central MAP kinase Hog1 is activated by the upstream MAPK kinase (MAPKK) Pbs2 through

two distinctive signal inputs (31). One of the inputs is dependent on the osmosensor Sho1 which activates the MAPKK Pbs2 in response to severe hyperosmotic stress and the other one is through a histidine-asparate phosphorelay module system Sln1-Ypd1-Ssk1 (31, 35). The phosphorelay system is active under iso-osmotic conditions, which represses Pbs2, while it gets inhibited by mild hyperosmotic stress, which leads to the activation of Ssk2 and Ssk22, two MAPKKKs, and thus the activation of the Pbs2. Once activated by Pbs2, a rapid translocation of the Hog1 from the cytoplasm to nucleus occurs, which results in the activation of its downstream targets followed by the expression of hundreds of genes in response to the osmotic stress. In contrast to *S. cerevisiae*, the HOG pathway plays a critical role in the cell response to weak organic acids, such as sorbic acid, in *C. glabrata* (36). In addition, the regulation of the pathway between the two species is different, and depending on the genetic background, *C. glabrata* might have a higher basal level of Hog1 activity even under the non-osmotic stress condition (37). Pheromone response pathway is another MAPK pathway involved in the response of *S. cerevisiae* to general environmental stress. Interestingly, although the *C. glabrata* is regarded as an asexual fungus and doesn't respond to the mating pheromones (38), it has a putative mating type locus, a pheromone gene, as well as orthologs of at least 31 genes involved in the mating and meiosis of *S. cerevisiae*, including some key components of the pheromone response pathway (39, 40). The ortholog of the *ScSTE20*, encoding a kinase in the pheromone response pathway of *S. cerevisiae*, in *C. glabrata*, *CgSTE20*, was shown to function for the hyperosmotic stress and cell wall integrity (41). Recently, the roles of the calcineurin signaling pathway in

thermotolerance and pH homeostasis of *C. glabrata* were characterized (42). The researchers found that the calcineurin signaling pathway is required for the growth of at least three different *C. glabrata* strains, including the genome-sequenced reference strain CBS138, at high temperature (*e.g.* 40°C) and the pathway seems to function for the maintenance of an intact plasma membrane structure at the high temperature. In addition, they found that the calcineurin signaling is essential for the growth of *C. glabrata* at pH 2.0 and pH 8.0, possibly through the regulation of a GPI-anchored aspartyl protease Yps1. Calcineurin is a calcium/calmodulin-dependent serine/threonine specific protein phosphatase that comprises a catalytic A (Cna1) and a regulatory B calcium-binding subunit (Cnb1). In the calcineurin signaling cascade of *C. glabrata*, the central regulator Crz1 is activated by dephosphorylation through the heterodimer calcineurin AB and the activity of the calcineurin AB was stimulated by calcium and regulated by a positive regulator Rcn1 and a feedback inhibitor Rcn2. Once activated, the Crz1 migrated from the cytoplasm into the nucleus to regulate the expression of many genes involved in a variety of cell processes.

In addition, there are many stress-induced transcription factors that regulate expression of genes involved in the protection against various environmental stressors in *C. glabrata*. The orthologs of *ScMSN2* and *ScMSN4* in *C. glabrata*, *CgMSN2* and *CgMSN4*, are involved in general environmental stress regulation and affect the expression of genes in response to osmotic and oxidative stress. In contrast, CgYap1 and CgSkn7 are dedicated to regulate the expression of genes in response to oxidative stress (43, 44). In *S. cerevisiae*, the Yap 1 is a central component of the oxidative stress

response. Depending on the oxidative stress source, Yap1 is regulated by different mechanisms. Upon the stimulation by H_2O_2, Yap1 is oxidized by Gpx3 and Ybp1 to form dual disulfide bridge, which results in the accumulation of the Yap1 in the nucleus and activates its downstream targets. When stimulated by diamide, Yap1 is oxidized in a different cysteine residue, which inhibits its interaction with a nuclear exportin Crm1 and results in its accumulation in the nucleus as well (45). In *C. glabrata*, the ortholog of Ybp1 in *S. cerevisiae* was identified and its role in the regulation of the Yap1 seems to be conserved between the *S. cerevisiae* and *C. glabrata*. In addition, the core oxidative stress response genes in *C. glabrata* have been well-characterized, including thioredoxin peroxidases (CgTsa1 and CgTsa2), thioredoxin reductases (CgTrr1 and CgTrr2), thioredoxin cofactor CgTrx2, glutathione peroxidase CgGpx2, and catalase CgCta1.

2.4. Strain development for enhanced tolerance to environmental stressors

A variety of engineering tools have been used to improve the tolerance of microorganisms to various environmental stresses of industrial relevance for better production performance, including single gene manipulation, transcription factor-based engineering, whole genome shuffling (WGS), small RNA-based posttranscriptional regulation, and evolutionary engineering.

Manipulation of single genes either via overexpression or deletion is a useful technique in rational engineering for desired phenotypes. Cellular tolerance to stressors involves activation of many signaling and regulatory pathways, which makes strain tolerance engineering through direct manipulation at the molecular level very difficult. Though challenging, several prior efforts have successfully improved tolerance to

fermentation conditions via single gene manipulation. Overexpression of *RSP5*, encoding an E3 ubiquitin ligase, was found to confer superior thermotolerance to *S. cerevisiae*, possibly by facilitating the removal of stress-damaged proteins by increasing the level of ubiquitination (46). In addition, overexpression of *TPS1*, encoding a trehalose6phosphate (T6P) synthase in yeast, results in enhanced ethanol production, from 37 to 60 g/L, and thermotolerance (improved critical growth temperature from 36 to 42 °C) (47). These examples suggest that some key components of the stress responses may be good targets to manipulate the stress tolerance.

Often times the cell is encountering multiple stressors at once. Thus, rational strain improvement will require knowledge of the major stressor(s) involved. The question of how to diagnose which stressor is the cause of poor fermentation performance is a challenging one to address, due to the presence of multiple stressors and potential synergistic effects of combinations of stressors. Transcriptomic and/or proteomic analysis may be a quick way to identify the major stressor(s) based on the cellular response in fermentation conditions using existing biological knowledge. Alternatively, if the identities and concentrations of the potential stressors are known, then controlled experiments involving each individual and combinations of stressors can be performed to identify the most relevant stressors (or combination of stressors) for which enhanced tolerance is needed to improve performance. However, if the above strategies are not possible, then more global approaches, such as the ones described below, may be applied.

Transcription factor-based engineering has become an important class of tools for strain development; the manipulation of transcriptional regulators allows perturbing the expression of multiple genes simultaneously. Global transcription machinery engineering (gTME) was initially developed in bacteria and yeast and represents the first systemic tool of this class. Since the initial development, gTME has been successfully applied in *Lactobacillus plantarum* to select for mutants with enhanced lactic and inorganic acid tolerance by targeting the principal σ factor, encoded by *RpoD* (48). The same technique that targets two components of RNA polymerase II transcription factor D (TFIID), TATA-binding protein Spt15p and TATA-binding associated factor Taf25p, of *S. cerevisiae* has been used to select mutants with enhanced tolerance to high concentrations of ethanol (6 % v/v) and glucose (120 g/L) (49). CRP is a well-known global regulator that controls the expression of over 400 genes in *E. coli* (50), and was successfully targeted for the strain development of osmotolerant (51) and acid tolerant mutants (52).

WGS has also been used to enhance *S. cerevisiae* tolerance to multi-stresses, including harsh fermentation conditions; where the DNA of similar but diversified cell populations is shuffled to recombine desirable genes or mutations. Shi et al. successfully improved the thermotolerance, ethanol tolerance, and ethanol productivity of an industrial yeast strain SM3 using this technique (53). Their starting population was created by protoplast ultraviolet irradiation and then subjected to three rounds of recursive protoplast fusion; positive colonies were screened for growth in the presence of combinations of different temperatures and ethanol concentrations. The best

performing strain, F34, was capable of growth in up to 55 °C, producing 9.95 % (w/v) ethanol, and tolerating 25 % (v/v) ethanol stress.

Small RNAs (sRNAs) are a group of small noncoding RNA molecules, which could modify the function of proteins and regulate gene expression by binding to target molecules (54). The sRNAs-based technique in metabolic engineering is emerging and has been applied to improve biological systems for stress tolerance. A recent successful example of sRNAs-based approach is the overexpression of *DsrA*, *RprA*, and *ArcZ* (individually and in combinations) in *E. coli* to significantly enhance the tolerance to low pH stress (pH 2.5) (55). Simultaneous overexpression of all three sRNAs resulted in an 8500-fold increase in survival in acid conditions compared with the control strain. In addition to the enhanced tolerance to low pH, overexpression of the three sRNAs also conferred significant protection to carboxylic acid and oxidative stress (55). The proposed mechanism by which the overexpression of the three sRNAs may protect cells from the stresses is by altering the mRNA levels of two critical regulators involved in stress tolerance, *RpoS* and *HNS*, and their downstream gene targets. Unlike tools based on gene overexpression, sRNA-based tools generally impose less metabolic burden on cells, and thus may be more effective in strain engineering.

Evolutionary engineering, as described earlier, was recently applied to improve the osmotolerance (NaCl) in *E. coli* (56). Compared to the unevolved parental strains, isolates from the evolution experiments had significantly improved growth rate under the osmotic stress and could grow in up to 0.8 M (47 g/L) NaCl in minimum media, a concentration that completely inhibits the parental strain.

3. THE ADAPTATION OF *C. GLABRATA* TO HYDROGEN PEROXIDE INVOLVES TRANSCRIPTIONAL REGULATION BY SEVERAL KEY PLAYERS

3.1. Introduction

C. glabrata has both industrial and medical importance. It is an important industrial producer of pyruvic acid, which was commercialized by the Toray Industry in the 1990's (11). Compared to the model yeast *Saccharomyces cerevisiae* (*S. cerevisiae*), this fungus has shown significantly higher resistance to various environmental stressors, including oxidative, osmotic, and cell wall stresses (34). These traits make it an attractive biocatalyst in the industrial biotechnology and recent work has demonstrated the potential use of *C. glabrata* in the production of various chemicals of industrial significance, including α-ketoglutarate, malate, and ethanol (18-20, 57, 58).

During fermentation, oxidative stress resulting from the exposure to reactive oxygen species (ROS) is frequently encountered. The highly aerobic nature of fungal growth due to the vigorous aeration and agitation and frequent temperature change due to the inhomogeneity of the fermentation liquid contribute to burst of intracellular ROS of the fungal producers (59). The oxidative stress to which *C. glabrata* is exposed in the industrial settings has damaging effects on biomolecules and potentially cause cell death (60). In addition, the oxidative stress has been shown to impact the production performance of industrial microorganisms by itself or with various other stressors (*e.g.* high temperature and limited nutrients), resulting in decreased growth rate, extended lag phase, and reduced productivity (61, 62). Thus, the cellular response to this stress and

the underlying mechanisms are critical to further improve the robustness of its production performance in hostile industrial settings.

Current knowledge on the oxidative stress response (OSR) of *C. glabrata* has increased significantly in the past decade, and the core elements have been characterized. These elements constitute two classes of defense mechanisms against oxidative stress, including detoxifying enzymes (*e.g.* catalase and superoxide dismutases) and non-enzymatic defenses (*e.g.* production of glutathione and pigments) (recent review on the topic can be found in (63)). Several key transcription factors (TFs) involved in the OSR have been identified, which includes Yap1, Skn7, Msn2, and Msn4 (43, 44). Yap1 and Skn7 are more dedicated to the response to the oxidative stress, while Msn2 and Msn4 are involved in the regulation of general stress response. However, there are additional components and pathways that remain unexplored in the OSR of *C. glabrata* so that the understanding of its molecular mechanisms is still far from being comprehensive.

Due to the complex nature of oxidative stress tolerance, rational engineering to further elevate the tolerance of the host based on limited knowledge of the underlying mechanisms would be very challenging. In contrast, adaptive laboratory evolution has been proven to be a useful tool to enhance the tolerance to various environmental stressors and to develop desired complex phenotypes in many different microorganisms without *a prior* knowledge (56, 64-67). The resulting adaptive mutants contain beneficial mutations and can be used to determine the mechanisms underlying the desired phenotypes. In this study, we are harnessing the power of the adaptive evolution

to improve the resistance of *C. glabrata* to H_2O_2 (a specie of the ROS); complemented with next-generation sequencing and genome-wide transcriptome analysis, we are able to identify potential mechanisms of oxidative stress tolerance in *C. glabrata*.

3.2. Materials and methods

3.2.1. Strains and culture medium

Unless specified, the culture medium used in this part of work is the YNB medium supplied with 2% (w/v) dextrose. *C. glabrata* strains, primers, and plasmids used in this part of work were listed in the table 1~3.

Table 1. List of primers used in the evolution under the hydrogen peroxide

Primer ID	Primer sequence (5'-->3')
HE1_F	CCCCCGAATTCATGAGTAAAGGAGAAGAACTT
HE1_R	CCCCCTCGAGTTATTTGTATAGTTCATCCATG
HE2_F	CCCCCGAATTCATGAGTAAAGGAGAAGAACTT
HE2_R	CCCCCTCGAGCTATTTGTATAGTTCATCCATG
HE3_F	GGCCAACACTTGTCACTACTTTCTC
HE3_R	TCTTTCGAAAGGGCAGATTGTGT
HE4_F	GTACCGCTCGAGCAGCTGTGATTGATTGAGGAGCGTCAAAACTAGAGAAT
HE4_R	ACTTAAGCCTTGGCAACGTGTTCAACCAAGACTTCACATATGTTAGGCGT
HE5_F	TAAACCATTGAGTGTCCGTTAGAATCATTTTGAAT
HE5_R	CTCAGTAACTGTGCTACTTCACATATGTTAGGCGT
HE6_F	CTCCCCGCGCGTTGGCCGATTCATTAATCG*GCATGC*TCTCTGTGGTAGCAGATTAT
HE6_R	AAATGATTCTAACGGACACTCAATGGTTTAGTAGC
HE7_F	TAACATATGTGAAGTAACGGAAGTGTCCAGTGAAT
HE7_R	CGGTGCGGGCCTCTTCGCTATTACGCCAGG*GCATGC*CGTAGCACCTTGCATGTTAT
HE8_F	CTTTACCATCTGGAACAAAG
HE8_R	ATATATTCTGTGTAACCCGC
HE9_F	GCATCGTCTCATCGGTCTCAAACGCTAAGCACGGACTACTAC
HE9_R	ATGCCGTCTCAGGTCTCACATATTATCCAACTATCAAATCATTTAG
HE10_F	GCATCGTCTCATCGGTCTCAATCCGTTCTAAGGTTAGAGCAATCG

Table 1. Continued

Primer ID	Primer sequence (5'-->3')
HE10_R	ATGCCGTCTCAGGTCTCACAGCGCTCATATGAACCAACGACA
HE11_F	GCATCGTCTCATCGGTCTCAAACGGAAGACTTTGTTGAACGAAG
HE11_R	ATGCCGTCTCAGGTCTCACATATTACCAGGTCATCTTTTGAAG
HE12_F	GCATCGTCTCATCGGTCTCAATCCTGTGCTGATTATCAGTTCTAATC
HE12_R	ATGCCGTCTCAGGTCTCACAGCTACATTAACAACGCTCATAAC
HE13_F	GCATCGTCTCATCGGTCTCATATGTGACCATGATTACGAATTCGAGC
HE13_R	ATGCCGTCTCAGGTCTCAGGATGCTCTAGAACTAGTGGATCTG
HE14_F	AACGGCATTCAGGGAGCAAT
HE14_R	TTGGGCGATGCGATTACCAT
HE15_F	CATCTGGCCTCTTTGAAGGGA
HE15_R	GTGGATCTGAAGTTCCTATTCTCTA
HE16_F	TGAGCAATCGAGATCCGGTG
HE16_R	CCTTGGTGTGCCAAAAGTGT
HE17_F	GGCACCTATACTGCAAACCCT
HE17_R	AGGGAAGCCATTCAAACACT
HE18_F	GCCAGGACTTAGCACAAGCA
HE18_R	CGTATGGGCAGTAACCAAGC
HE19_F	CGCAAGAAGTTCCACATCCA
HE19_R	TGACGAGGGCCTGACCATATT

Table 2. List of strains used in evolution under the hydrogen peroxide

Strain ID	Genotype	Source
KK-CA-24	ATCC2001	ATCC
KKY	ATCC2001 CAGL0C01067g::ScTDH3p-YFP-*SAT1*	this study
KKG	ATCC2001 CAGL0C01067g::ScTDH3p-GFP-*SAT1*	this study
H2-8Y	evolved mutants	this study
H2-11G	evolved mutants	this study
H2-18Y	evolved mutants	this study
H2-22Y	evolved mutants	this study
sMH098	ATCC2001 CAGL0F06831gΔ::CAGL0F06831g-FRT	this study
sMH099	ATCC2001 CAGL0F06831gΔ::CAGL0F06831g(opal)-FRT	Not constructed yet
sMH100	ATCC2001 cth2Δ::CTH2-FRT	this study
sMH101	ATCC2001 cth2Δ::cth2(amber)-FRT	this study

Table 3. The list of the plasmids used in evolution under the hydrogen peroxide

Plasmid ID	Description	Markers	Source
yEPGAP-cherry	yEMRFP	*URA3* *AmpR*	Sabine Keppler-Ross, et al., 2008
yEPGAP-GFP	GFP	*URA3* *AmpR*	This work
yEPGAP-YFP	YFP	*URA3* *AmpR*	This work
pKKGS4	source of green fluorescent gene	*AmpR*	Katy Kao's lab
pKKGS5	source of yellow fluorescent gene	*AmpR*	Katy Kao's lab
yEP352-*SAT1*	source of the *SAT1-FLP* marker	*URA3* *AmpR* *SAT1*	This work
yEPGAP-GFP-*SAT1*	GFP *SAT1-FLP*	*URA3* *AmpR* *SAT1*	This work
yEPGAP-YFP-*SAT1*	YFP *SAT1-FLP*	*URA3* *AmpR* *SAT1*	This work
yMH-CgI-GFP	for integration of green fluorescent cassette at CAGL0C01067g	*URA3* *AmpR* *SAT1*	This work
yMH-CgI-YFP	for integration of yellow fluorescent cassette at CAGL0C01067g	*URA3* *AmpR* *SAT1*	This work
pYTK001	Part Plasmid Entry Vector	GFP *CmR*	Michael E. Lee, et al., 2015
pYTK002	ConLS	*CmR*	Michael E. Lee, et al., 2016
pYTK067	ConR1	*CmR*	Michael E. Lee, et al., 2017
pYTK095	*AmpR*-ColE1	*AmpR*	Michael E. Lee, et al., 2018
pMH033	type 3 plasmid containing *SAT1-FLP*	*CmR* *SAT1-FLP*	This work
pMH045	type 2 plasmid containing partial coding sequence of wild-type CAGL0F06831g	*CmR*	This work
pMH046	type 2 plasmid containing partial coding sequence of CAGL0F06831g(opal) from H2-11G	*CmR*	This work
pMH047	type 2 plasmid containing partial coding sequence of CTH2	*CmR*	This work
pMH048	type 2 plasmid containing partial coding sequence of cth2(amber) from H2-18Y	*CmR*	This work
pMH049	type 4 plasmid containing 3 prime UTR of CAGL0F06831g	*CmR*	This work

Table 3. Continued

Plasmid ID	Description	Markers	Source
pMH050	type 4 plasmid containing 3 prime UTR of CTH2	*CmR*	This work
pMH051	cassette plasmid for replacement of CAGL0F06831g with CAGL0F06831g-*SAT1-FLP*	*AmpR SAT1-FLP*	This work
pMH052	cassette plasmid for replacement of CAGL0F06831g with CAGL0F06831g(opal)-*SAT1-FLP*	*AmpR SAT1-FLP*	This work
pMH053	cassette plasmid for replacement of CTH2 with CTH2-*SAT1-FLP*	*AmpR SAT1-FLP*	This work
pMH054	cassette plasmid for replacement of CTH2 with cth2(amber)-*SAT1-FLP*	*AmpR SAT1-FLP*	This work

3.2.2. Construction of fluorescent *C. glabrata* strains

The fluorescent *C. glabrata* strains, KKY and KKG, were constructed as follows: Gene encoding Green fluorescent protein (GFP) was amplified from pKKGS4 plasmid using primer pair of HE1_F and HE1_R; gene encoding yellow fluorescent protein (YFP) was amplified from pKKGS5 plasmid using primer pair of HE2_F and HE2_R. They were then cut with EcoRI and XhoI and ligated to the plasmid yEPGAP-cherry that was digested with the same two restriction enzymes. The resulting plasmids (yEPGAP-GFP and yEPGAP-YFP) have the yEMRFP gene replaced by corresponding fluorescent genes. The *SAT1* marker, amplified from yEP352-*SAT1* plasmid using the primer pair of HE4_F and HE4_R, was assembled with the Sal1-digested yEPGAP-GFP and yEPGAP-YFP by Gibson reaction (68) to create plasmid yEPGAP-GFP-*SAT1* and yEPGAP-YFP-*SAT1* respectively. The 5 prime and 3 prime flanking regions for fluorescent integration cassettes were amplified from the genomic DNA (gDNA) of KK-CA-24 using the primer pair of HE6_F and HE6_R and primer pair of HE7_F and HE7_R respectively, which are homologous to a pseudo gene CAGL0C01067g. The green and yellow

fluorescent cassettes were amplified from yEPGAP-GFP-*SAT1* and yEPGAP-YFP-*SAT1* respectively; and were then assembled with the two flanking regions and BamHI-digested yEPGAP-cherry by Gibson assembly to create yMH-CgI-GFP and yMH-CgI-YFP. The fluorescent integration cassettes were then cut from the yMH-CgI-GFP and yMH-CgI-YFP by restriction enzyme SphI and integrated into the genome of KK-CA-24 by electroporation (69).

3.2.3. Introduction of identified mutations in CAGL0F06831g and CAGL0E01243g

Mutants were constructed as follows: Partial coding sequences containing the desired mutations of the CAGL0F06831g and CAGL0E01243g were amplified from the gDNA of H2-11G with primer pair of HE9_F and HE9_R and from the gDNA of H2-18Y with primer pair of HE11_F and HE11_R respectively. The partial coding sequences of their wild-type version were amplified from the gDNA of KK-CA-24 with the same primer pairs as well. 3 prime untranslated regions (3UTRs) of these genes were amplified from the gDNA of KK-CA-24 with the primer pair of HE10_F and HE10_R (CAGL0F06831g) and the primer pair of HE12_F and HE12_R (CAGL0E01243g). In addition, the *SAT1-FLP* cassette was amplified from the plasmid yEP352-*SAT1* with the primer pair of HE13_F and HE13_R. These DNA fragments were all first cloned into the plasmid pYTK001 to create a new set of part plasmids (pMH033, pMH045~ pMH050); and then were assembled with fragments from pYTK002, pYTK067, and pYTK095 to construct four cassette plasmids that contain the replacement cassettes for CAGL0F06831g (both wild-type and mutant) and CAGL0E01243g (both wild-type and mutant). These plasmid constructions follow a MoClo-derived assembly by Michael E.

Lee *et al.* (70). The replacement cassettes were cut from the cassette plasmids (pMH051~ pMH054) by BsmbI (Thermo scientific) and integrated into the genome of KK-CA-24 using the Easy Frozen-EZ Yeast Transformation II Kit (Zymo Research) according to the manufacturer's protocol. The loop out of the *SAT1-FLP* cassettes were induced by growing the resulting transformants in YPD medium and verified by both colony PCR and DNA sequencing. The DNA fragments of part plasmids for construction of the cassette plasmids and the mutations in the CAGL0F06831g and CAGL0E01243g were verified by Sanger sequencing and analyzed with Unipro UGENE.

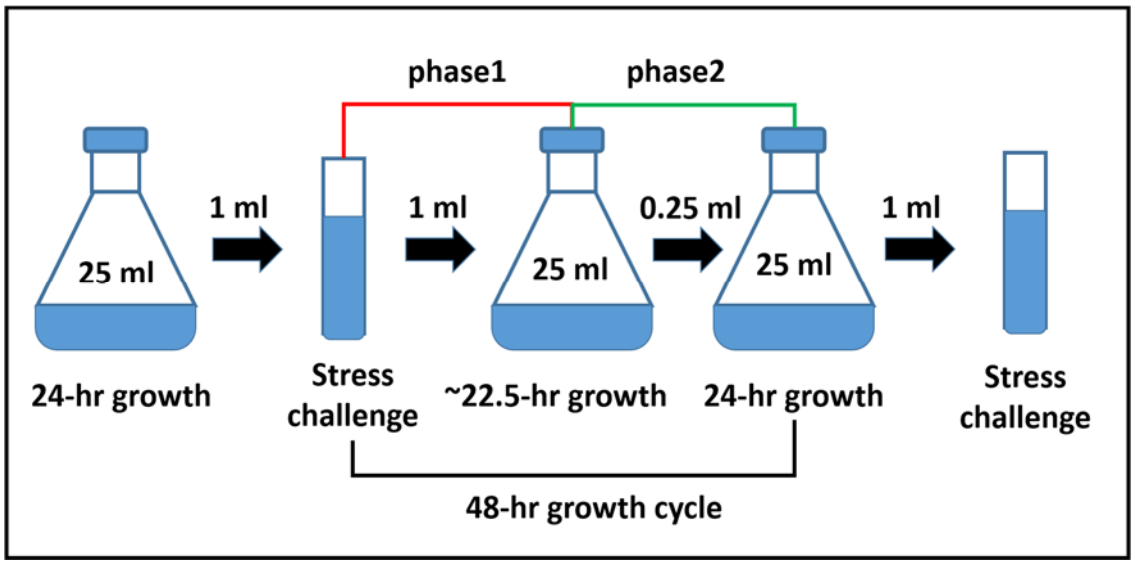

Figure 3. The scheme of two-phase based periodic shock strategy for adaptive evolution of *C. glabrata* under the inhibition of thermal/oxidative (H_2O_2) stress**.**

3.2.4. Adaptive evolution of *C. glabrata* to H_2O_2

Founding populations consist of approximately equal number of cells labeled by green fluorescent protein (GFP) and yellow fluorescent protein (YFP); and they were cultured in 25 ml of growth medium in flasks in a shaking water bath at 30°C. The populations were transferred daily and periodically shocked by H_2O_2 following a two-phase strategy (**figure 3**). During the phase 1 (P1), 1 ml of cell culture after 24-hour growth was challenged by H_2O_2 for 1 hour, which was followed by pelleting the cells to remove the H_2O_2, washing with 1 ml of 0.85% NaCl solution, re-suspending in 1 ml of growth medium, and inoculation into 24 ml of fresh growth medium for overnight growth. In the phase 2 (P2), 250 µl of the overnight culture from the P1 phase was transferred into 24.75 ml of growth medium; and the cells were grown for 24 hours so that they can recover from the H_2O_2 shock. These two phases were repeated until the end of the evolution. During the evolution, the OD_{600} of the evolving populations were measured by sampling cells before and right after each transfer. Frozen stocks of the evolving populations sampled right before each stress challenge were made for further characterizations and storage. When the OD_{600} significantly increased, the H_2O_2 IC_{50}s of the evolving populations were measured using the H_2O_2 susceptibility assay to check if any improvements in the tolerance to this oxidant. The selective stress (concentration of H_2O_2 in the challenge) was ramped up to the new IC_{50} value if an increase was observed. The relative proportions of the two subpopulations (GFP and YFP) for stored samples of selected evolving populations were measured using a FACScan flow cytometer (BD Biosciences, San Jose, CA). The isolation of the adaptive mutant for a given population

sample was performed as follows: At least 8 colonies from the given population sample were isolated for analysis. Their tolerance to H_2O_2 was estimated by H_2O_2 susceptibility assay and those with the highest H_2O_2 IC_{50}s were chosen as the adaptive mutants. If multiple colonies have the same H_2O_2 IC_{50} values, the colony with the highest viability at the H_2O_2 IC_{50}, measured as the ratio of the biomass (OD_{600}) accumulated after the challenge over the biomass (OD_{600}) accumulated in the absence of challenge for 48 hours, was selected as the adaptive mutant. These selected adaptive mutants from stored population samples were named based on the population samples from which they were isolated and the color of fluorescent protein expressed. For example, mutant H2-8Y was isolated from the YFP subpopulation of population sample H2-8.

3.2.5. H_2O_2 susceptibility assay

We defined the H_2O_2 IC_{50} of our evolving populations and adaptive mutants as the concentration of H_2O_2 used in the 1-hr challenge at 30°C that results in about 50% reduction of biomass (OD_{600}) as compared to the control (incubated at 30°C for 1 hour in the absence of H_2O_2). The H_2O_2 susceptibility assay was used to quantify the H_2O_2 IC_{50} for both populations and adaptive mutants by following steps. We grew the test subjects to an OD_{600} between 2.0~3.0 in culture medium at 30°C; measured and normalized the OD_{600} of all samples to about 1.0 before the H_2O_2 challenge using a spectrophotometer (Thermo Scientific inc., MA, United States); challenged 500 µl of normalized samples by an appropriate concentration gradient of H_2O_2 for 1 hour at 30°C in a shaker; the cells were pelleted after the challenge to remove the residual H_2O_2 and were subjected to serial 10-fold dilutions using the culture medium; 200 µl of the challenged cell cultures

and their diluted products (10-fold to 1000-fold) were incubated in 96-well plates at 30°C without agitation for 48 hours; and finally, the ODs were measured for each sample using a microplate reader (Tecan Group Ltd., Switzerland). The average mean of the H_2O_2 IC_{50} determined from at least three biological replicates of each sample was used for comparison.

3.2.6. Survival rate after stress challenge

The tolerance of our mutants and population samples to H_2O_2 was quantified in terms of its survival rate after the treatment of 100 mM of H_2O_2 for 1 hour as well. We grew the test subjects to an OD_{600} between 2.0~3.0 in the culture medium at 30°C; measured and normalized the OD_{600} of all samples to about 1.0 before the H_2O_2 challenge using a spectrophotometer (Thermo Scientific inc., MA, United States); challenged 500 µl of normalized samples by 100 mM of H_2O_2 for 1 hour at 30°C in a shaker; cells in the control group were incubated in the absence of H_2O_2 for 1 hour at 30°C in a shaker; pelleted the cells after the challenge to remove the residual H_2O_2 and diluted them in serial 10-fold dilutions by the culture medium; plated the 10000-fold diluted cells on YNB plates and incubated the plates at 30°C for two days before counting the colony formation units (CFUs). The survival rate was the ratio of the CFUs of H_2O_2-challenged cells to CFUs of the control group; and its average mean of at least three biological replicates of each sample was used for comparison.

3.2.7. Characterize the resistance to continuous exposure to H_2O_2

To estimate the resistance of our mutants and population samples to a long-term exposure to H_2O_2, we grew 200 µl of cells with the OD_{600} normalized to ~0.02 in YNB

medium in the presence and absence of 4 mM of H_2O_2 in 96-well plates at 30°C and 200 rpm. The OD_{600} was measured periodically during the entire growth phase using the microplate reader (Tecan Group Ltd., Switzerland). Growth curve fitting of OD_{600} data with the late-stationary-phase time points excluded (distorted the model fit) was performed using DMFit (www.ifr.ac.uk/safety/DMfit) to measure growth parameters, including specific growth rates and the lag times, using the model of Baranyi and Roberts (71). We had at least four biological replicates for each sample under each conditions. The means of the specific growth rates and the lag times of our samples were reported.

3.2.8. H_2O_2 clearance assay

To estimate the difference in H_2O_2 degradation and growth initiation in response to this stressor between the mutants and their parental strains, cells were grown to mid-exponential phase (OD_{600} between 0.4 and 0.6) at 30°C in 25 ml of culture medium and were pelleted to remove the supernatant. The cell pellets were then suspended in 1 ml of fresh medium; and OD_{600} of the cell suspensions were measured and normalized the to be about 2.5. 1 ml of each normalized cell suspension was added into 24 ml of growth medium containing H_2O_2 and incubated at 30°C in a shaking water bath. The initial concentration of H_2O_2 is about ~4 mM of H_2O_2. We sampled the cells right after the inoculation and several time points later for determining their OD_{600} and H_2O_2 concentration. To estimate the H_2O_2 concentration in the culture medium, we pelleted the cells of our samples and measured the H_2O_2 in the supernatant using the Amplex Red Hydrogen Peroxide/Peroxidase kit (Life Technologies, Carlsbad, CA) according to the

manufacturer's instructions. For each sample, we had at least three biological replicates and the means of the OD_{600} and H_2O_2 concentration were reported. In addition, the concentration of H_2O_2 at which the cells can tolerate and start to grow was defined as the H_2O_2 concentration measured at the first time point of a period when the OD_{600} of cells continuously increases for at least three successive time points.

3.2.9. Characterizations of H_2O_2 tolerance by plate dilution assay

Cells were grown to an OD_{600} between 2.0~3.0 in culture medium at 30°C; and the OD_{600} was measured and normalized to about 1.0 before the stress challenge using a spectrophotometer (Thermo Scientific inc., MA, United States). 500 µl of normalized samples were then challenged by 100 mM of H_2O_2 for 1 hour at 30°C in a shaker. For the control group, cells were incubated in the absence of H_2O_2 for 1 hour at 30°C in a shaker. The cells (both control and H_2O_2-treated group) were pelleted after the challenge to remove the residual H_2O_2 and subjected to serial 10-fold dilutions using the culture medium. 5 µl of diluted cells (10-fold, 10^2-fold, 10^3-fold, and 10^4-fold) were spotted on YNB plates supplemented with 2% dextrose and incubated at 30°C for two days. The images of the plates after 2-day incubation were taken for further analysis. The growth of the diluted cells on the plates were then compared between different samples.

3.2.10. Genome Sequencing

For evolutionary studies under the H_2O_2 stress, the adaptive clones, H2-8Y, H2-11G, H2-18Y, and H2-22Y, from population H2 and the two unevolved parental strains, KKY and KKG, were sequenced to identify the genotypes underlying the observed H_2O_2 tolerance. Genomic library preparation and sequencing were performed by the Texas

A&M Genomics Center for sequencing on the Illumina HiSeq 2500 platform using 100-bp pair-end reads. An average coverage of more than 238-fold was obtained for each clone. Reads were assembled against the CBS138 reference genome, and each mutant genome was compared to the parental sequences to identify any de novo mutations using the CLC Genomics workbench (version 6.0.1). For the variants calling, the frequency threshold was set to be 90% and the forward/reverse balance was set ≥ 0.3. Otherwise, the default setting was used for the CLC Genomics workbench. Selected mutations were verified with Sanger sequencing and analyzed with Unipro UGENE.

3.2.11. Microarray analysis

3.2.11.1. Sample harvest and total RNA extraction

Two biological replicates of H2-8Y, H2-11G, H2-18Y, H2-22Y, KKY and KKG were used for microarray analysis. Two colonies of each strain were inoculated into 1 ml of growth medium in 24-well plates and grown overnight at 30°C with shaking. An appropriate amount of overnight culture was diluted into 125-ml flasks containing 25 ml of growth medium to make an initial OD_{600} of about 0.01. Samples were grown until reaching an OD_{600} in a range between 0.4 and 0.6 (mid-exponential phase); and were then challenged by 1 mM of H_2O_2 for 30 minutes at 30°C in a shaker. The challenged cells were then harvested by rapid filtration (Nalgene) followed by immediate resuspension in 5 ml of RNAlater (AMBION). Total RNA was extracted from 3 ml of RNAlater suspension for each sample using the ZR Fungal/Bacterial RNA MiniPrep kit (Zymo Research Corp) according to the manufacturer's instructions.

3.2.11.2. Labeled cDNA Generation and Microarray Hybridization

The SuperScript indirect cDNA labeling system (Invitrogen) was used to generate cDNA incorporating amino-allyl dUTP. Cy3 and Cy5 (GE Healthcare) were used to label the cDNA samples. Custom cDNA microarrays (Agilent) containing 14645 probes (excluding positive and negative controls) were designed using the software package Picky (72) with the default parameters except that the number of probes per gene was set to be 2. The arrays contain probes covering ~99.98% of all identified ORFs in CSB138 strain with at least two probes per ORF. Labeled cDNA was hybridized onto the cDNA arrays for 18 hours, washed with Agilent Wash Buffers 1 and 2, and then immediately scanned using a GenePix 4200A reader according to the manufacturer's protocol as described for Agilent two-color prokaryotic microarrays.

3.2.11.3. Data Analysis

The local background intensity was subtracted from the recorded signal from each array spot. Arrays were then subjected to LOWESS normalization individually using the MIDAS software package (TM4) (73). The arithmetic average of the biological and technical replicate sample and reference signals were used for downstream analysis (74). Differentially expressed (DE) genes of our mutants as compared to their parental strains in the presence of H_2O_2 were identified using the rank product method with a critical p-value ($p<0.01$) using the MeV (TM4) microarray analysis software (75). The currently known functional annotations for *C. glabrata* genes were obtained from the Candida Genome Database (CGD) (23). Since most of the *C. glabrata* genes haven’t

been characterized yet, functions of these genes were inferred from their *S. cerevisiae* orthologs from Saccharomyces Genome Database (SGD)(76).

3.2.12. Bioinformatics analysis

The tools of GO term analysis from both CGD and SGD were used to analyze the significantly enriched biological processes and functional categories for the mutated genes and DE genes as compared to the parental strains. The regulatory enrichment assay was performed with the tool of "Rank by TF" provided by Yeastract for *S. cerevisiae* orthologs of the genes in our mutants whose expression is different from their parental strains at a statistically significant level (p-value <0.01) (77).

3.3. Results

3.3.1. Population dynamics of *C. glabrata* evolving with periodic H_2O_2 challenge

Three parallel populations (H1, H2, and H3) were evolved in YNB medium at 30ºC via serial batch transfers. Visualizing evolution in real-time (VERT) (78) was used to track the population dynamics during evolution using two otherwise isogenic strains that are labeled with either yellow fluorescent protein (YFP) or green fluorescent protein (GFP). An adaptive evolutionary strategy using periodic challenge with H_2O_2 was employed (**see figure 3 and Materials and Methods for details**). A control population (HC) which was serially transferred at 30°C in the absence of periodic H_2O_2 challenge was included. The populations were evolved for more than 180 generations and their optical densities at 600 nm (OD_{600}) prior to the transfer after each stress challenge (the end of phase 1) were shown in **figure 4**, which exhibited a step-wise increase in the OD_{600} for the evolving populations over the course of evolution. This data suggested that

evolved populations may acquire increased tolerance to H_2O_2. The IC_{50} for H_2O_2, as defined in the Materials and Methods section, was measured when a significant increase in cell densities was observed at the end of Phase 1 in each cycle (**figure 3**); and the selective pressure (concentration of H_2O_2) was ramped up to be the new IC_{50} value if an increase was observed. Following this strategy, the H_2O_2 challenge was ramped up from 80 mM at the beginning of the evolution experiment to 350 mM at the end.

All three evolved populations significantly improved their tolerance to H_2O_2. At the end of the evolution, the population-average H_2O_2 IC_{50}s ranged between approximately 17 to nearly 26 fold higher than that of the initial founding population, HC-1 (**figure 5**). Population H2 was chosen for more detailed characterizations, because one of its samples, H2-18, has the highest H_2O_2 IC_{50} (**figure 5 and figure 7)**. Its population dynamics was estimated with VERT by quantifying the relative proportions of GFP and YFP colored subpopulations (**figure 6**). As expected, each increase in the average OD_{600} at the population level was accompanied by an expansion in the relative proportion of a colored subpopulation (**figure 6**). For example, the average OD_{600} at the population level changed significantly from generation ~31 to ~39, and this was accompanied by an observed expansion in the YFP subpopulation (**figure 6**). These changes observed in the average cell density at the population level are likely due to the occurrence of mutations that benefit cell growth; and these beneficial mutations likely occurred in the expanding colored subpopulation. The data also suggests that VERT may be more sensitive in identifying the occurrence of adaptive mutations. The observed increase in the cell densities for population H2 indicates that one or more

adaptive mutations occurred at generation ~31. In contrast, the observed expansion in the YFP subpopulation suggests that the mutation or mutations may have already taken place at generation ~25. In addition, VERT can also be used to identify the subpopulation where the beneficial mutation arose (YFP or GFP subpopulation), which helps to facilitate the isolation of adaptive mutants for subsequent analyses.

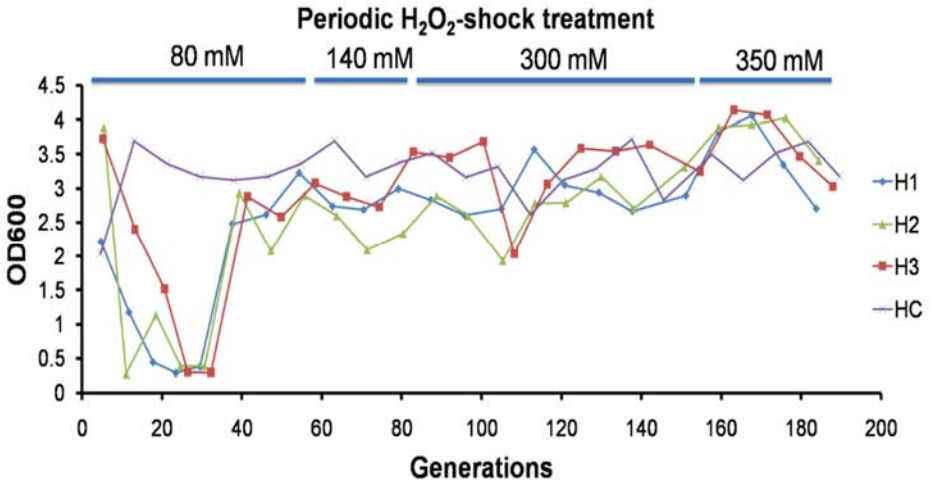

Figure 4. The dynamics of the population cell density (OD_{600}) during the evolution of *C. glabrata* exposed to periodic H_2O_2 treatment.

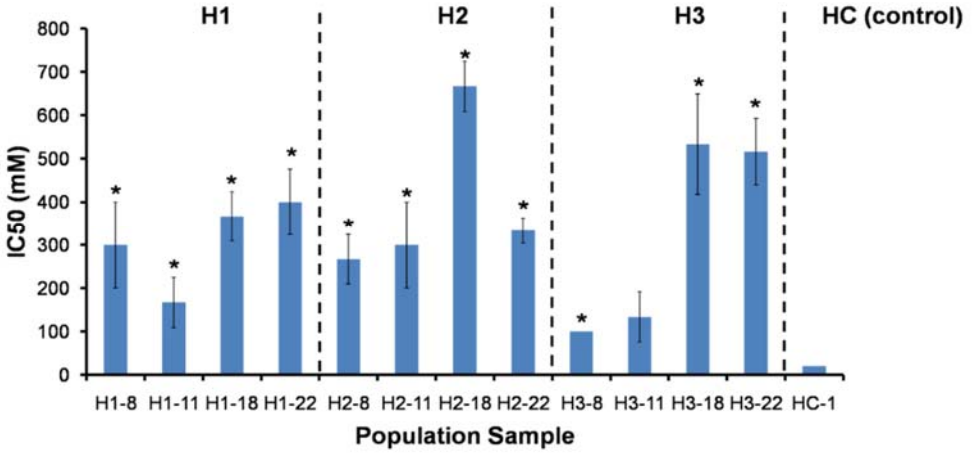

Figure 5. H_2O_2 IC_{50} values of the evolved populations after H_2O_2 shock treatment in a shaker (1 hour at 30°C). The asterisks indicate that the H_2O_2 IC_{50} values of evolved populations are statistically different from the control population, HC-1 ($P<0.05$, unpaired student t test with unequal variance).

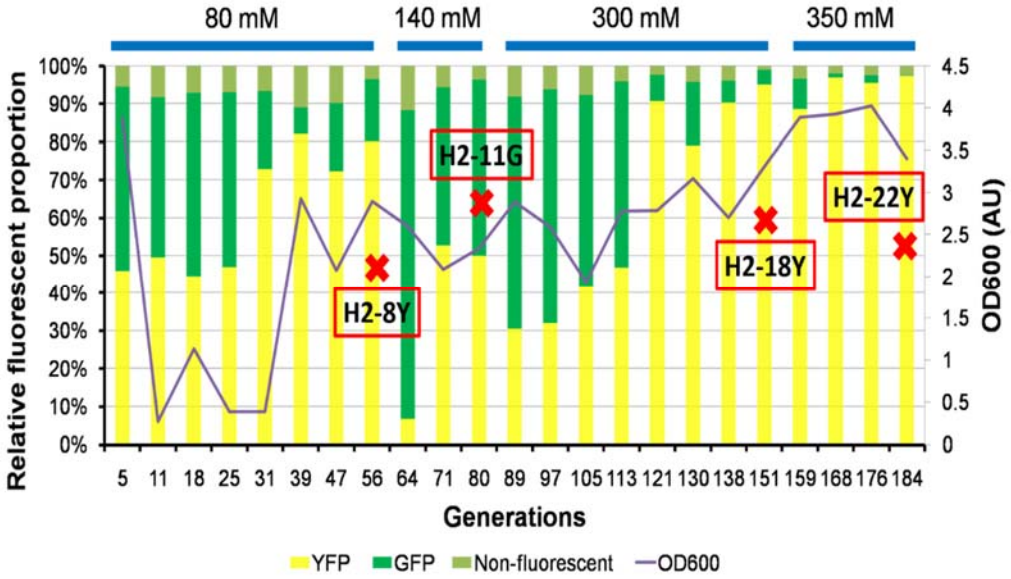

Figure 6. Population dynamics of H2 during the evolution under the inhibition of H_2O_2. The colored bar represented the relative fluorescent proportions of green fluorescent subpopulation (dark green), yellow fluorescent subpopulation (yellow), and non-fluorescent subpopulation (light green) and the purple line represents the optical densities of the populations measured at 600 nm. The concentrations of the H_2O_2 used in the shock during the evolution were shown on the top. The isolated adaptive mutants were highlighted in red box; and the red crosses indicated the time points when they were isolated and the subpopulations form which they were isolated.

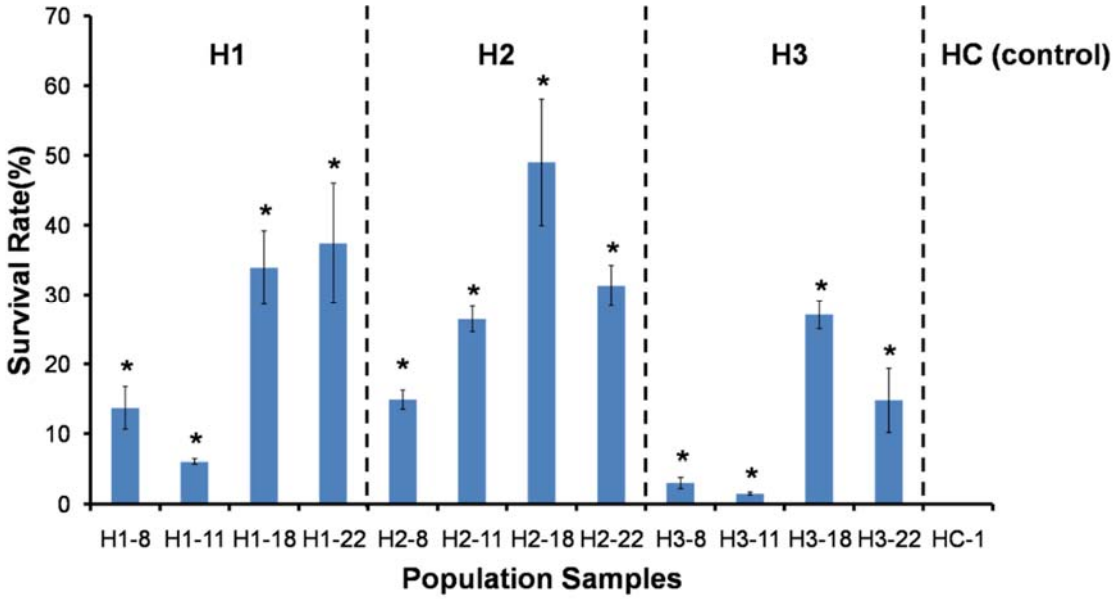

Figure 7. The survival rates of the evolved populations after 1-hr shock treatment with 100 mM H_2O_2 in a shaker at 30°C. The asterisks indicate that the survival rates of evolved populations are statistically different from the control population, HC-1 ($P<0.05$, unpaired student t test with unequal variance).

3.3.2. Adaptive mutants developed improved resistance to H_2O_2 and faster detoxification of H_2O_2

Time course samples from population H2 were selected for further phenotypic characterizations. Adaptive mutants H2-8Y, H2-11G, H2-18Y, and H2-22Y were isolated from time points immediately prior to each ramp-up in selective pressure, from populations H2-8, H2-11, H2-18, and H2-22, respectively (**figure 6**). The isolated adaptive mutants were chosen based on their H_2O_2 IC_{50} measurements among at least 8 isolates from each population sample (**see method and material**). Each isolated adaptive mutant and selected population samples from H1~H3 were analyzed for tolerance (survival and IC_{50}) to short-term exposures of high concentration of H_2O_2

(**figure 5, figure 7, and table 4**), and resistance (growth kinetics) to continuous exposure in a lower concentration of H_2O_2 (**figure 8 and table 4**). According to these characterizations, significant increases were observed in the H_2O_2 tolerance for adaptive mutants and population samples. The highest IC_{50} and survival rate was observed in mutant H2-18Y, which exhibited an IC_{50} of 600 mM and a 100% survival rate after a 1-hr exposure to 100 mM of H_2O_2, which were ~12-fold and ~555-fold higher than those of the parental strain, KKY, respectively (**table 4**). In contrast to survival rate, the IC_{50} measurements also consider the rate of recovery after challenge with the stressor in addition to the killing effects. Therefore, the increased IC_{50} observed in the adaptive mutants may also suggest an increased rate of recovery from the cell damage imposed by the H_2O_2 compared with the parental strains. Continuous exposure of both isolated mutants and populations to 4 mM of H_2O_2 showed significantly reduced growth lag phases (by approximately 6 hours) but no increase in specific growth rates compared with the parental strains; and the isolated mutants and evolved populations showed no significant difference in lag time in the absence of H_2O_2 (**figure 8A and table 4**). The observed decreased lag time suggests that the evolved mutants and populations are able to adjust more rapidly to H_2O_2 than the parental strains, possibly via faster H_2O_2 detoxification or higher level of H_2O_2 resistance.

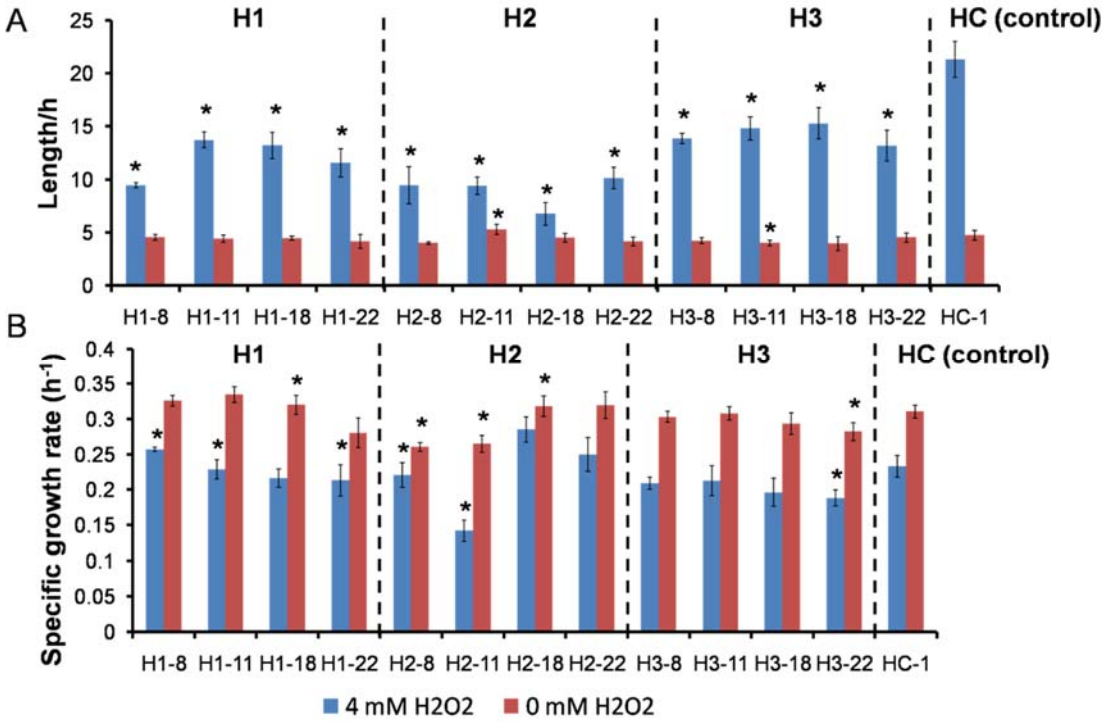

Figure 8. Growth kinetics of evolved populations in the presence and absence of H_2O_2. The length of the lag phase (A) and the specific growth rate (B) of the evolved populations as well as control population, HC-1, measured in YNB liquid medium supplemented with 2% (w/v) dextrose at 30°C in the presence and absence of 4 mM hydrogen peroxide. The average value of six biological replicates was reported for each sample and the asterisks indicate that the measured properties of evolved populations are statistically different from the control population, HC-1 ($P<0.05$, unpaired student t test with unequal variance).

Table 4. Properties of the Adaptive Mutants Isolated from the Evolution Under the inhibition of H_2O_2

Strain	Population	Generation	Fluorescence	Lag phase[a] (hr)		Specific growth rate[b] (h^{-1})		IC50[c] (mM)	Survival rate[d] (%)
				4 mM H_2O_2	0 mM H_2O_2	4 mM H_2O_2	0 mM H_2O_2		
H2-8Y	H2	56	YFP	8.8*	4.3	0.2*	0.31	225*	2.8*
H2-11G	H2	80	GFP	10*	5.3	0.12*	0.22*	500*	36.6*
H2-18Y	H2	151	YFP	9.7*	5.4*	0.17*	0.26*	600*	105.4*
H2-22Y	H2	184	YFP	9.6*	5.2	0.31*	0.38*	350*	42.8*
KKY	NA	NA	YFP	13.6	3.7	0.26	0.31	53	0.2
KKG	NA	NA	GFP	15.8	3.5	0.24	0.29	53	0.1

a. the mean value of the lag time based on four biological replicates was reported for each strain.

b. the mean value of the specific growth rate based on four biological replicates was reported for each strain.

c. The mean hydrogen peroxide IC50 value of at least three biological replicates was reported for each strain.

d. The mean survival rate of at least three biological replicates was reported for each strain.

The asterisks indicate that phenotypic traits of corresponding strains are statistically different from the parental strains, KKY and KKG ($P<0.05$, unpaired student t test with unequal variance).

To determine which one or both of these mechanisms is/are responsible for the increased H_2O_2 resistance, we measured the rate of H_2O_2 degradation and studied the initiation of cell growth in batch cultures in the presence of 4mM of H_2O_2 by the H_2O_2 clearance assay (**figure 9 and figure 10, see materials and methods**). Results showed that the H_2O_2 concentration decreased faster in cultures of adaptive mutants than the parental strains; the rate of H_2O_2 degradation is also faster in mutants isolated later during the adaptive evolution (adapted to higher selective pressure). The isolated mutant that exhibited the highest H_2O_2 detoxification rate is H2-18Y, which is able to reduce the H_2O_2 concentration from 4mM to less than 2 μM within 8 hours. In contrast, the parental strain KKY required more than 11 hours to reduce the H_2O_2 from the same initial level to about 34 μM. The data suggests that the isolated mutants gained the ability to more efficiently detoxify the exogenous H_2O_2. We also analyzed whether the isolated adaptive mutants are able to initiate growth at a higher concentration of H_2O_2

compared with the parental strains (**figure 10**). The results showed that the best isolated mutant, H2-8Y, can start growing at about 2.25 mM, which is a 61% increase compared to the parental strain KKY (Fig 5). Taken together, the data suggests that the adaptive mutants gained both improved resistance to H_2O_2 and faster detoxification of H_2O_2.

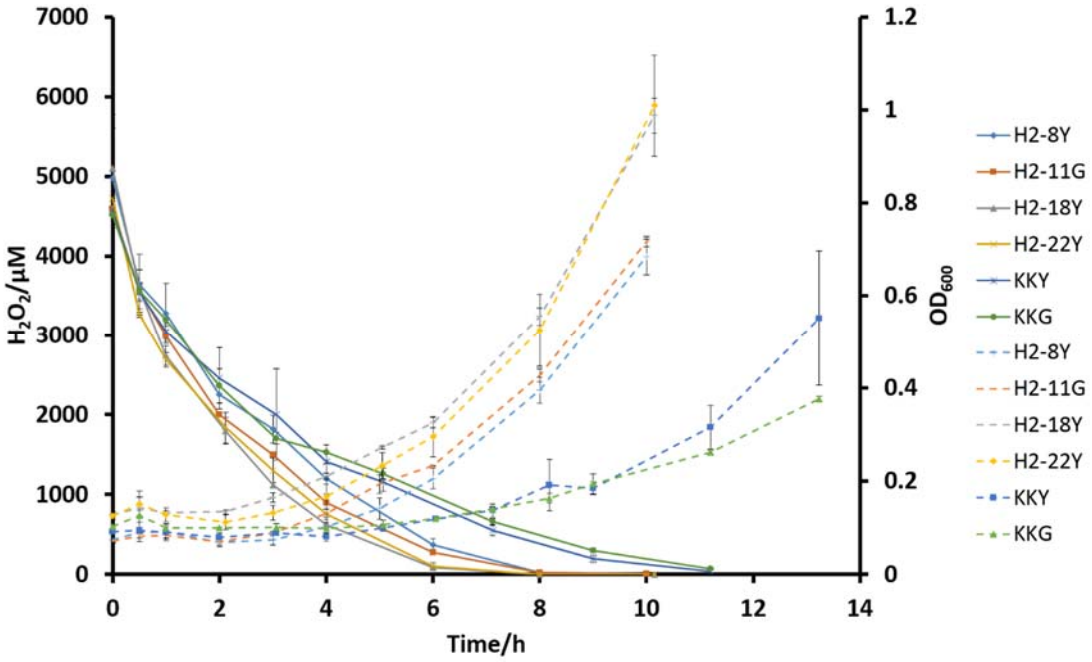

Figure 9. H_2O_2 degradation and the accumulation of biomass by adaptive mutants. The degradation of H_2O_2 and the accumulation of biomass (OD_{600}) by *C. glabrata* mutants and their parental strains in 25 ml of YNB medium supplemented with 2% (w/v) dextrose containing 4 mM of H_2O_2. The average values of at least three biological replicates for H_2O_2 concentration and OD_{600} were plotted against the time.

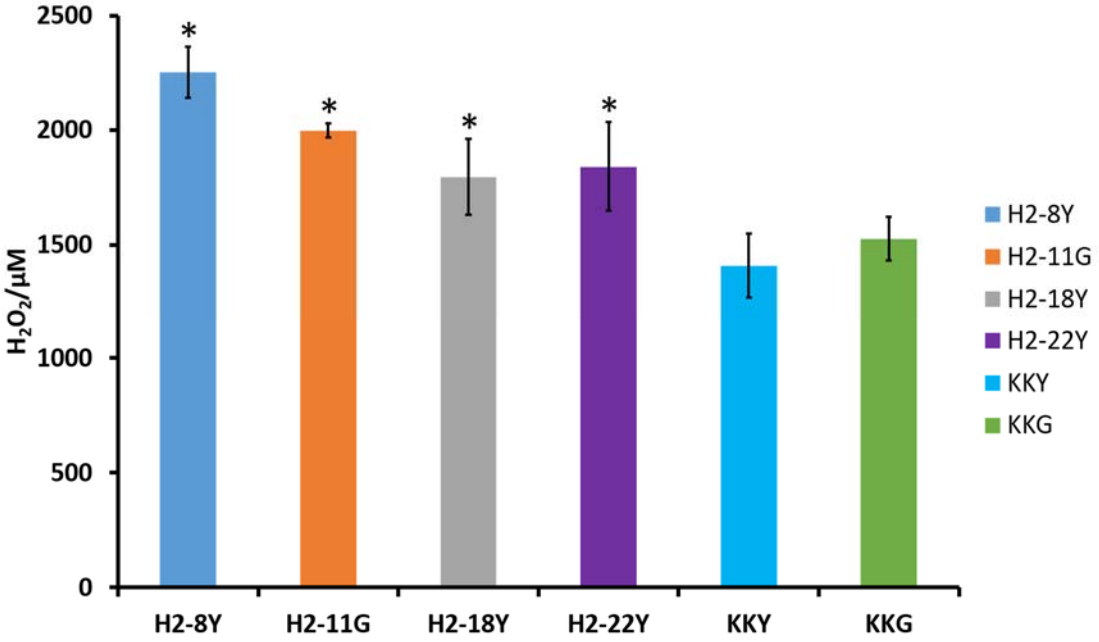

Figure 10. The resistance of adaptive mutants as well as parental strains (KKY and KKG) to H_2O_2. The concentration of H_2O_2 when cells initiated their grow in YNB medium supplemented with 2% (w/v) dextrose and 4 mM of H_2O_2 at 30°C in a shaker was measured for each strain. The average values of at least three biological replicates for the H_2O_2 concentrations were reported. The asterisks indicate that the H_2O_2 concentration of adaptive mutants are statistically different from the parental strains, KKY or KKG ($P<0.05$, unpaired student t test with unequal variance).

3.3.3. Next-generation sequencing revealed diverse evolutionary trajectories for adaptation to H_2O_2

We sequenced all four adaptive mutants (H2-8Y, H2-11G, H2-18Y, and H2-22Y) that were isolated from population H2. We found 47 mutations in total (**table 5**). Among these mutations, 28 are present in coding sequences and 19 are within 1 kbp of at least one coding sequence (**table 5**). Interestingly, there is only one mutation in CAGL0D00110g (pseudogene) which was identified across more than one adaptive

mutant. This lack of convergence in genes mutated across adaptive mutants and parallel populations suggests multiple adaptive routes involved in developing H_2O_2 resistance.

Table 5. The list of mutations identified in all adaptive mutants isolated from population H2 by next-generation sequencing

SID	Gene[a]	Amino acid change	Non-synonymous	nearby geneID[b]
H2-8Y	CAGL0B00105g, CAGL0B00110g-T	[Arg18fs]; [Asp642fs]	Yes	NA
H2-8Y	CAGL0B03113g	Gly107Val	Yes	NA
H2-8Y	CAGL0C00385g	Pro24Arg	Yes	NA
H2-8Y	NA	NA	-	CAGL0D05874g(WU); CAGL0D05852g(CD);
H2-8Y	NA	NA	-	CAGL0E01397g(CD); CAGL0E01419g(WU);
H2-8Y	NA	NA	-	CAGL0H01067g(CD); CAGL0H01089g(CU);
H2-8Y	NA	NA	-	CAGL0H01067g(CD); CAGL0H01089g(CU);
H2-8Y	NA	NA	-	CAGL0K12034g(CD);
H2-11G	CAGL0A02112g	His233Gln	Yes	NA
H2-11G	CAGL0B05093g-T	Pro559fs	Yes	NA
H2-11G	CAGL0F04983g	NA	No	NA
H2-11G	CAGL0F06831g	Leu807*	Yes	NA
H2-11G	CAGL0H02475g	NA	No	NA
H2-11G	CAGL0J01353g	Leu190Phe	Yes	NA
H2-11G	CAGL0M07546g	Phe6Tyr	Yes	NA
H2-18Y	NA	NA	-	CAGL0A04829g(CD);
H2-18Y	CAGL0D00110g-T	His610fs	Yes	NA
H2-18Y	CAGL0E01243g	Ser72*	Yes	NA
H2-18Y	CAGL0E05940g	Lys646fs	Yes	NA
H2-18Y	NA	NA	-	NA
H2-18Y	CAGL0I01694g	NA	No	NA
H2-18Y	CAGL0I07469g	NA	No	NA
H2-18Y	NA	NA	-	CAGL0J05918g(CD); CAGL0J05940g(WU);
H2-18Y	CAGL0K06083g	Tyr154His	Yes	NA
H2-18Y	CAGL0K09856g	Val307Ile	Yes	NA
H2-18Y	NA	NA	-	CAGL0L06094g(WU);
H2-18Y	NA	NA	-	CAGL0M08536g(CU);

Table 5. Continued

SID	Gene[a]	Amino acid change	Non-synonymous	nearby geneID[b]
H2-18Y	NA	NA	-	CAGL0M09581g(CD);
H2-22Y	CAGL0B00110g-T	His348fs	Yes	NA
H2-22Y	CAGL0B05093g-T, CAGL0B05148g	[Ser992Asn]; NA	Yes	NA
H2-22Y	CAGL0C05599g	Leu372fs	Yes	NA
H2-22Y	CAGL0D00110g-T	His610fs	Yes	NA
H2-22Y	CAGL0E01573g	Asp69Glu	Yes	NA
H2-22Y	NA	NA	-	CAGL0F03003g(WU); CAGL0F02959g(WD);
H2-22Y	NA	NA	-	CAGL0G01716g(CD); CAGL0G01738g(WU);
H2-22Y	NA	NA	-	CAGL0G03729g(CU); CAGL0G03707g(CD);
H2-22Y	NA	NA	-	CAGL0G05445g(CU);
H2-22Y	NA	NA	-	CAGL0G07513g(CD); CAGL0G07529g(WU); CAGL0G07535g(WU);
H2-22Y	CAGL0H00132g-T	Phe877fs	Yes	NA
H2-22Y	CAGL0H02827g	Glu185Gly	Yes	NA
H2-22Y	CAGL0H05137g	NA	No	NA
H2-22Y	CAGL0J01774g	Ser1263Pro	Yes	NA
H2-22Y	CAGL0K11990g	Pro349Leu	Yes	NA
H2-22Y	NA	NA	-	CAGL0L01111g(WD);
H2-22Y	NA	NA	-	CAGL0L12650g(WD); CAGL0L12672g(CU);
H2-22Y	CAGL0M00528g	NA	No	NA
H2-22Y	NA	NA	-	CAGL0M00924g(WU);
H2-22Y	CAGL0M12474g	NA	No	NA

a. the '-T' following the name of a gene indicates that the gene is a pseudogene.
b. the letters in the parenthesis following the gene ID describe the positions of identified mutations relative to the affected genes: W/C indicates the affected gene is in Watson strand/Crick strand; U/D indicates the mutations is in the upstream/downstream of the affected gene. For example, WU indicates that the affected gene is on Watson strand and the mutation is in its upstream.

Gene Ontology (GO) term analysis was used to identify if there is any enriched biological process or molecular function among the genes with mutations in either the coding sequences or in potential regulatory regions in the adaptive mutants. The GO

term analysis for the genes which are potentially affected by mutations across all four mutants did not yield any significantly (p-value<0.05) enriched functional categories or biological processes. Since most ORFs in *C. glabrata* have not been verified or characterized, we performed the GO term analysis using their orthologs or genes with the highest sequence similarities if orthologs are not available in *Saccharomyces cerevisiae* (*S. cerevisiae*) as well. Similarly, we didn't find any significantly (p-value<0.05) enriched functional category or biological process. When the potentially affected genes from each individual mutant were analyzed, we found that genes involving in the purine ribonucleoside triphosphate binding (p-value<0.04719) and cellular chemical homeostasis (p-value<0.02225) are significantly enriched in H2-11G and H2-18Y respectively.

To identify the mutations in our *C. glabrata* mutants that impact the cellular tolerance to H_2O_2, we checked the phenotypic data of the *S. cerevisiae* orthologs of the affected genes or *S. cerevisiae* genes with the highest sequence similarity to the affected ones in Saccharomyces Genome Database (SGD). We found that eleven *S. cerevisiae* genes were reported to directly impact H_2O_2 resistance when inactivated (**table 6**). Among the eleven *S. cerevisiae* genes that play roles in H_2O_2 resistance, most result in decreased H_2O_2 resistance, and three confer increased H_2O_2 resistance when nullified. There are only three orthologs (CAGL0F06831g, CAGL0H02827g, and CAGL0E01573g) of these *S. cerevisiae* genes in our adaptive mutants have mutations in their coding sequences. Interestingly, the CAGL0F06831g in H2-11G mutant is nullified and it has high sequence similarities to two genes in *S. cerevisiae* (*SPT23* and *MGA2*);

previous reports showed that a null mutation in *MGA2* led to increased resistance to H_2O_2 (79) in *S. cerevisiae*, suggesting that the null mutation in CAGL0F06831g may be responsible for the enhanced H_2O_2 resistance in H2-11G. In addition, five affected genes identified from the next-generation sequencing (NGS) analysis are possible orthologs of transcription factors (TFs) in *S. cerevisiae*; they are CAGL0E01243g (ortholog of *ScTIS11*/*CTH1*), CAGL0F06831g (ortholog of Sc*MGA2*/*ScSPT23*), CAGL0G05445g (ortholog of *ScSPS18*), CAGL0G03729g (ortholog of *ScNDD1*), and CAGL0L12650g (ortholog of *ScSSN3*). Two of these TFs in *S. cerevisiae*, *MGA2/SPT23* and *SSN3*, have been found to regulate the H_2O_2 resistance. Thus, we hypothesized that some of these potential TFs are likely to result in global transcriptional changes in our mutants to contribute their improved H_2O_2 resistance. Moreover, one affected gene (CAGL0K11990g) with sequence similarity to *AKL1* in *S. cerevisiae* may also impact H_2O_2 resistance of our mutants (**table 6**), because its *S. cerevisiae* ortholog affects glutathionin excretion.

Table 6. Phenotypic annotation of affected genes in adaptive mutants whose ortholog in yeast impact the H_2O_2 tolerance

SID	Gene Name	Mutation position[a]	Mutation type[b]	Ortholog[c]	Phenotype[d]
H2-22Y	CAGL0H05137g	CDS	S	*ALD6*	decreased when nullified; "Ng CH, et al. (2008)"
H2-22Y	CAGL0G07513g	ITR	NA	*ATP12*	decreased when nullified; "Brown JA, et al. (2006)"
H2-22Y	CAGL0E01573g	CDS	AAC	*EMW1*	decreased when nullified; "Okada N, et al. (2014)"
H2-22Y	CAGL0G05445g	ITR	NA	*GCS1*	decreased when nullified; "Brown JA, et al. (2006)"
H2-22Y	CAGL0G01716g	ITR	NA	*ISR1*	increased when nullified; "Brown JA, et al. (2006)"
H2-22Y	CAGL0H02827g	CDS	AAC	*JEM1*	decreased when nullified; "Brown JA, et al. (2006)"
H2-11G	CAGL0F06831g	CDS	NS	*MGA2*	increased when nullified; "Brown JA, et al. (2006)"
H2-8Y	CAGL0H01067g	ITR	NA	*NSE3*	decreased when nullified; "Okada N, et al. (2014)"
H2-22Y	CAGL0G01738g	ITR	NA	*PIL1*	decreased when nullified; "Martinez-Pastor M, et al. (2010)"
H2-22Y	CAGL0L12650g	ITR	NA	*SSN3*	increased when nullified; "Brown JA, et al. (2006)"
H2-8Y	CAGL0E01397g	ITR	NA	*TAF12*	decreased when nullified; "Okada N, et al. (2014)"

a. CDS indicates that the mutation occurred in coding sequence of an affected gene; ITR indicates that the mutation occurred within a 1 kb from the ORF of an affected gene;
b. AAC refers to amino acid change; FS refers to frame shift mutation; S refers to synonymous mutation; NS refers to nonsense mutation;
c. *S. cerevisiae* orthologs for given genes were inferred based on sequence similarities if not characterized;
d. phenotypes of affected *C. glabrata* genes were inferred from their yeast orthologs.

3.3.4. Putative transcription factors may function in the regulation of H_2O_2 tolerance

To identify potential molecular mechanisms underlying the improved H_2O_2 tolerance in the isolated mutants, we compared the whole-genome transcriptomic profiles between the adaptive mutants and the parental strains after exposure to 1 mM H_2O_2 for 30 minutes. A total of 612 genes were differentially expressed in at least one of the four mutants compared with the parental strain; 82 of these genes were differentially regulated in 3 or more mutants and 358 genes were differentially regulated in only one mutant (**see table A-1 in appendix**). Thus, while there may be similar mechanisms for H_2O_2 tolerance between individual mutants, the data also supports the existence of multiple adaptive routes to improved H_2O_2 resistance. The GO term analysis of the 82 genes with commonly perturbed expression shows that genes with roles in the organic acid biosynthetic process are significantly enriched (p-value ~0.025, false discovery rate ~2%). These enriched genes include those functioning in the biosynthetic process of the long-chain fatty acid (CAGL0D00528g, CAGL0E06138g, and CAGL0L10780g) and various amino acids (*e.g.* CAGL0C05115g and CAGL0I09592g for arginine synthesis, CAGL0H06369g for cysteine synthesis, CAGL0C03443g for lysine synthesis, CAGL0E01133g for homoserine synthesis). Interestingly, all of these enriched genes with roles in the biosynthesis of fatty acids or amino acids were commonly up-regulated, suggesting these organic acids may play an important role in the adaptation of *C. glabrata* to H_2O_2.

We further compared the list of differentially expressed genes found in our mutants and the list of genes that impact the H_2O_2 resistance in *Candida glabrata* from

the Candida Genome Database; and found that the two shared only one gene (CAGL0M13189g) which encodes a putative transcription factor similar to the *S. cerevisiae* Msn4p. The CAGL0M13189g is reported to result in a decreased resistance to H_2O_2 when nullified (43). This gene is down-regulated in our mutant, H2-22Y, and thus it would be expected to decrease the resistance to H_2O_2 rather than the opposite. There must be some other genes involved in the enhanced resistance to H_2O_2 in our mutants. Since only a few genes in *C. glabrata* have been characterized, we searched the phenotypic data of *S. cerevisiae* orthologs or genes with high sequence similarity to the differentially expressed gene in our *C. glabrata* mutants in the Saccharomyces Genome Database. In total, we found 99 genes with orthologs in *S. cerevisiae* (**see table A-1 in appendix**) affecting the resistance to H_2O_2 when mutated (mostly nullified) and ~42 of them are potentially involved in the improved resistance to H_2O_2 in our mutants according to their inferred functions based on sequence similarities to genes in *S. cerevisiae*. Among these genes with commonly perturbed expression in our mutants, there is only one, CAGL0J09966g (ortholog of *YDJ1* in *S. cerevisiae*), that is up-regulated in all four mutants; and two genes (CAGL0M07920g and CAGL0B03069g) are up-regulated in three mutants. Orthologs of these three genes in *S. cerevisiae* decrease the H_2O_2 resistance when nullified (79-81), suggesting that their up-regulation may have impacts on the H_2O_2 resistance of our mutants.

Relative to the parental strains, the expression of the five potential TFs with mutations that may affect their activity (CAGL0E01243g, CAGL0F06831g, CAGL0G05445g, CAGL0G03729g, and CAGL0L12650g) were not significantly

different at the transcription level in any of the isolated mutants. Three of the TFs contain mutations nearby but not directly in their coding sequences; the lack of differential gene expression relative to their parental strains suggests that these three may not play important roles in H_2O_2 resistance. The other two TFs (CAGL0F06831g and CAGL0E01243g) contain nonsense mutations in strains H2-11G and H2-18G respectively, which likely inactivated these TFs; and warrant further analysis.

CAGL0F06831g is a potential ortholog of *MGA2/SPT23* in *S. cerevisiae*, and there is prior experimental evidence showing that inactivation of *MGA2* in *S. cerevisiae* increases H_2O_2 resistance in yeast (79). Thus, it is likely that the nonsense mutation of CAGL0F06831g found in the strain H2-11G altered the transcription of its downstream targets involved in OSR, and increased the resistance to the stressor. The transcriptome analysis of H2-11G revealed 317 differentially expressed genes compared to its parental strain KKG; 298 of these genes have potential orthologs in *S. cerevisiae* based on their sequence similarities. Consistent with our hypothesis that the mutation in CAGL0F06831g can impact the expression of the genes regulated by *ScMGA2*, 28.14% of the differentially regulated genes in H2-11G with potential orthologs in *S. cerevisiae* are known members of the *ScMGA2* regulon, which is statistically enriched based on the use of "Rank by TF" in the Yeastract (with p-value ~6.67×10^{-9}). In addition to CAGL0F06831g, the same TF enrichment analysis revealed additional genes with their orthologs functioning as TFs in *S. cerevisiae* that may also impact the H_2O_2 resistance of H2-11G mutant (**see table A-2 in appendix**).

CAGL0E01243g has recently been characterized as a post-transcriptional inhibitor of iron consumption processes (82) with high sequence similarity to both *TIS11* and *CTH1* in *S. cerevisiae*. It has a nonsense mutation in the strain H2-18Y and the transcriptome analysis of the mutant revealed 290 genes with differential expression compared with the parental strain KKY in the presence of H_2O_2. Analysis revealed that 263 *S. cerevisiae* genes have high sequence similarities to the 264 differentially expressed genes in H2-18Y and thus could be their orthologs. Regulatory information for 258/263 genes are documented in the Yeastract database. The regulatory enrichment analysis tool on Yeastract found 8.46% of these potential orthologs to be regulated by *TIS11* with a p-value of ~1.65×10^{-5}. These findings suggest that the ortholog of the *S. cerevisiae TIS11* in *C. glabrata*, CAGL0E01243g, is likely to play a role in the improved H_2O_2 resistance. Moreover, an additional 14 TFs were significantly enriched from the analysis (**see table A-2 in appendix**) for H2-18Y as well; and one of them, the Hmo1 , has been reported to impact the H_2O_2 resistance in *S. cerevisiae* as well (83). Taken all together, mutations in orthologs of some of these *S. cerevisiae* TFs might contribute to the improved H_2O_2 tolerance in our mutants.

3.3.5. The role of putative transcription factors, CAGL0F06831g and CAGL0E01243g, in tolerance to H_2O_2

Given on the challenges of molecular cloning in *C. glabrata* (*e.g.* limited selective markers, and dominant non-homologous end joining over homologous recombination) (84), we selected only a few candidate mutations for reconstruction in our wild-type background (KK-CA-24) using a strategy based on a MoClo-derived

assembly (**see materials and methods for details**) (70). Mutations identified in CAGL0F06831g from H2-11G and in CAGL0E01243g from H2-18Y were chosen based on their potential roles as TFs and the fact that their potential regulatory targets were significantly enriched in genes which are differentially expressed in mutants compared to parental strains. We successfully introduced one of the two aforementioned mutations, the nonsense mutation in CAGL0E01243g from H2-18Y, into KK-CA-24. The resulting strain, sMH101, carries the mutation with a FRT scar of about 109 bp that was left after the loop out of our selective marker. Since the scar that was left between the coding sequence of the gene and their original 3 prime UTR might impact the expression of the gene (85), we introduced the wild-type CAGL0E01243g from KK-CA-24 to create strain sMH100 in the same way to evaluate the phenotypic effects of the altered structure of the 3 prime UTR due to the presence of the FRT scar. For the mutation in CAGL0F06831g from H2-11G, we only were able to constructed the strain with the wild-type CAGL0F06831g and the FRT scar, sMH098. These strains (sMH098, sMH100~sMH101) with the KK-CA-24 were challenged by 50 and 100 mM of H_2O_2 for 1 hour in a shock assay (**see materials and methods**); and the results (**figure 11**) showed that the sMH101 has acquired significantly improved tolerance to the H_2O_2 as compared to both KK-CA-24 and the control with the wild-type gene and the scar, sMH100. Interestingly, the two control strains, sMH098 and sMH100, both exhibited higher tolerance to H_2O_2 as compared to the KK-CA-24 as well. Since the mutations in these two genes are nonsense, the affected genes may be non-functional. If this is the case, the improved tolerance to H_2O_2 in our control strains could be attributed to the

reduced gene expression by the altered 3 prime UTR structure. Taken together, these data suggest that CAGL0F06831g and CAGL0E01243g may have a negative impact on the cellular tolerance to H_2O_2.

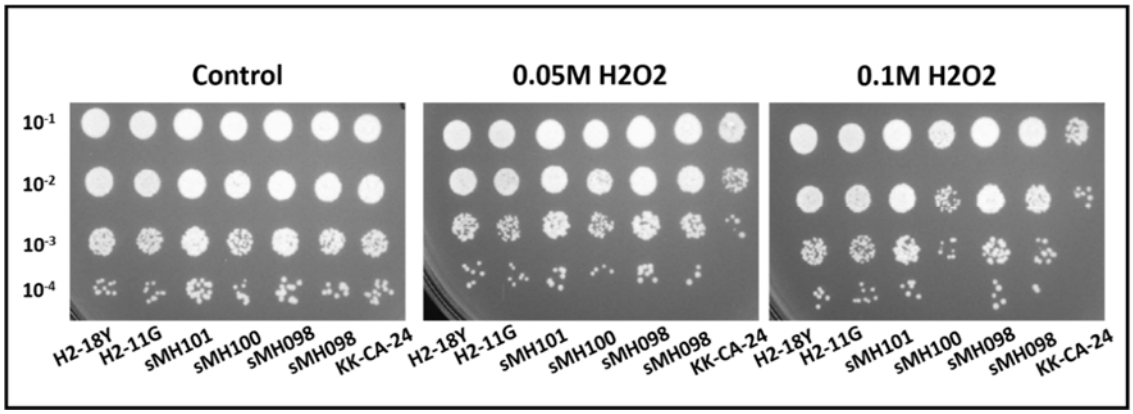

Figure 11. Characterization of the H_2O_2 tolerance for strains with introduced mutation from adaptive mutants. The cells were subjected to 50 mM and 100 mM of H_2O_2 for 1 hour in a shaker at 30°C; for the control group, cells were incubated in a shaker at 30°C for 1 hour in the absence of the stress; diluted cells (10^{-1}, 10^{-2}, 10^{-3}, and 10^{-4}) were plated on the YNB plates supplemented with 2% (w/v) dextrose at 30°C for two days.

3.4. Discussion

3.4.1. Modulation of membrane composition by CAGL0F06831g could result in enhanced H_2O_2 tolerance

Based on the high sequence similarity, CAGL0F06831g has a *S. cerevisiae* ortholog, *MGA2*, which involves in the membrane fatty acid biosynthesis. One of the most well-characterized targets of Sc*MGA2* is *OLE1*, which encodes a Δ9 fatty acid desaturase required for monounsaturated fatty acid synthesis (86). Another characterized target of Sc*MGA2* is *ERG1*, which encodes a squalene epoxidase required for ergosterol

synthesis (87). In addition to these targets, *ScMGA2* were also reported to affect expression of many genes which impact resistance to H_2O_2 (Yeastract and SGD database). As mentioned earlier, the null mutation of the *S. cerevisiae MGA2* has been shown to increase the H_2O_2 resistance. Interestingly, the adaptive mutant, H2-11G, has a nonsense mutation close to the 3 prime end of the CAGL0F06831g (ortholog of *ScMGA2*), which results in the expression of a truncated protein. The regulatory enrichment analysis revealed that *C. glabrata* orthologs of targets regulated by *ScMGA2* overrepresented at a statistically significant level ($P<6.7x10^{-9}$, Yeastract database). The GO term analysis of all *S. cerevisiae* orthologs which are differentially regulated in H2-11G as compared to its parent showed that those involved in fatty acid synthesis are significantly enriched (p-value~0.024, with Benjamini Hochberg test correction). Most of the *S. cerevisiae* orthologs in the enriched category are direct regulatory targets of *ScMGA2* (Yeastract database), namely, *FAS1*, *FAS2*, *ELO1*, *ELO2*, and *ELO3*; and they are all significantly up-regulated (p-value<0.01), which might favor the synthesis of long-chain saturated fatty acid (88). The resistance to hydrogen peroxide was reported to be affected by the saturation and chain length of membrane fatty acids in *S. cerevisiae* (89, 90). The nonsense mutation of the CAGL0F06831g in H2-11G could either result in a loss-of-function protein or a constitutively active protein due to the absence of C-terminal membrane-anchoring domains which is reported to repress the protein activity (86). It would be expected that both cases could significantly alter the expression profiles of the downstream targets of the CAGL0F06831g and thus possibly change the composition of membrane fatty acid. Taken together, all these evidence suggests that in

C. glabrata modulation of membrane fatty acid composition by CAGL0F06831g could contribute to the increased H_2O_2 resistance.

3.4.2. CAGL0E01243g may affect the tolerance of *C. glabrata* to H_2O_2 through multiple mechanisms

S. cerevisiae TIS11 encodes a mRNA-binding protein that binds to 3 prime UTR of specific genes to mediate their degradation. In *C. glabrata*, the ortholog of *S. cerevisiae TIS11* is CAGL0E01243g based on sequence similarity; and as mentioned before, its function has been characterized recently. According to the Yeastract database, *TIS11* in *S. cerevisiae* has about 319 documented direct regulatory targets with various functions in distinct cellular processes and some have transcription factor activity. In our mutant H2-18Y, CAGL0E01243g has a nonsense mutation occurred close to the 5 prime end of the gene, which possibly results in a non-functional truncated protein. The transcriptome analysis of the H2-18Y mutant suggests that putative targets of the CAGL0E01243g over-represents in the genes with differential expression as compared to the parental strain (p-value~1.65×10^{-5}, Yeastract database). The same regulation enrichment analysis revealed genes with putative TF activities that could be responsible in large part for the differential expression of genes in the mutant, including CAGL0E00737g (ortholog of *ScHMO1*), CAGL0E02475g (ortholog of *ScSIN3*), and CAGL0M04323g (ortholog of *ScACE2*) (**see table A-2 in appendix**). In addition, these genes themselves were all up-regulated in the mutant relative to the parental strain at statistically significant levels (p-value<0.01); many of their differentially expressed targets are reported to affect the H_2O_2 resistance in *S. cerevisiae*. Particularly, the

absence of *ScHMO1* is reported to decrease the H_2O_2 resistance in *S. cerevisiae* (83). These data suggest that their orthologs in *C. glabrata* might involve in the adaptation of H2-18Y to H_2O_2. Furthermore, the regulatory association analysis using the database of Yeastract revealed possible connections between these genes and CAGL0E01243g, suggesting that some or all of them might be the indirect regulatory targets of the latter.

GO term analysis of the *S. cerevisiae* orthologs of differentially regulated genes in H2-18Y showed that genes involved in many categories of biological processes are significantly enriched, including those involved in the nicotinamide nucleotide metabolism (p-value~$3.4X10^{-3}$, with Benjamini Hochberg test correction, SGD), lipid biosynthesis (p-value~$3.3\ X10^{-3}$, with Benjamini Hochberg test correction, SGD), and cellular amino acid biosynthesis (p-value~$3.8\ X10^{-4}$, with Benjamini Hochberg test correction, SGD). As discussed before, membrane composition may play a critical role in the H_2O_2 resistance in H2-11G and thus it is not surprising to see relevant genes are enriched in H2-18Y. Interestingly, *FAS1*, *FAS2*, *ELO1*, and *ELO2* showed similar up-regulation in H2-18Y as in H2-11G, although the ortholog of *ScMGA2* was neither mutated nor differentially expressed in the H2-18Y. This result suggests that other regulator may also contribute to the change in the membrane composition in response to the challenge by H_2O_2. Another discovery in the GO term analysis is that genes involved in nicotinamide nucleotide metabolism, including those play critical roles in the glycolysis and pentose phosphate pathway (PPP), are significantly enriched. The expression pattern of this group of genes in H2-18Y favors the redirection of carbon flux from glycolysis to PPP to produce cellular reducing power NADPH, which is consumed

rapidly during the detoxification of ROS by glutathione- and thioredoxin-dependent enzymes (91, 92). As to the effects of the amino acids on the oxidative stress, a limited number of relevant researches on fungi are available. The restriction of methionine and accumulation of proline were reported to protect cells against the oxidative damages (93, 94). Interestingly, othologs of many *S. cerevisiae* genes involves in the synthesis of methionine (CAGL0L06094g, CAGL0H06369g, CAGL0K06677g, and CAGL0E01133g) and the precursor of the proline, glutamate (CAGL0I07227g, CAGL0G02673g, and CAGL0L01089g), are differentially regulated relative to the parental strain in H2-18Y. Together, we hypothesized that CAGL0E01243g (ortholog of *ScTIS11*) might regulate several putative TFs directly or indirectly, such as those encoded by CAGL0E00737g (ortholog of *ScHMO1*), CAGL0E02475g (ortholog of *ScSIN3*), and CAGL0M04323g (ortholog of *ScACE2*), to alter the expression of their targets involving in NADPH regeneration, modulation of membrane composition, and synthesis of amino acids with protective effects against oxidants, which impacts the H_2O_2 tolerance in *C. glabrata*.

3.4.3. Potential role of chromatin remodeling in the adaptation of *C. glabrata* to H_2O_2

We sequenced the genome of the adaptive mutant H2-8Y and found that the mutation of one gene, CAGL0C00385g, is of particular interest. In H2-8Y, the CAGL0C00385g has a mutation in its coding sequence which causes the amino acid change. Although it is not characterized in *C. glabrata*, CAGL0C00385g has an otholog in *S. cerevisiae*, *IOC2*, which functions in the chromatin remodeling. We have some data

showing that the CAGL0C00385g might regulate the H_2O_2 resistance in *C. glabrata* by chromatin remodeling.

In eukaryotic cells, chromatin remodeling plays a critical role in gene expression by regulating the accessibility of condensed gDNA to regulatory transcription machinery proteins (*e.g.* TFs and RNAPII); it is also required for other processes involving DNA molecules, such as transcription, recombination, DNA repair and replication (95, 96). In *S. cerevisiae*, Ioc2 forms a nucleosome-stimulated ATP-dependent chromatin remodeling complex Isw1b with two other components, Isw1 (catalytic subunit) and Ioc4. It is proposed that Isw1b functions as a transcription elongation checkpoint (TEC) to coordinate the early and late events in the transcription cycle (97). In the Isw1b-dependent transcription regulation, Isw1 is essential for all functions of the complex; and the associated protein Ioc2 is required for the pausing of the RNAPII at a putative TEC near the promoter of target genes. In addition, Ioc2 promotes the dissociation of the RNAPII from the DNA templates at the TEC. These negative impacts of the Ioc2 on the transcription of its target genes are consistent with the transcriptome analysis of a Ioc2 mutant in a microarray study where most target genes are de-repressed (98).

Given on the role of Ioc2 in *S. cerevisiae*, it is likely that the mutation of its ortholog (CAGL0C00385g) in H2-8Y strain altered the interaction between the components of its Isw1b complex and therefore affected the transcription profiles of the mutant in response to the H_2O_2. In agreement with our hypothesis, the transcriptome analysis of H2-8Y showed that the putative targets of the CAGL0C01683g, ortholog of *S. cerevisiae ISW1*, were over-represented with a p-value of ~0.074 (**see table A-2 in**

appendix) in the cluster of genes which showed different expression from its parent at a statistically significant level (p-value <0.01). In addition, the analysis revealed that the orthologs of *S. cerevisiae ZAP1* (CAGL0J05060g) and *CAD1* (CAGL0F03069g) were all up-regulated as compared to the parental strain at a statistically significant level (p-value<0.01) and the putative targets of CAGL0J05060g (the ortholog of the *ScZAP1*) were overrepresented (**see table A-2 in appendix**) in the differentially regulated gene cluster of H2-8Y as well (p-value <0.015). These two genes encode TFs in *S. cerevisiae* that are well-known to affect the resistance of *S. cerevisiae* to oxidative stress (99, 100). Although *ISW1* has no known targets directly involved in the tolerance or resistance to the H_2O_2, it might play an indirect role by regulating the expression of the *RLM1* in *S. cerevisiae* (101). The CAGL0M06325g has some sequence similarities to the *S. cerevisiae RLM1* and this gene is up-regulated at a statistically significant level (p-value<0.01) in H2-8Y relative to its parental strain. The analysis using the module "search for associations" of yeastract database showed that the *S. cerevisiae RLM1* have many targets involved in the H_2O_2 resistance; and some of their *C. glabrata* orthologs were actually expressed differentially in H2-8Y as compared to its parent (**see table A-1 in appendix**), including orthologs of *ADH1*(CAGL0I07843g), *ATP7*(CAGL0L09713g), *PDC1*(CAGL0M07920g), *HMX1*(CAGL0A03905g), *VPS1*(CAGL0L02299g), and *YBL028C*(CAGL0F04103g). Moreover, the *RLM1* could potentially regulate the expression of *GIS1* and *YER130C* thus the expression of *ZAP1* and *YAP1* according to the regulatory association database in Yeastract. Taken together, our data suggests a possibility that putative Isw1b complex plays a role in the adaptation of *C. glabrata* to

H_2O_2 through transcriptional regulation cascades of putative TFs that are involved in the OSR. The introduction of the mutation in CAGL0C00385g from H2-8Y into the wild-type KK-CA-24 in the future will help to answer the question.

4. MAPK SIGNALING CASCADS HAVE A CRUCIAL IMPACT ON THE ADAPTATION OF *C. GLABRATA* TO MULTIPLE ENVIRONMENTAL STRESSES

4.1. Introduction

Adaptation to the ever-changing environment is one of the biggest challenges facing each of living organisms. One of the ubiquitous environmental variables that have profound impacts on the physiology of living organisms is the temperature. When the ambient temperature falls outside of the normal range which an organism could tolerate, it may cause a wide range of cellular damages and ultimately the death of the organism (102, 103). As a potential producer for many chemicals of industrial significance, the adaptation of *C. glabata* to elevated temperatures is of particular interest (104). Studies have shown that microbial fermentation at high temperature could help to reduce the cooling costs, prevent contamination, and improve the productivities of simultaneous saccharification and fermentation (SSF) (105-107). Thus, understanding of the adaptive mechanisms to the thermal stress are critical to improve the thermal tolerance of the *C. glabrata* and could benefit its production performance in hostile industrial settings.

We have made many significant advances in our understanding of the temperature sensing and the heat stress response (HSR) using the model yeast *Saccharomyces cerevisiae* (*S. cerevisiae*) in the past two decades. Many transcription factors and their downstream targets that involve in the response to thermal stress have been characterized, including *HSF1*, *MSN2*, and *MSN4*(108-110). In addition, many temperature sensing mechanisms have been proposed with experiment evidence, such as

the membrane fluidity change, unfolded protein responses, and RNA thermometer (reviewed in (111)). However, the current knowledge on the adaptation of *S. cerevisiae* to thermal stress is still far from being comprehensive and many key components have not been identified, such as the primary sensors of the change in the ambient temperature. As to the *C. glabrata*, there has been little work on its adaptation to thermal stress.

Due to the complex nature of thermo-tolerance and limited prior knowledge, we decided to perform the laboratory adaptive evolution (LAE) to study the adaptation of *C. glabrata* to high temperatures (≥ 47°C) using the periodic hyperthermal challenge. The resulting adaptive mutants constitute a precious genetic database which is rich in beneficial mechanisms regarding the affected phenotypes. In this study, we are harnessing the power of the adaptive evolution to improve the resistance of *C. glabrata* to the challenge at high temperatures (≥ 47°C); studying the underlying mechanisms using the next generation sequencing. We found that the acquisition of cross-tolerance to stresses other than the heat is common in our parallely evolved populations. Moreover, we identified several beneficial mutations that are responsible in large part for the observed cross-tolerance; and showed that the MAPK pathway, especially the HOG pathway, may have an important role not only in the temperature adaptation but also adaptation to various other stresses in *C. glabrata*. To our knowledge, this is the first report that studied the acquisition of resistance to thermal stress and other stresses in *C. glabrata* in the context of short-term adaptive evolution.

4.2. Materials and methods

4.2.1. Strains and culture media

Unless specified, the culture medium used in this part of work is the YNB medium supplied with 2% (w/v) dextrose. *C. glabrata* strains, primers, and plasmids used in this part of work were listed in the table 7~9.

Table 7. List of primers used in the evolution under the hyper-thermal stress

Primer ID	Primer sequence (5'-->3')
TE9_F	GCATCGTCTCATCGGTCTCAAACGAGGAAGGTAAGGATAAACTACGG
TE9_R	TGATTCTCCTGGTTTAGTGGTGA
TE10_R	ATGCCGTCTCAGGTCTCACATACTATATGATATGACTCTCGAGCC
TE11_F	GCATCGTCTCATCGGTCTCAATCCGATGAATATATTAACGAGAATG
TE11_R	ATGCCGTCTCAGGTCTCACAGCACTTTGAAATACCAGACCG
TE12_F	GCATCGTCTCATCGGTCTCATATGTGACCATGATTACGAATTCGAGC
TE12_R	ATGCCGTCTCAGGTCTCAGGATGCTCTAGAACTAGTGGATCTG
TE13	CCTCTGACTTGAGCGTCG
TE14	AATGCCTGCATCTGTGAG
TE15	GGGTTGTGTCAAGATCAC
TE16	CCAATCTTTGAATTATTC
TE17	CCACGGTTAATAACATCC
TE18	ACAACATTAGTCAACTCC
TE19	AGGAATTCTGAACCAGTC
TE20	TGGTGAGAACAGCGACCG
TE21	TGTTGTGGGTGTGTGCTA
TE22	GCCATAGCAAGCAGAGTC
TE23	ATAGAAGAAGTTGCTGCT
TE24_F	GCAAACTACTCAAGAATCCTCCG
TE24_R	CCCAGGATGGTATCTCCGGT
TE25_F	ATCGTGACATCAAGGGTGCC
TE25_R	TTCGTGTTCATCGAGGGGAC
TE26	ACTATTCAAAGAACGTGC
TE27	AATGCCTGCATCTGTGAG
TE28	GGGTTGTGTCAAGATCAC

Table 8. List of strains used in the evolution under the hyper-thermal stress

Strain ID	Genotype	Source
KK-CA-24	ATCC2001	ATCC
KKY	ATCC2001 CAGL0C01067g::ScTDH3p-YFP-*SAT1*	this study
KKG	ATCC2001 CAGL0C01067g::ScTDH3p-GFP-*SAT1*	this study
T1-27G	evolved mutants	this study
T2-5G	evolved mutants	this study
T2-10G	evolved mutants	this study
T2-17G	evolved mutants	this study
T2-27G	evolved mutants	this study
T3-24Y	evolved mutants	this study
sMH080	ATCC2001 ste11Δ::*STE11*-FRT	this study
sMH081	ATCC2001 ste11Δ::*STE11*(T554I)-FRT	this study
sMH082	ATCC2001 ste11Δ::*STE11*(P256T)-FRT	this study
sMH083	ATCC2001 ste11Δ::*STE11*(P256S)-FRT	this study

Table 9. The list of the plasmids used in the evolution under the hyper-thermal stress

Plasmid ID	Description	Markers	Source
pYTK001	Part Plasmid Entry Vector	GFP *CmR*	Michael E. Lee, et al., 2015
pYTK002	ConLS	*CmR*	Michael E. Lee, et al., 2016
pYTK067	ConR1	*CmR*	Michael E. Lee, et al., 2017
pYTK095	*AmpR*-ColE1	*AmpR*	Michael E. Lee, et al., 2018
pMH032	type 2 plasmid containing partial coding sequence of *STE11*	*CmR*	This work
pMH033	type 3 plasmid containing *SAT1-FLP*	*CmR SAT1-FLP*	This work
pMH034	type 4 plasmid containing 3 prime UTR of *STE11*	*CmR*	This work
pMH035	cassette plasmid for replacement of *STE11* with *STE11-SAT1-FLP*	*AmpR SAT1-FLP*	This work
pMH036	cassette plasmid for replacement of *STE11* with *STE11*(T554I)-*SAT1-FLP*	*AmpR SAT1-FLP*	This work

Table 9. Continued

Plasmid ID	Description	Markers	Source
pMH037	cassette plasmid for replacement of *STE11* with *STE11*(P256T)-*SAT1-FLP*	*AmpR SAT1-FLP*	This work
pMH038	cassette plasmid for replacement of *STE11* with *STE11*(P256S)-*SAT1-FLP*	*AmpR SAT1-FLP*	This work
pMH041	type 2 plasmid containing partial coding sequence of *STE11*(T554I)	*CmR*	This work
pMH042	type 2 plasmid containing partial coding sequence of *STE11*(P256T)	*CmR*	This work
pMH043	type 2 plasmid containing partial coding sequence of *STE11*(P256S)	*CmR*	This work

4.2.2. Introduction of identified mutations in CAGL0B02739g

Introduction of the identified mutations in CAGL0B02739g from all three evolving populations (T1~T3) in KK-CA-24 was performed as follows: 1st part of partial coding sequences containing the desired mutations of the CAGL0B02739g were amplified from the gDNA of T1-27G, T2-5G, and T3-24Y with primer pair of TE9_F and TE9_R. The 2nd part (~367 bp) was synthesized as a gBlock DNA fragments (Integrated DNA Technologies, Inc) to remove the BsaI site by a single nucleotide substitution without causing the amino acid change; and was joined to the 1st part by overlapping PCR using the primer pair of TE9_F and TE10_R. The partial coding sequence of their wild-type version was constructed in a similar way using the gDNA of KK-CA-24 as the template with the same primer pairs as well. 3 prime untranslated region (3UTR) of CAGL0B02739g was amplified from the gDNA of KK-CA-24 with

the primer pair of TE11_F and TE11_R. In addition, the *SAT1-FLP* cassette was amplified from the plasmid yEP352-*SAT1* with the primer pair of TE12_F and TE12_R. These DNA fragments were all first cloned into the plasmid pYTK001 to create a new set of part plasmids (pMH032~pMH034, and pMH041~ pMH043); and then were assembled with fragments from pYTK002, pYTK067, and pYTK095 to construct four cassette plasmids (pMH035~pMH038) that contain the replacement cassettes for CAGL0B02739g (both wild-type and mutant from population T1~T3). These plasmid constructions follow a MoClo-derived assembly by Michael E. Lee, *et al.* (70). The replacement cassettes were then cut from the cassette plasmids by BsmbI (Thermo scientific) and integrated into the genome of KK-CA-24 using the Easy Frozen-EZ Yeast Transformation II Kit (Zymo Research) according to the manufacturer's protocol. The loop out of the *SAT1-FLP* cassettes were induced by growing the resulting transformants in YPD medium and verified by both colony PCR and DNA sequencing. The DNA fragments of part plasmids for construction of the cassette plasmids and the mutations in the CAGL0B02739g were verified by Sanger sequencing and analyzed with Unipro UGENE.

4.2.3. Adaptive evolution of *C. glabrata* to hyper-thermal stress

Founding populations consist of approximately equal number of cells labeled by green fluorescent protein (GFP) and yellow fluorescent protein (YFP); and they were cultured in 25 ml of growth medium in flasks in a shaking water bath at 30°C. The populations were transferred daily and periodically heat-challenged following a two-phase strategy (**figure 3**). During the phase 1 (P1), 1 ml of cell culture after 24-hour

growth was challenged by hyperthermal stress for 30 minutes, which was followed by inoculation into 24 ml of fresh growth medium for overnight growth. In the phase 2 (P2), 250 μl of the overnight culture from the P1 phase was transferred into 24.75 ml of growth medium; and the cells were grown for 24 hours so that they can recover from the heat challenge. These two phases were repeated until the end of the evolution. During the evolution, the OD_{600} of the populations were measured by sampling cells before and right after each transfer. Frozen stocks of the evolving populations sampled right before each stress challenge were made for further characterizations and storage. When the OD_{600} significantly increased, thermo-tolerance of the evolving populations was measured using a modified method of the general stress tolerance to check if any improvements. Briefly, the cells of the populations were challenged by a temperature gradient from the current selective level to 2°C above for 30 minutes and other steps are the same. The selective stress (temperature) was ramped up to the new level that gave at least 10-fold reduction in the biomass as compared to the heat-free control. The relative proportions of the two subpopulations (GFP and YFP) for stored samples of selected evolving populations were measured using a FACScan flow cytometer (BD Biosciences, San Jose, CA). The isolation of the adaptive mutant for a given population sample was performed as follows: At least 8 colonies from a given population sample were isolated for analysis. Their thermo-tolerance was estimated using the same method as describe in the general stress tolerance and the one with the highest thermo-tolerance was selected as the adaptive mutant. The adaptive mutants were named based on the population samples from which they were isolated and the color of fluorescent protein expressed.

For example, mutant T2-5G was isolated from the GFP subpopulation of population sample T2-5.

4.2.4. Survival rate after stress challenge

The thermo-tolerance of our mutants and population samples was quantified in terms of its survival rate after challenged by 47°C and temperatures to which our samples exposed in the evolution for 1 hour. The test subjects were grown to an OD_{600} between 2.0~3.0 in culture medium at 30°C; and their OD_{600}s were measured and normalized to about 0.5 before the heat challenge using a spectrophotometer (Thermo Scientific inc., MA, United States). Then, 500 µl of the normalized samples were challenged by hyperthermal stress for 1 hour in a shaker; cells in the control group were incubated at 30°C for 1 hour in a shaker. After the challenge, the cells (both control and heat-challenged group) were placed on ice for 5 minute to cool down the temperature and then subjected to serial 10-fold dilutions using culture medium; and the 10000-fold diluted cells were plated on YNB plates and incubated the plates at 30C for two days before counting the colony formation units (CFUs). The survival rate was the ratio of the CFUs of heat-challenged cells to CFUs of the control group; and the average mean of at least three biological replicates of each sample was used for comparison.

4.2.5. Characterizations of general stress tolerance

The stress tolerance of our mutants and samples was characterized using following steps: Cells were grown to an OD_{600} between 2.0~3.0 in culture medium at 30°C; and the OD_{600} was measured and normalized to about 0.5 for heat and 1.0 for other stresses before the challenge using a spectrophotometer (Thermo Scientific inc.,

MA, United States). 500 µl of normalized samples were then challenged by stresses of interest for 1 hour in a shaker. For the control group, cells were incubated in the absence of the stresses for 1 hour at 30°C in a shaker. The stresses of our choice include 4% (v/v) isobutanol, 4% (v/v) 1-butanol, 16% (v/v) ethanol, 0.2M of HCl, 0.2M of acetic acid, 100 mM of H_2O_2, and heat at 50°C. For stresses other than heat, the cells (both control and stress-challenged group) were pelleted after the challenge to remove the supernatant and subjected to serial 10-fold dilutions using culture medium. For heat, the cells (both control and heat-shocked group) were placed on ice for 5 minutes to cool down the temperature after the challenge and subjected to serial 10-fold dilutions using culture medium. 5 µl of diluted cells (10-fold, 10^2-fold, 10^3-fold, and 10^4-fold) were spotted on YNB agar medium supplemented with 2% dextrose and incubated at 30°C for two days. The images of the cell growth on the solid medium after 2-day incubation were taken for further analysis.

4.2.6. Plate dilution with Radicicol

The impacts of HSP90 on the thermo-tolerance of our adaptive mutants, along with parental strains, were studied using the radicicol. Radicicol functions as an inhibitor of HSP90 (112) and we dissolved the radicicol in DMSO to make the stock solution (~2 mg/ml). We characterized the tolerance of our C. glabrata strains to radicicol as follows: Cells were grown to an OD_{600} between 2.0~3.0 in culture medium at 30°C; and the OD_{600} was measured and normalized to about 0.5 using a spectrophotometer (Thermo Scientific inc., MA, United States). The normalized cells were then subjected to serial 10-fold dilutions using culture medium. 5 µl of diluted cells (10-fold, 10^2-fold, 10^3-fold,

and 10^4-fold) were spotted on YNB agar medium supplemented with 2% (w/v) dextrose and 5 μM of radicicol; and for the control group, the diluted cells (10-fold, 10^2-fold, 10^3-fold, and 10^4-fold) were spotted on YNB agar medium supplemented with 2% (w/v) dextrose and YNB agar medium supplemented with 2% (w/v) dextrose and DMSO (~0.09%(v/v)). These plates (both experimental subjects and control group) were incubated at 30°C and 41°C for two days. The images of the cell growth on the solid medium after 2-day incubation were taken for further analysis.

4.2.7. Genome sequencing

The adaptive clones, T1-27G, T2-5G, T2-10G, T2-17G, T2-27G, and T3-24Y, from population T1~T3 and the two unevolved parental strains, KKY and KKG, were sequenced to identify the genotypes underlying the observed thermo-tolerance. Genomic library preparation and sequencing were performed by the Texas A&M Genomics Center for sequencing on the Illumina HiSeq 2500 platform using 100-bp pair-end reads. An average coverage of more than 32-fold was obtained for each clone. Reads were assembled against the CBS138 reference genome, and each mutant genome was compared to the parental sequences to identify any de novo mutations using the CLC Genomics workbench (version 6.0.1). For the variants calling, the frequency threshold was set to be 90% and the forward/reverse balance was set ≥ 0.3. Otherwise, the default setting was used for the CLC Genomics workbench. Selected mutations were verified with Sanger sequencing and analyzed with Unipro UGENE.

4.2.8. Bioinformatics analysis

The tools of GO term analysis from Candida Genome Database (CGD) (23) was used to determine if any significantly biological processes and functional categories is enriched for the mutated genes that were identified across all adaptive mutants. Since most of the genes in *C. glabrata* haven't been well-characterized, their functions were inferred according to their *S. cerevisiae* orthologs using the information from the Saccharomyces Genome Database (SGD)(76).

4.3. Results

4.3.1. Adaptive evolution of *C. glabrata* in periodic heat shock treatment

Three parallel populations (T1~T3) were evolved in YNB medium at 30°C via serial batch transfers. Visualizing evolution in real-time (VERT) (17) was used to track the population dynamics during evolution using two otherwise isogenic strains that are labeled with either yellow fluorescent protein (YFP) or green fluorescent protein (GFP). An adaptive evolutionary strategy using periodic challenge at high temperatures (≥47°C) was employed (**see figure 3 and Materials and Methods for details**). A control population (TC) which was serially transferred at 30°C in the absence of periodic challenge at high temperature was included. All populations were cultured for more than 180 generations and their optical densities at 600 nm (OD_{600}) were measured prior to the transfer after each stress challenge (the end of phase 1), which exhibited a significant increase over the course of evolution (**figure 12**). Thermo-tolerance of populations was determined (**see Materials and Methods for details**) when a significant increase in cell densities was observed after the heat challenge in the

evolution, at the end of Phase 1 in each cycle (**figure 3**), and the selective pressure (temperature) was ramped up accordingly. For the adaptive evolution, the stress was ramped up from 47°C at the beginning to 50°C at the end.

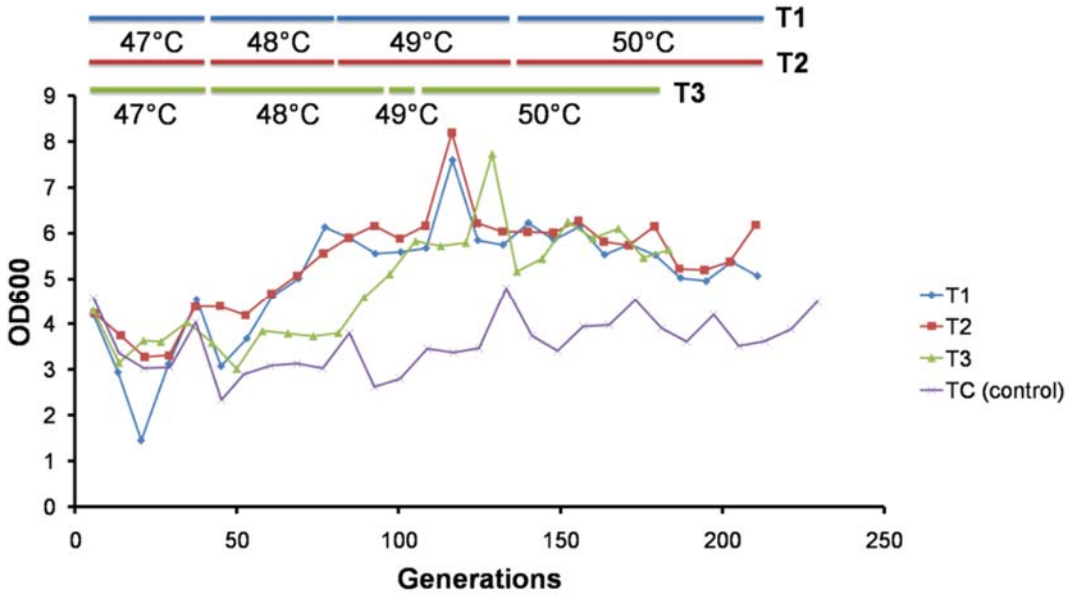

Figure 12. The dynamics of the population cell density (OD_{600}) in response to periodic heat shock. Temperatures used in the heat shock during the evolution were specified by the colored bars (blue for T1 and T2, orange for T3) on the top. The population, TC, in control group for the adaptive evolution was transferred similarly in the absence of the exposure to the stress.

All parallel populations gained significantly improved thermo-tolerance to heat challenge through the adaptive evolution (**figure 13**). The sample with the highest thermo-tolerance, T2-27, came from the population T2, which has an average viability of ~37% after heat shock at 50°C for 1 hour. In contrast, the average viability of the founding strains, KKY and KKG, is about 0.35% after challenged at a much lower

temperature (47°C) for 1 hour. Given on the source of the T2-27, we selected population T2 for further studies. The population dynamics of T2 was estimated with VERT by quantifying the relative proportions of GFP and YFP colored subpopulations (**figure 14**). Surprisingly, we observed a rapid increase in the proportion of the GFP colored subpopulation from the early state of the evolution (~generation 6) and then swept the entire population shortly, which indicates occurrence of adaptive mutations with significant fitness advantages in thermo-tolerance in the GFP subpopulation. Tracking the optical densities (OD) at the population level fails to capture the adaptive event (occurrence of adaptive mutations) in the same time period, suggesting that the VERT is more sensitive. However, the dynamics of the population OD can overcome a drawback of the VERT, that is, the loss of use when one colored subpopulation swept the entire population. The observation of continuously increased population OD (from generation 53 to 93) after the end of the expansion of GFP subpopulation size is a good example, suggesting other mutations continue to drive the adaptation of T2 population to the thermo-tolerance.

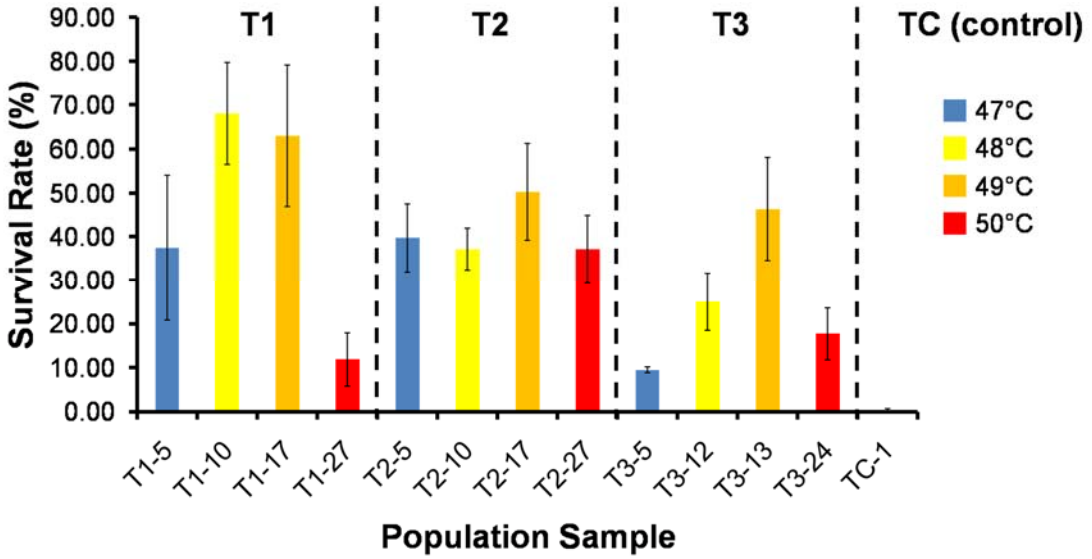

Figure 13. The survival rates of evolved populations after 1-hr heat shock treatments at specified temperatures. The colored bars represent the mean values of the survival rates based on three biological replicates.

4.3.2. Cross-tolerance acquired by mutants evolved under the hyper-thermal stress

Time course samples from population T2 and the last samples from the other two population, T1 and T3, were selected for further phenotypic characterizations. Adaptive mutants T2-5G, T2-10G, T2-17G, and T2-27G were isolated from time points immediately prior to each ramp-up in selective pressure, from populations T2-5, T2-10, T2-17, and T2-27, respectively (**figure 14**). The two adaptive mutants, T1-27G and T3-24Y, were isolated from the last sample of population T1 and T3 respectively. Each adaptive mutant was analyzed for its tolerance (survival) to 1-hour heat challenge at the temperature to which they were exposed during the evolution (**figure 15**). We observed significant increases in the viability after the heat challenge for the adaptive mutants as compared to the two parental strains, KKY and KKG. The highest viability after heat

shock at 50°C among the mutants was observed in T3-24Y, which has an average survival rate of about 74%. In contrast, the two parental strains have a survival rate of about 0.2% after heat challenge at 47°C for 1 hour. In addition, we also compared the viability of the mutants as well as the two parental strains after challenged at 47°C for 1 hour (**figure 16**); and found that all of the mutants have a much higher survival rate as compared to the parental strains.

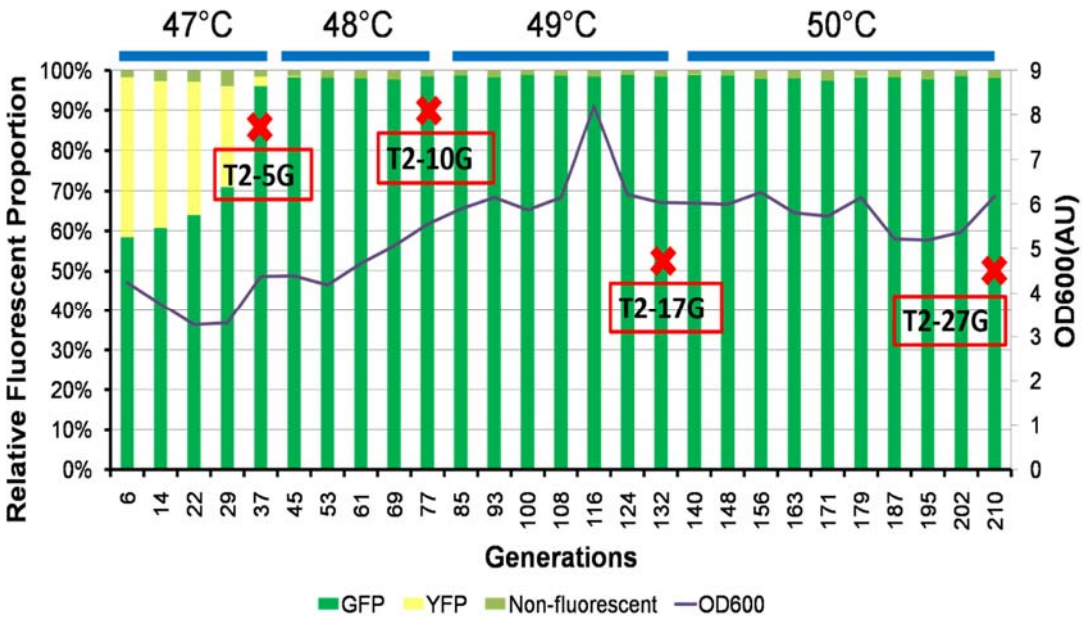

Figure 14. Population dynamics of T2 during the evolution under the inhibition of thermal stress. The colored bars represent the relative fluorescent proportions of green fluorescent subpopulation (dark green), yellow fluorescent subpopulation (yellow), and non-fluorescent subpopulation (light green) and the purple line represents the optical densities of the populations measured at 600 nm. The temperatures used in the 30-minute-heat-shock treatment during the evolution were shown on the top. The isolated adaptive mutants were highlighted in red box; and the red crosses indicated the time points when they were isolated and the subpopulations from which they were isolated.

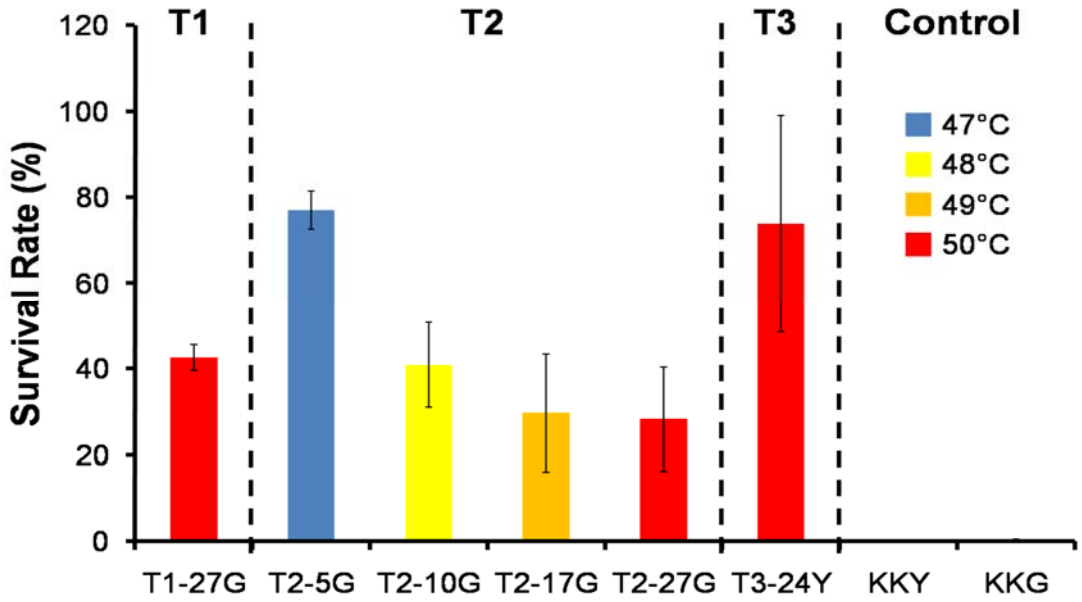

Figure 15. The survival rates of adaptive mutants and starting strains (KKY and KKG) after 1-hr heat shock treatments at specified temperatures. The colored bars represent the mean values of the survival rates based on three biological replicates.

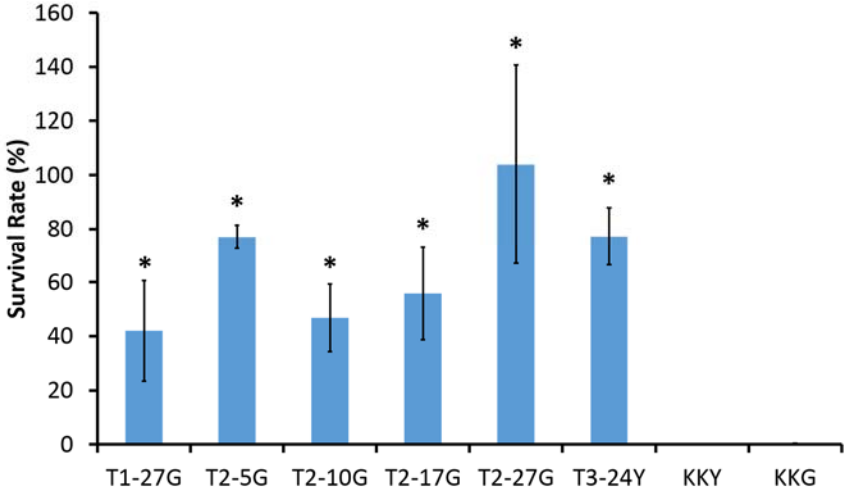

Figure 16. The survival rates of adaptive mutants and starting strains (KKY and KKG) after 1-hr heat shock treatments at 47°C. The bars represent the mean values of the survival rates based on three biological replicates. The asterisks indicate that the survival rates of adaptive mutants are statistically different from the parental strain, KKG ($P<0.05$, unpaired student t test with unequal variance).

Prior work in other species (*e.g. Escherichia coli*, *Salmonella typhimurium*, and *Corynebacterium glutamicum*) has shown that strains evolved under one stress can acquire cross-tolerance to other stresses (18-20). For example, researchers found that the evolved Corynebacterium glutamicum under the thermal stress has acquired cross-tolerance for isobutanol (20). In order to study the cross-tolerance behavior for our mutants, we performed shock assays using a wide variety of stresses (**table 10 and figure 17**), including oxidative stress (H_2O_2), acids (HCl and acetic acid), and solvents (ethanol, 1-butanol, iso-butanol). As compared to the parental strains, our mutants have acquired significantly improved tolerance to many of these stresses if not all. For some of the stresses (H_2O_2 and HCl), we observed that the cellular tolerance increases over the time in population T2 during the evolution. These results together suggested that the adaptation to thermal stress in *C. glabrata* may share some similar mechanisms with its adaptation to many other stresses, possibly by some key components in stress sensing, signal transduction, and stress response.

Table 10. Summary of the cross-tolerance for adaptive mutants

Strain ID	Oxidative Shock	Acid Shock		Solvent Shock		
	H_2O_2 (100 mM)	HCl (pH~1)	Acetic acid (pH~3)	EtOH (16%, v/v)	1-butanol (4%, v/v)	Isobutanol (4%, v/v)
T1-27G	++	++	++++	+++	+++	++++
T2-5G	N	+	+++	N	N	+++
T2-10G	++	+	+++	+	N	+++
T2-17G	++	++	+++	++	N	+++
T2-27G	+	++	++++	+++	N	+++
T3-24Y	+	++	+++	++	+	+++

Note: Cells in the test were challenged by stresses for 1 hour at 30°C in a shaker; N indicates not more resistant than parental strains; the more number of '+' a given strain has for a given stress challenge, the more tolerant to that stress as compared to the parental strains. Each '+" represents ~10 times more biomass as compared to parental strains after the stress challenge.

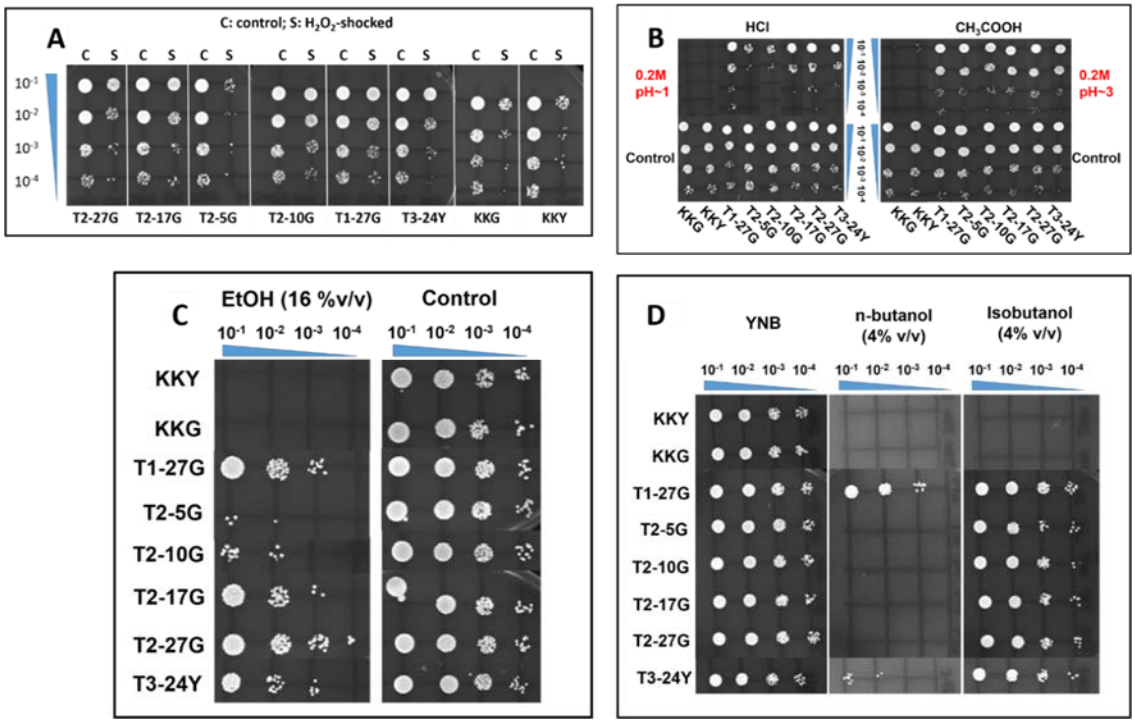

Figure 17. Tolerance to general environmental stresses for adaptive mutants. Cross-tolerance to H_2O_2 (A), HCl and acetic acid (B), ethanol (C), n-butanol and isobutanol (D) for adaptive mutants as well as the parental strains (KKY and KKG). Cross-tolerance was characterized after 1-hour exposure to given stresses and challenged cells after 10-fold serial dilutions were plated on YNB medium supplemented with 2% (w/v) dextrose at 30°C for two days.

4.3.3. HSP90 is required for innate and acquired thermo-tolerance in *C. glabrata*

In addition, it is well-established that the heat shock proteins (HSP) play a crucial role for cells to survive the stressed conditions and many of them are significantly induced by heat. To test if they would affect the thermo-tolerance of *C. glabrata*, we grew all adaptive mutants from the three parallel populations and the two parental strains (KKY and KKG) at different temperatures (30°C and 41°C) in the presence and absence of 5μM of radicicol (dissolved in DMSO), an inhibitor of HSP90, on YNB plates (**figure 18**). The control with cells growing on YNB agar medium supplemented with DMSO was also included to evaluate the effects of DMSO on the thermo-tolerance. As a result, we found that the radicicol didn't inhibit the growth of any test strain at normal growth temperature (30°C), but it completely inhibited the growth of all strains at 41°C. In contrast, all strains grew well at 41°C in the absence of the radicicol. These results showed that HSP90 is required for the thermo-tolerance in *C. glabrata* and the adaptation to the thermal stress in our mutants is HSP90-dependent.

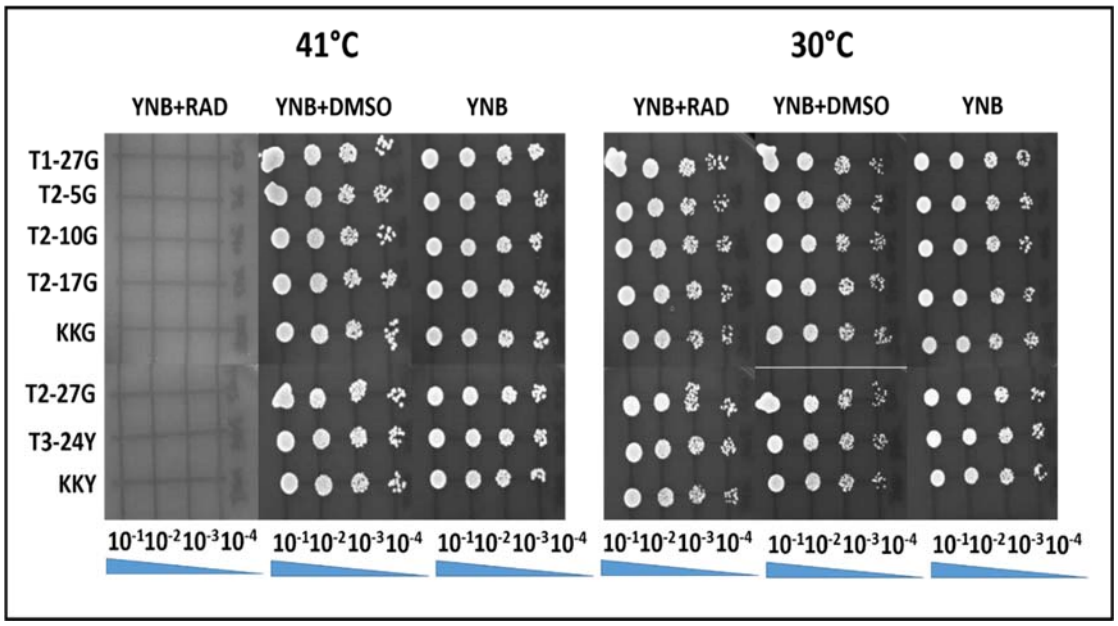

Figure 18. The effects of Radicicol (RAD) on the thermo-tolerance of adaptive mutants as well as the parental strains (KKY and KKG). The cells were grown on YNB plates supplemented with 2% (w/v) dextrose in the presence and absence of 5 μM of RAD at both 30°C and 41°C. Cells after 10-fold serial dilutions were spotted on the plates.

4.3.4. Potential beneficial mutations revealed by next-generation sequencing

We sequenced all six adaptive mutants that were isolated from population T1~T3; and found 20 mutations from these mutants in total (**table 11**). Among these mutations, there are four which was identified across more than one adaptive mutant; and the three of the four are present in two pseudogenes (CAGL0F00110g and CAGL0B05093g). The rest is present in all four adaptive mutants that were isolated from the population T2 and the affected gene CAGL0B02739g encodes a mitogen activated protein kinase kinase kinase(MAPKKK/MEKK) Ste11, which is reported to function in hypertonic stress response, filamentous growth, and virulence in *C. glabrata* (21). Interestingly, we also found mutations in CAGL0B02739g in other two adaptive

mutants from population T1 and T3; the mutation in the T3-24Y from population T3 occurred at the same position as those identified in mutants from population T2, but caused a different amino acid change; the mutation in T1-27G from population T1 is far away from those in population T2 and T3. Population sequencing of time-course samples from T1~T3 (data not shown) revealed that the frequency of these mutations in the populations increased significantly over time and they all fixed at the end of the evolution experiments. Taken together, these evidence plus previous phenotypic characterizations strongly suggested that CAGL0B02739g play an important role in the adaptation of *C. glabrata* to general stresses (heat, oxidative stress, acids, and solvents) and the underlying adaptive mechanisms may be similar to these stresses.

Table 11. The list of mutations identified in all adaptive mutants isolated from population T1~T3 by next-generation sequencing

SID	Gene[a]	Amino acid change	Non-synonymous	nearby gene ID[b]
T1-27G	CAGL0M11748g	Met188Ile	Yes	NA
T3-24Y	NA	NA	-	CAGL0L09955g(WU); CAGL0L09933g(WD);
T3-24Y	CAGL0G08602g	Pro732fs	Yes	NA
T2-10G	NA	NA	-	CAGL0I07843g(CD); CAGL0I07865g(WU);
T1-27G	CAGL0D06732g-T	Phe623fs	Yes	NA
T2-17G	CAGL0H06567g	Pro544Gln	Yes	NA
T3-24Y	CAGL0H06281g	Lys244fs	Yes	NA
T1-27G	CAGL0M05709g	Gln185Pro	Yes	NA
T2-27G	CAGL0C05599g	Glu531*	Yes	NA
T3-24Y	CAGL0B05093g-T, CAGL0B05148g	[Ser992Asn]	Yes	NA
T2-5G	CAGL0B05093g-T	Pro559fs	Yes	NA
T2-17G	CAGL0B05093g-T	Pro559fs	Yes	NA
T2-27G	CAGL0B05093g-T	Pro559fs	Yes	NA
T2-10G	CAGL0B05093g-T	*260Tyr	Yes	NA
T2-27G	CAGL0F03311g	Lys683*	Yes	NA

Table 11. Continued

SID	Gene[a]	Amino acid change	Non-synonymous	nearby gene ID[b]
T2-5G	CAGL0B02739g	Pro256Thr	Yes	NA
T2-10G	CAGL0B02739g	Pro256Thr	Yes	NA
T2-17G	CAGL0B02739g	Pro256Thr	Yes	NA
T2-27G	CAGL0B02739g	Pro256Thr	Yes	NA
T3-24Y	CAGL0B02739g	Pro256Ser	Yes	NA
T1-27G	CAGL0B02739g	Thr554Ile	Yes	NA
T2-17G	NA	NA	-	NA
T2-5G	CAGL0C01067g-T, CAGL0C01078g	[Ala5fs]	Yes	NA
T1-27G	CAGL0F00110g-T	Leu763Gln	Yes	NA
T2-10G	CAGL0F00110g-T	Leu763Gln	Yes	NA
T2-27G	CAGL0F00110g-T	Leu763Gln	Yes	NA
T3-24Y	CAGL0F00110g-T	Leu763Gln	Yes	NA
T1-27G	CAGL0F00110g-T	NA	No	NA
T2-10G	CAGL0F00110g-T	NA	No	NA
T2-17G	CAGL0F00110g-T	NA	No	NA
T2-27G	CAGL0F00110g-T	NA	No	NA
T3-24Y	CAGL0F00110g-T	NA	No	NA

a. the '-T' following the name of a gene indicates that the gene is a pseudogene; the '*' indicates a nonsense mutation;
b. the letters in the parenthesis following the gene ID describe the positions of identified mutations relative to the affected genes: W/C indicates the affected gene is in Watson strand/Crick strand; U/D indicates the mutations is in the upstream/downstream of the affected gene. For example, WU indicates that the affected gene is on Watson strand and the mutation is in its upstream.

Gene Ontology (GO) term analysis was used to identify if there is any enriched biological process or molecular function among the genes with mutations in the coding regions or in potential regulatory regions in the mutants. The result revealed that genes functioning in the osmosensory signaling pathway (CAGL0H06567g, CAGL0B02739g, and CAGL0M11748g) are significantly enriched with a p-value of ~0.0028, which suggests the involvement of the components of osmosensory signaling pathway in the adaptation to general stresses. Interestingly, the gene CAGL0B02739g plays a crucial

role in the osmosensory signaling in *C. glabrata*, which further supports its role in the mediation of general stress response. Since these mutated genes were not well-characterized in *C. glabrata*, I analyzed the functions of their *S. cerevisiae* orthologs (based on sequence similarities) to search for potential candidates contributing to the improved general stress tolerance in *C. glabrata*. In total, we found 9 candidates whose orthologs impact the tolerance to at least one of the stresses of our choice in *S. cerevisiae* (**table 12**). Surprisingly, we got five of them with either a non-sense mutation or a frame shift mutation (CAGL0C05599g, CAGL0D06732g, CAGL0F03311g, CAGL0G08602g, and CAGL0H06281g). If they share the similar functions as their *S. cerevisiae* orthologs, mutations for most of them except the CAGL0C05599g probably will impair the tolerance to corresponding stresses in *C. glabrata*. For CAGL0C05599g, it is predicted to be the ortholog of *S. cerevisiae LRG1*, which is reported to increase the thermo-tolerance and acetic acid when nullified (22, 23). Thus, its non-sense mutation in T2-27G could be responsible for the improved tolerance to thermal stress and acetic acid in this mutant. Moreover, we got 2 (CAGL0M05709g and CAGL0M11748g) of the 9 candidates with amino acid change in their coding sequences. The *S. cerevisiae* ortholog of CAGL0M05709g, *SGF73*, is reported to impact the resistance to H_2O_2 and ethanol (24, 25) and the *S. cerevisiae* ortholog of CAGL0M11748g, *HOG1*, is reported to impact the resistance to boric acid and H_2O_2 (24, 26). Together, we identified many potential candidates that could be responsible for improved stress tolerance and requires further studies.

Table 12. Phenotypic annotation of affected genes in adaptive mutants whose ortholog in yeast impact environmental stress tolerance

Gene	Ortholog[a]	Phenotype[b]
CAGL0C05599g	*LRG1*	increased tolerance to heat and acetic acid when nullified; "Jarolim S, et al. (2013)"; "Ding J, et al. (2013)"
CAGL0D06732g	*FLO1*	decreased tolerance to ethanol when nullified; "Smukalla S, et al. (2008)";
CAGL0F03311g	*KSP1*	decreased tolerance to H2O2 when nullified; "Brown JA, et al. (2006)";
CAGL0G08602g	*RPI1*	decreased tolerance to propionic acid, heat, and H2O2 when nullified; "Mira NP, et al. (2009)"; "Jarolim S, et al. (2013)"; "Brown JA, et al. (2006)"
CAGL0H06281g	*TPD3*	decreased tolerance to HCl, H2O2, acetic acid, and ethanol when nullified; "Banuelos MG, et al. (2010) "; "Outten CE, et al. (2005) "; "Kawahata M, et al. (2006) "; "Auesukaree C, et al. (2009) "
CAGL0I07843g	*ADH1*	increased tolerance to heat when nullified; "Jarolim S, et al. (2013)"
CAGL0L09955g	*WHI2*	decreased tolerance to propionic acid, heat, H2O2, and ethanol when nullified; "Mira NP, et al. (2009)"; "Jarolim S, et al. (2013)"; "Brown JA, et al. (2006)"; "Teixeira MC, et al. (2009)"
CAGL0M05709g	*SGF73*	decreased tolerance to H2O2 and ethanol when nullified; "Brown JA, et al. (2006)"; "Teixeira MC, et al. (2009)"
CAGL0M11748g	*HOG1*	decreased tolerance to boric acid and H2O2 when nullified; "Schmidt M, et al. (2012)"; "Pascual-Ahuir A and Proft M (2007)"; "Brown JA, et al. (2006)"

a. *S. cerevisiae* orthologs for given genes were inferred based on sequence similarities if not characterized;
b. Phenotypes of affected *C. glabrata* genes were inferred from their yeast orthologs.

4.3.5. Mutations in CAGL0B02739g contribute to the improved general stress tolerance

Given on the challenges of molecular cloning in *C. glabrata* (*e.g.* limited selective markers, and dominant non-homologous end joining over homologous recombination) (27), we selected only a few candidate mutations for reconstruction in our wild-type background (KK-CA-24) using a strategy based on a MoClo-derived assembly (**see materials and methods for details**) (13). Mutations identified in CAGL0B02739g from all three parallel populations (T1~T3), namely, C1661T (T1 mut), C766A (T2 mut), and C766T (T3 mut), were chosen due to the prevalence of

mutated CAGL0B02739g in parallel populations and the role of the gene in osmosensory signaling pathway whose components were significantly enriched in the GO term analysis. We successfully introduced the three aforementioned mutations in KK-CA-24; and each of the resulting strains, sMH081~sMH083, carries a mutated CAGL0B02739g from population T1~T3 respectively with a scar of about 109 bp that was left after the loop out of our selective marker. Since the scar that was left between the coding sequence of CAGL0B02739g and its 3 prime UTR could potentially impact the expression of the gene (28), we also introduced the wild-type CAGL0B02739g from KK-CA-24 to create strain sMH80 in the same way to assay the phenotypic effects of the altered structure of the 3 prime UTR due to the presence of the FRT scar. These strains (sMH080~sMH083) with the KK-CA-24 were challenged by stresses that were used for adaptive mutants before; and the results (**figure 19**) showed that strains with mutated CAGL0B02739g all have acquired significantly improved tolerance to many stresses, including heat, hydrogen peroxide, ethanol, acetic acid, and others, as compared to both KK-CA-24 and sMH080. In addition, there is no significant difference in the tolerance to these stresses between the KK-CA-24 and sMH080. These results suggested that the acquisition of cross-tolerance to various stresses in our adaptive mutants is in large part attributed to the mutations in CAGL0B02739g.

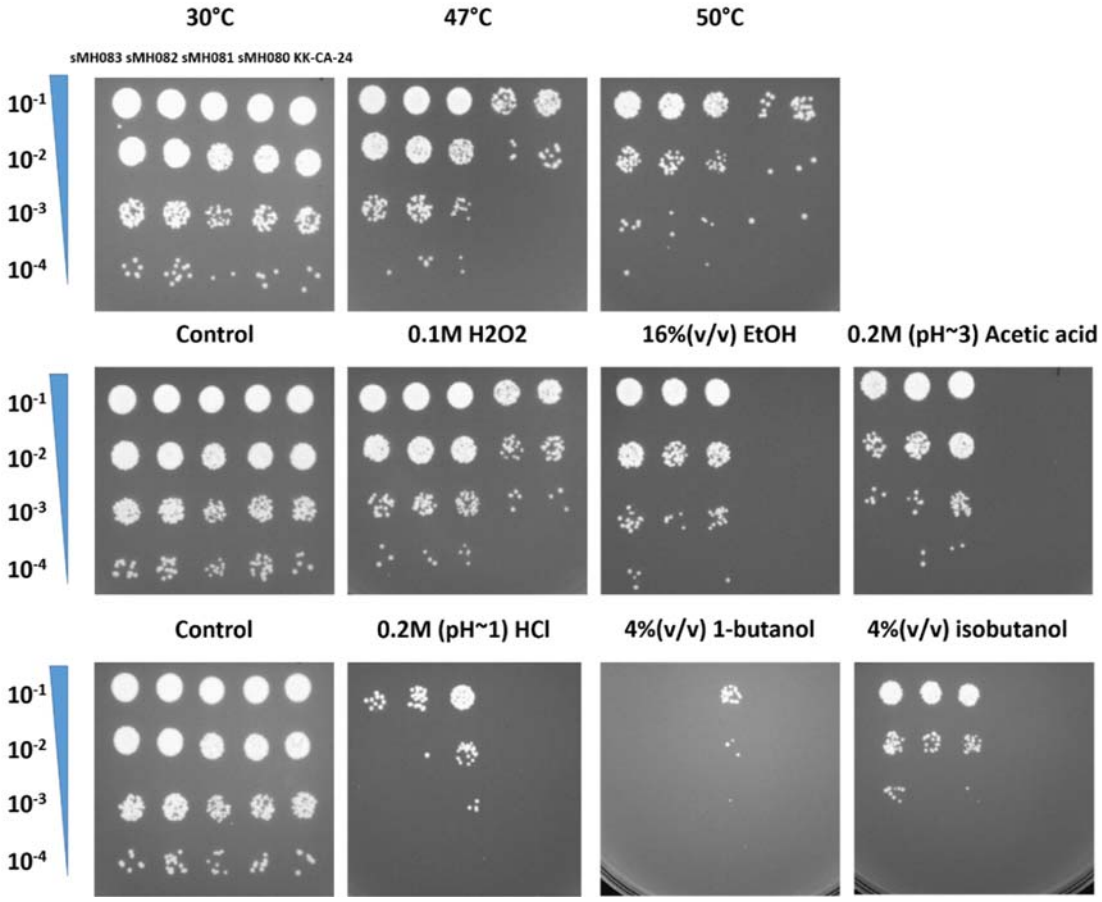

Figure 19. The general stress tolerance characterized for strains introduced with three identified ste11 mutations by 1-hr shock assays.

4.4. Discussion

We have shown that all three identified mutations in the CAGL0B02739g (ortholog of *S. cerevisiae STE11*) of our mutants contribute to the cross-tolerance to a wide range of different stresses. This observation showed that in *C. glabrata* the CAGL0B02739g may play a key role in cellular response to general environmental stresses. Previously, the functional analysis of the *C. glabrata* ste11 null mutant demonstrated that *STE11* is required for tolerance to hyperosmotic stress, filamentation

induced by nitrogen starvation, and virulence (113). In addition, the absence of the CAGL0B02739g in the ATCC2001 background seems to be dispensable for the maintenance of the cell wall integrity, since the null mutant is no more sensitive to the cell-wall perturbing agents, such as SDS and calcofluor white, as compared to the wild-type (113). Interestingly, we didn't observe improved tolerance to common osmotic agents, including NaCl and Sorbitol (data not shown), in our adaptive mutants whose *STE11* are mutated. Given on the role of CAGL0B02739g in signaling transduction, our data suggests that it may function differently in response to osmotic stress from other stresses (*e.g.* thermal stress, oxidative stress, solvents, and acids).

Little information is available on the roles of the CAGL0B02739g in cellular response to other stresses. There is one report showing that the *SHO1* branch of High-Osmolarity Glycerol (HOG) signaling in *C. glabrata* influences the cellular tolerance to high temperature and weak organic acids (36). The CAGL0B02739g is assumed to be a key component in the *SHO1* branch of HOG signaling based on its ability to partially complement the loss of *STE11* in the model yeast *S. cerevisiae* (113). Thus, it is very likely that CAGL0B02739g functions in the modulation of the thermo-tolerance and weak acid tolerance. In agreement with this idea, our experimental data showed that the mutations in CAGL0B02739g significantly improved the tolerance of *C. glabrata* to thermal stress and weak organic acids, such as acetic acid. These evidence suggested that the mutated CAGL0B02739g may improve the stress tolerance, at least to thermal stress and weak acids, by increasing the activity of HOG signaling in *C. glabrata*.

In response to various environmental stresses, the cross talk between different signaling cascades in fungi is necessary to coordinate the regulation of the gene expression to survive in the suboptimal or hostile conditions, especially when stress level exceeds the capacity of a single signaling cascade (114, 115). Much of our knowledge for fungal signaling cascades came from the studies on the model yeast *S. cerevisiae*. One of the well-characterized MAPK signaling cascades that are activated by various stresses is the cell wall integrity (CWI) pathway, which orchestrates the cell wall biosynthesis, actin organization, and other necessary events to withstand various stresses, including thermal, osmotic, and oxidative stress (116). More and more evidence from recent studies showed that *STE11* play a critical role in the cross talk between the CWI pathway and the HOG pathway in *S. cerevisiae* to endure the environmental stresses, such as oxidative and thermal stress (32, 117). Gang Leng and Kiwon Song found that the Ste11 interacts with Mkk1/2 through the Nst1 to connect the HOG and pheromone pathways to CWI pathway in response to heat and pheromone (117). In addition, Chunyan Jin et al. have shown that in *S. cerevisiae* the Ste11 may activate the Mkk1/2 and thus the Slt2 and Kdx1, which results in the nuclear release and subsequent destruction of the repressor cyclin C in response to high levels of oxidative stress to promote stress-responsive gene expression (32). Consistent with these reports, our data showed that mutations in the CAGL0B02739g (ortholog of *ScSTE11* in *C. glabrata*) conferred improved tolerance to both oxidative stress and thermal stress. Although differences exist, most of the components from the HOG and CWI pathway are conserved among fungi. Given on the high level of stresses that were used to challenge

our mutants, it could be expected that the cross talk between multiple signaling cascades, such as HOG and CWI pathways, may involve in the adaptation of our mutants to these stresses. Hypothetical translation of many of these putative signaling proteins in HOG and CWI pathways in *C. glabrata* (*e.g.* Ste11 (64% identity, 77% similarity), Mkk1 (58% identity, 67% similarity), Mkk2 (68% identity, 81% similarity), Nst1 (77%identity, 90%similarity), Slt2 (77%identity, 84%similarity)) showed that they have both high similarity and identity at the amino acid level to their *S. cerevisiae* orthologs, and thus it is very interesting to see whether their relationships observed in the yeast are conserved in *C. glabrata* as well.

In addition to signaling components, heat shock proteins (HSP) play a crucial role for cells to survive the stressed conditions, which function in the promotion of protein folding, prevention of protein aggregation, degradation and repair of damaged proteins. HSP90 family is one of predominant groups of HSPs in yeast and its members are abundant and well-conserved among eukaryotic cells (118). In *S. cerevisiae*, the HSPs family has two isomers, encoded by two genes *HSP82* and *HSC82*(119). Although to different extent, the expression of both two isomers of HSP90 are significantly induced in response to acute temperature upshift in *S. cerevisiae* (119). Researches on the HSP90 family have shown its role as an evolutionary capacitor to facilitate the evolutionary changes over a long timescale (120-123) and also a biological transistor to regulate activities of core signaling pathways in response to dynamic environmental conditions over a short timescale (118). Among the numerous proteins that interact with the members of HSP90 family are two kinases in MAPK signaling cascades, Ste11 and

Slt2 (124, 125). Hsp90 is reported to impact the kinase activity of the Ste11 in *S. cerevisiae* (124, 126). In addition, it has also been reported that appropriate post-translational modifications of HSP90 is necessary for its efficient chaperoning of the Ste11 and Slt2 (127). These evidence suggested that the chaperoning by HSP90 is important for *STE11* to function properly in signaling transduction to regulate appropriate cellular response to environmental stresses. Consistent with this idea, our data showed that both the parental strains and adaptive mutants with mutated CAGL0B02739g (ortholog of *S. cerevisiae STE11*) that gained improved thermotolerance are hypersensitive to the long-term high temperature exposure (41°C) in the presence of radicicol (5μM), an inhibitor to HSP90(112). Together, we postulated that the activity of the CAGL0B02739g depends on the chaperoning of the HSP90 in *C. glabrata* in a similar fashion to *S. cerevisiae*.

5. CONCLUSION

In our study, we combined the laboratory evolution and next-generation genome sequencing to study the adaptation of *C. glabrata* to two environmental stresses of both industrial and medical relevance, H_2O_2 and heat. For H_2O_2, we further studied the cellular response at the transcriptional level using the whole genome gene expression microarray. The combination of these technologies showed its power in identifications of various adaptive mechanisms to complex phenotypes.

Here, we focus on the gene-phenotype relationship in isolated adaptive clones and for the first time we showed the importance of several genes in *C. glabrata* that contribute to their tolerance and adaptation to thermal stress and oxidative stress (H_2O_2). For H_2O_2 stress, we identified a beneficial nonsense mutation in CAGL0E01243g and confirmed that it significantly improved the tolerance of *C. glabrata* to H_2O_2. For thermal stress, we identified three beneficial mutations in CAGL0B02739g and showed that they all significantly improved the thermo-tolerance of *C. glabrata*. Moreover, the three mutations resulted in cross-tolerance to various other environmental stresses. In addition, our studies also revealed that many other mutations that were not fully characterized in this studies may involve in the stress tolerance. For example, the nonsense mutation in CAGL0F06831g is very likely to contribute to the improved H_2O_2 tolerance as well.

In order to understand the mechanisms underlying the adaptation to H_2O_2, we performed the microarray analysis for both mutants and parental strains in the presence

of this stress and the data revealed that many potential mechanisms, including NADPH regeneration, modulation of membrane composition, cell wall remodeling and global regulatory changes. We postulated that the absence of functional products encoded by the mutated CAGL0E01243g may activate some or all of these mechanisms in response to the oxidative stress (H_2O_2). For strains evolved under the hyper-thermal stress, we further characterized the thermo-tolerance of our mutants in the absence of functional HSP90 members and found that the observed improved tolerance to heat depends on the HSP90. With these results, we postulated that the identified mutations in CAGL0B02739g may function with the help of HSP90 in multiple MAPK signaling transduction cascades to help cells to resist various environmental stresses. Follow-up studies are required to characterize the effects of these mutations on the transcriptome of *C. glabrata* in response to these stresses by either Microarray or RNAseq to fill in the details of the regulatory mechanisms. We believe what we gained here could benefit the understanding of the mechanisms underlying the rapid adaptation of *C. glabrata* to various environmental stresses.

REFERENCES

1. **Pfaller MA, Diekema DJ.** 2007. Epidemiology of invasive candidiasis: a persistent public health problem. Clin Microbiol Rev **20:**133-163.

2. **Pfaller MA, Diekema DJ, Gibbs DL, Newell VA, Ellis D, Tullio V, Rodloff A, Fu W, Ling TA.** 2010. Results from the ARTEMIS DISK Global Antifungal Surveillance Study, 1997 to 2007: a 10.5-year analysis of susceptibilities of Candida Species to fluconazole and voriconazole as determined by CLSI standardized disk diffusion. J Clin Microbiol **48:**1366-1377.

3. **Krcmery V, Barnes AJ.** 2002. Non-albicans *Candida spp*. causing fungaemia: pathogenicity and antifungal resistance. J Hosp Infect **50:**243-260.

4. **Pfaller MA, Messer SA, Bolmstrom A.** 1998. Evaluation of Etest for determining in vitro susceptibility of yeast isolates to amphotericin B. Diagn Microbiol Infect Dis **32:**223-227.

5. **Bennett JE, Izumikawa K, Marr KA.** 2004. Mechanism of increased fluconazole resistance in Candida glabrata during prophylaxis. Antimicrob Agents Chemother **48:**1773-1777.

6. **Redding SW, Kirkpatrick WR, Saville S, Coco BJ, White W, Fothergill A, Rinaldi M, Eng T, Patterson TF, Lopez-Ribot J.** 2003. Multiple patterns of resistance to fluconazole in Candida glabrata isolates from a patient with oropharyngeal candidiasis receiving head and neck radiation. J Clin Microbiol **41:**619-622.

7. **Sanglard D, Ischer F, Bille J.** 2001. Role of ATP-binding-cassette transporter genes in high-frequency acquisition of resistance to azole antifungals in Candida glabrata. Antimicrob Agents Chemother **45:**1174-1183.

8. **Ogoina D.** 2011. Fever, fever patterns and diseases called 'fever'--a review. J Infect Public Health **4:**108-124.

9. **Vieira OV, Botelho RJ, Grinstein S.** 2002. Phagosome maturation: aging gracefully. Biochem J **366:**689-704.

10. **Haas A.** 2007. The phagosome: compartment with a license to kill. Traffic **8:**311-330.

11. **Li Y, Chen J, Lun SY.** 2001. Biotechnological production of pyruvic acid. Appl Microbiol Biotechnol **57:**451-459.

12. **Yonehara T, Miyata R, Matsuno H, Goto M, Yahanda S.** 2000. Development of fermentative production of pyruvate by metabolic control - Monograph. Seibutsu-Kogaku Kais **78:**56-62.

13. **Li Y, Chen J, Lun SY, Rui XS.** 2001. Efficient pyruvate production by a multi-vitamin auxotroph of Torulopsis glabrata: key role and optimization of vitamin levels. Appl Microbiol Biotechnol **55:**680-685.

14. **Li Y, Hugenholtz J, Chen J, Lun SY.** 2002. Enhancement of pyruvate production by Torulopsis glabrata using a two-stage oxygen supply control strategy. Appl Microbiol Biotechnol **60:**101-106.

15. **Liu L, Li Y, Du G, Chen J.** 2006. Redirection of the NADH oxidation pathway in Torulopsis glabrata leads to an enhanced pyruvate production. Appl Microbiol Biotechnol **72:**377-385.

16. **Xu S, Zhou J, Qin Y, Liu L, Chen J.** 2010. Water-forming NADH oxidase protects Torulopsis glabrata against hyperosmotic stress. Yeast **27:**207-216.

17. **Liu L, Xu Q, Li Y, Shi Z, Zhu Y, Du G, Chen J.** 2007. Enhancement of pyruvate production by osmotic-tolerant mutant of Torulopsis glabrata. Biotechnol Bioeng **97:**825-832.

18. **Liu L, Li Y, Zhu Y, Du G, Chen J.** 2007. Redistribution of carbon flux in Torulopsis glabrata by altering vitamin and calcium level. Metab Eng **9:**21-29.

19. **Zhang D, Liang N, Shi Z, Liu L, Chen J, Du G.** 2009. Enhancement of α-ketoglutarate production in Torulopsis glabrata: redistribution of carbon flux from pyruvate to α-ketoglutarate. Biotechnol Bioproc E **14:**134-139.

20. **Chen X, Xu G, Xu N, Zou W, Zhu P, Liu L, Chen J.** 2013. Metabolic engineering of Torulopsis glabrata for malate production. Metab Eng **19:**10-16.

21. **Watanabe I, Nakamura T, Shima J.** 2008. A strategy to prevent the occurrence of Lactobacillus strains using lactate-tolerant yeast Candida glabrata in bioethanol production. J Ind Microbiol Biotechnol **35:**1117-1122.

22. **Watanabe I, Nakamura T, Shima J.** 2010. Strategy for simultaneous saccharification and fermentation using a respiratory-deficient mutant of Candida glabrata for bioethanol production. J Biosci Bioeng **110:**176-179.

23. **Skrzypek MS, Binkley J, Binkley G, Miyasato SR, Simison M, Sherlock G.** 2017. The Candida Genome Database (CGD): incorporation of Assembly 22, systematic identifiers and visualization of high throughput sequencing data. Nucleic Acids Res **45:**D592-D596.

24. **Pfaller MA, Diekema DJ, Rinaldi MG, Barnes R, Hu B, Veselov AV, Tiraboschi N, Nagy E, Gibbs DL.** 2005. Results from the ARTEMIS DISK Global Antifungal Surveillance Study: a 6.5-year analysis of susceptibilities of Candida and other yeast species to fluconazole and voriconazole by standardized disk diffusion testing. J Clin Microbiol **43:**5848-5859.

25. **Pfaller MA, Messer SA, Boyken L, Hollis RJ, Rice C, Tendolkar S, Diekema DJ.** 2004. In vitro activities of voriconazole, posaconazole, and fluconazole against 4,169 clinical isolates of *Candida spp*. and Cryptococcus neoformans collected during 2001 and 2002 in the ARTEMIS global antifungal surveillance program. Diagn Microbiol Infect Dis **48:**201-205.

26. **Pfaller MA, Boyken L, Hollis RJ, Messer SA, Tendolkar S, Diekema DJ.** 2005. In vitro susceptibilities of clinical isolates of Candida species, Cryptococcus neoformans, and Aspergillus species to itraconazole: global survey of 9,359 isolates tested by clinical and laboratory standards institute broth microdilution methods. J Clin Microbiol **43:**3807-3810.

27. **Ostrosky-Zeichner L, Rex JH, Pappas PG, Hamill RJ, Larsen RA, Horowitz HW, Powderly WG, Hyslop N, Kauffman CA, Cleary J, Mangino JE, Lee J.** 2003.

Antifungal susceptibility survey of 2,000 bloodstream Candida isolates in the United States. Antimicrob Agents Chemother **47:**3149-3154.

28. **Cuenca-Estrella M, Gomez-Lopez A, Mellado E, Buitrago MJ, Monzon A, Rodriguez-Tudela JL.** 2006. Head-to-head comparison of the activities of currently available antifungal agents against 3,378 Spanish clinical isolates of yeasts and filamentous fungi. Antimicrob Agents Chemother **50:**917-921.

29. **Li S, Chen X, Liu L, Chen J.** 2013. Pyruvate production in Candida glabrata: manipulation and optimization of physiological function. Crit Rev Biotechnol.

30. **Merico A, Sulo P, Piskur J, Compagno C.** 2007. Fermentative lifestyle in yeasts belonging to the Saccharomyces complex. FEBS J **274:**976-989.

31. **Chen RE, Thorner J.** 2007. Function and regulation in MAPK signaling pathways: lessons learned from the yeast Saccharomyces cerevisiae. Biochim Biophys Acta **1773:**1311-1340.

32. **Jin C, Kim SK, Willis SD, Cooper KF.** 2015. The MAPKKKs Ste11 and Bck1 jointly transduce the high oxidative stress signal through the cell wall integrity MAP kinase pathway. Microb Cell **2:**329-342.

33. **Liu S, Hou Y, Liu W, Lu C, Wang W, Sun S.** 2015. Components of the Calcium-Calcineurin Signaling Pathway in Fungal Cells and Their Potential as Antifungal Targets. Eukaryotic Cell **14:**324-334.

34. **Nikolaou E, Agrafioti I, Stumpf M, Quinn J, Stansfield I, Brown AJ.** 2009. Phylogenetic diversity of stress signalling pathways in fungi. BMC Evol Biol **9:**44.

35. **Maeda T, Takekawa M, Saito H.** 1995. Activation of yeast PBS2 MAPKK by MAPKKKs or by binding of an SH3-containing osmosensor. Science **269:**554-558.

36. **Gregori C, Schuller C, Roetzer A, Schwarzmuller T, Ammerer G, Kuchler K.** 2007. The high-osmolarity glycerol response pathway in the human fungal pathogen Candida glabrata strain ATCC 2001 lacks a signaling branch that operates in baker's yeast. Eukaryot Cell **6:**1635-1645.

37. **Jandric Z, Schuller C.** 2011. Stress response in Candida glabrata: pieces of a fragmented picture. Future Microbiol **6:**1475-1484.

38. **Muller H, Hennequin C, Gallaud J, Dujon B, Fairhead C.** 2008. The asexual yeast Candida glabrata maintains distinct a and alpha haploid mating types. Eukaryot Cell **7:**848-858.

39. **Butler G.** 2010. Fungal sex and pathogenesis. Clin Microbiol Rev **23:**140-159.

40. **Wong S, Fares MA, Zimmermann W, Butler G, Wolfe KH.** 2003. Evidence from comparative genomics for a complete sexual cycle in the 'asexual' pathogenic yeast Candida glabrata. Genome Biol **4:**R10.

41. **Calcagno AM, Bignell E, Rogers TR, Canedo M, Muhlschlegel FA, Haynes K.** 2004. Candida glabrata Ste20 is involved in maintaining cell wall integrity and adaptation to hypertonic stress, and is required for wild-type levels of virulence. Yeast **21:**557-568.

42. **Chen YL, Konieczka JH, Springer DJ, Bowen SE, Zhang J, Silao FG, Bungay AA, Bigol UG, Nicolas MG, Abraham SN, Thompson DA, Regev A,**

Heitman J. 2012. Convergent Evolution of Calcineurin Pathway Roles in Thermotolerance and Virulence in Candida glabrata. G3 (Bethesda) **2:**675-691.

43. **Cuellar-Cruz M, Briones-Martin-del-Campo M, Canas-Villamar I, Montalvo-Arredondo J, Riego-Ruiz L, Castano I, De Las Penas A.** 2008. High resistance to oxidative stress in the fungal pathogen Candida glabrata is mediated by a single catalase, Cta1p, and is controlled by the transcription factors Yap1p, Skn7p, Msn2p, and Msn4p. Eukaryot Cell **7:**814-825.

44. **Saijo T, Miyazaki T, Izumikawa K, Mihara T, Takazono T, Kosai K, Imamura Y, Seki M, Kakeya H, Yamamoto Y, Yanagihara K, Kohno S.** 2010. Skn7p is involved in oxidative stress response and virulence of Candida glabrata. Mycopathologia **169:**81-90.

45. **Gulshan K, Lee SS, Moye-Rowley WS.** 2011. Differential oxidant tolerance determined by the key transcription factor Yap1 is controlled by levels of the Yap1-binding protein, Ybp1. J Biol Chem **286:**34071-34081.

46. **Shahsavarani H, Sugiyama M, Kaneko Y, Chuenchit B, Harashima S.** 2012. Superior thermotolerance of Saccharomyces cerevisiae for efficient bioethanol fermentation can be achieved by overexpression of RSP5 ubiquitin ligase. Biotechnol Adv **30:**1289-1300.

47. **An MZ, Tang YQ, Mitsumasu K, Liu ZS, Shigeru M, Kenji K.** 2011. Enhanced thermotolerance for ethanol fermentation of Saccharomyces cerevisiae strain by overexpression of the gene coding for trehalose-6-phosphate synthase. Biotechnol Lett **33:**1367-1374.

48. **Klein-Marcuschamer D, Stephanopoulos G.** 2008. Assessing the potential of mutational strategies to elicit new phenotypes in industrial strains. Proc Natl Acad Sci U S A **105:**2319-2324.

49. **Alper H, Moxley J, Nevoigt E, Fink GR, Stephanopoulos G.** 2006. Engineering yeast transcription machinery for improved ethanol tolerance and production. Science **314:**1565-1568.

50. **Khankal R, Chin JW, Ghosh D, Cirino PC.** 2009. Transcriptional effects of CRP* expression in Escherichia coli. J Biol Eng **3:**13.

51. **Zhang H, Chong H, Ching CB, Jiang R.** 2012. Random mutagenesis of global transcription factor cAMP receptor protein for improved osmotolerance. Biotechnology and Bioengineering **109:**1165-1172.

52. **Basak S, Geng H, Jiang R.** 2014. Rewiring global regulator cAMP receptor protein (CRP) to improve E. coli tolerance towards low pH. J Biotechnol **173:**68-75.

53. **Shi DJ, Wang CL, Wang KM.** 2009. Genome shuffling to improve thermotolerance, ethanol tolerance and ethanol productivity of Saccharomyces cerevisiae. J Ind Microbiol Biot **36:**139-147.

54. **Vogel J, Wagner EG.** 2007. Target identification of small noncoding RNAs in bacteria. Curr Opin Microbiol **10:**262-270.

55. **Gaida SM, Al-Hinai MA, Indurthi DC, Nicolaou SA, Papoutsakis ET.** 2013. Synthetic tolerance: three noncoding small RNAs, DsrA, ArcZ and RprA, acting supra-additively against acid stress. Nucleic Acids Res **41:**8726-8737.

56. **Winkler JD, Garcia C, Olson M, Callaway E, Kao KC.** 2014. Evolved osmotolerant Escherichia coli mutants frequently exhibit defective N-acetylglucosamine catabolism and point mutations in cell shape-regulating protein MreB. Appl Environ Microbiol **80:**3729-3740.

57. **Watanabe I, Nakamura T, Shima J.** 2008. A strategy to prevent the occurrence of Lactobacillus strains using lactate-tolerant yeast Candida glabrata in bioethanol production. Journal of industrial microbiology & biotechnology **35:**1117-1122.

58. **Watanabe I, Nakamura T, Shima J.** 2010. Strategy for simultaneous saccharification and fermentation using a respiratory-deficient mutant of Candida glabrata for bioethanol production. Journal of bioscience and bioengineering **110:**176-179.

59. **Li Q, Harvey LM, McNeil B.** 2009. Oxidative stress in industrial fungi. Crit Rev Biotechnol **29:**199-213.

60. **Imlay JA.** 2003. Pathways of oxidative damage. Annu Rev Microbiol **57:**395-418.

61. **O'Donnell A, Bai Y, Bai Z, McNeil B, Harvey LM.** 2007. Introduction to bioreactors of shake-flask inocula leads to development of oxidative stress in Aspergillus niger. Biotechnol Lett **29:**895-900.

62. **Kelsall D, Lyons T.** 1999. Management of fermentations in the production of alcohol: moving toward 23% ethanol. The alcohol textbook: a reference for the beverage, fuel and industrial alcohol industries, 3rd edn. Nottingham University Press, Nottingham, UK**:**26-38.

63. **Briones-Martin-Del-Campo M, Orta-Zavalza E, Juarez-Cepeda J, Gutierrez-Escobedo G, Canas-Villamar I, Castano I, De Las Penas A.** 2014. The oxidative stress response of the opportunistic fungal pathogen Candida glabrata. Rev Iberoam Micol **31:**67-71.

64. **Huang M, McClellan M, Berman J, Kao KC.** 2011. Evolutionary dynamics of Candida albicans during in vitro evolution. Eukaryot Cell **10:**1413-1421.

65. **Demeke MM, Dietz H, Li Y, Foulquie-Moreno MR, Mutturi S, Deprez S, Den Abt T, Bonini BM, Liden G, Dumortier F, Verplaetse A, Boles E, Thevelein JM.** 2013. Development of a D-xylose fermenting and inhibitor tolerant industrial Saccharomyces cerevisiae strain with high performance in lignocellulose hydrolysates using metabolic and evolutionary engineering. Biotechnol Biofuels **6:**89.

66. **Almario MP, Reyes LH, Kao KC.** 2013. Evolutionary engineering of Saccharomyces cerevisiae for enhanced tolerance to hydrolysates of lignocellulosic biomass. Biotechnol Bioeng **110:**2616-2623.

67. **Koppram R, Albers E, Olsson L.** 2012. Evolutionary engineering strategies to enhance tolerance of xylose utilizing recombinant yeast to inhibitors derived from spruce biomass. Biotechnol Biofuels **5:**32.

68. **Gibson DG, Young L, Chuang RY, Venter JC, Hutchison CA, 3rd, Smith HO.** 2009. Enzymatic assembly of DNA molecules up to several hundred kilobases. Nat Methods **6:**343-345.

69. **Reuss O, Vik A, Kolter R, Morschhauser J.** 2004. The *SAT1* flipper, an optimized tool for gene disruption in Candida albicans. Gene **341:**119-127.

70. **Lee ME, DeLoache WC, Cervantes B, Dueber JE.** 2015. A Highly Characterized Yeast Toolkit for Modular, Multipart Assembly. ACS Synth Biol **4:**975-986.

71. **Baranyi J, Roberts TA.** 1994. A dynamic approach to predicting bacterial growth in food. International journal of food microbiology **23:**277-294.

72. **Chou HH, Hsia AP, Mooney DL, Schnable PS.** 2004. Picky: oligo microarray design for large genomes. Bioinformatics **20:**2893-2902.

73. **Saeed AI, Sharov V, White J, Li J, Liang W, Bhagabati N, Braisted J, Klapa M, Currier T, Thiagarajan M, Sturn A, Snuffin M, Rezantsev A, Popov D, Ryltsov A, Kostukovich E, Borisovsky I, Liu Z, Vinsavich A, Trush V, Quackenbush J.** 2003. TM4: a free, open-source system for microarray data management and analysis. Biotechniques **34:**374-378.

74. **Rutherford BJ, Dahl RH, Price RE, Szmidt HL, Benke PI, Mukhopadhyay A, Keasling JD.** 2010. Functional genomic study of exogenous n-butanol stress in Escherichia coli. Applied and environmental microbiology **76:**1935-1945.

75. **Breitling R, Armengaud P, Amtmann A, Herzyk P.** 2004. Rank products: a simple, yet powerful, new method to detect differentially regulated genes in replicated microarray experiments. FEBS Lett **573:**83-92.

76. **Cherry JM, Hong EL, Amundsen C, Balakrishnan R, Binkley G, Chan ET, Christie KR, Costanzo MC, Dwight SS, Engel SR, Fisk DG, Hirschman JE, Hitz BC, Karra K, Krieger CJ, Miyasato SR, Nash RS, Park J, Skrzypek MS, Simison**

M, Weng S, Wong ED. 2012. Saccharomyces Genome Database: the genomics resource of budding yeast. Nucleic Acids Res **40:**D700-705.

77. **Teixeira MC, Monteiro PT, Guerreiro JF, Goncalves JP, Mira NP, dos Santos SC, Cabrito TR, Palma M, Costa C, Francisco AP, Madeira SC, Oliveira AL, Freitas AT, Sa-Correia I.** 2014. The YEASTRACT database: an upgraded information system for the analysis of gene and genomic transcription regulation in Saccharomyces cerevisiae. Nucleic Acids Res **42:**D161-166.

78. **Kao KC, Sherlock G.** 2008. Molecular characterization of clonal interference during adaptive evolution in asexual populations of Saccharomyces cerevisiae. Nat Genet **40:**1499-1504.

79. **Brown JA, Sherlock G, Myers CL, Burrows NM, Deng C, Wu HI, McCann KE, Troyanskaya OG, Brown JM.** 2006. Global analysis of gene function in yeast by quantitative phenotypic profiling. Mol Syst Biol **2:**2006 0001.

80. **Outten CE, Falk RL, Culotta VC.** 2005. Cellular factors required for protection from hyperoxia toxicity in Saccharomyces cerevisiae. Biochem J **388:**93-101.

81. **Ng CH, Tan SX, Perrone GG, Thorpe GW, Higgins VJ, Dawes IW.** 2008. Adaptation to hydrogen peroxide in Saccharomyces cerevisiae: the role of NADPH-generating systems and the SKN7 transcription factor. Free Radic Biol Med **44:**1131-1145.

82. **Gerwien F, Safyan A, Wisgott S, Hille F, Kaemmer P, Linde J, Brunke S, Kasper L, Hube B.** 2016. A Novel Hybrid Iron Regulation Network Combines Features from Pathogenic and Nonpathogenic Yeasts. MBio **7**.

83. **Ando A, Nakamura T, Murata Y, Takagi H, Shima J.** 2007. Identification and classification of genes required for tolerance to freeze-thaw stress revealed by genome-wide screening of Saccharomyces cerevisiae deletion strains. FEMS Yeast Res **7:**244-253.

84. **Ho HL, Haynes K.** 2015. Candida glabrata: new tools and technologies-expanding the toolkit. FEMS Yeast Res **15**.

85. **Curran KA, Morse NJ, Markham KA, Wagman AM, Gupta A, Alper HS.** 2015. Short Synthetic Terminators for Improved Heterologous Gene Expression in Yeast. ACS Synth Biol **4:**824-832.

86. **Chellappa R, Kandasamy P, Oh CS, Jiang Y, Vemula M, Martin CE.** 2001. The membrane proteins, Spt23p and Mga2p, play distinct roles in the activation of Saccharomyces cerevisiae OLE1 gene expression. Fatty acid-mediated regulation of Mga2p activity is independent of its proteolytic processing into a soluble transcription activator. J Biol Chem **276:**43548-43556.

87. **Rice C, Cooke M, Treloar N, Vollbrecht P, Stukey J, McDonough V.** 2010. A role for MGA2, but not SPT23, in activation of transcription of ERG1 in Saccharomyces cerevisiae. Biochem Biophys Res Commun **403:**293-297.

88. **Rossler H, Rieck C, Delong T, Hoja U, Schweizer E.** 2003. Functional differentiation and selective inactivation of multiple Saccharomyces cerevisiae genes involved in very-long-chain fatty acid synthesis. Mol Genet Genomics **269:**290-298.

89. **Steels EL, Learmonth RP, Watson K.** 1994. Stress tolerance and membrane lipid unsaturation in Saccharomyces cerevisiae grown aerobically or anaerobically. Microbiology **140 (Pt 3):**569-576.

90. **Matias AC, Pedroso N, Teodoro N, Marinho HS, Antunes F, Nogueira JM, Herrero E, Cyrne L.** 2007. Down-regulation of fatty acid synthase increases the resistance of Saccharomyces cerevisiae cells to H2O2. Free Radic Biol Med **43:**1458-1465.

91. **Grant CM.** 2008. Metabolic reconfiguration is a regulated response to oxidative stress. Journal of Biology **7:**1.

92. **Larochelle M, Drouin S, Robert F, Turcotte B.** 2006. Oxidative stress-activated zinc cluster protein Stb5 has dual activator/repressor functions required for pentose phosphate pathway regulation and NADPH production. Molecular and cellular biology **26:**6690-6701.

93. **Takagi H.** 2008. Proline as a stress protectant in yeast: physiological functions, metabolic regulations, and biotechnological applications. Applied Microbiology and Biotechnology **81:**211.

94. **Johnson JE, Johnson FB.** 2014. Methionine restriction activates the retrograde response and confers both stress tolerance and lifespan extension to yeast, mouse and human cells. PLoS One **9:**e97729.

95. **Mellor J, Morillon A.** 2004. ISWI complexes in Saccharomyces cerevisiae. Biochim Biophys Acta **1677:**100-112.

96. **Venkatesh S, Workman JL.** 2015. Histone exchange, chromatin structure and the regulation of transcription. Nat Rev Mol Cell Biol **16:**178-189.

97. **Morillon A, Karabetsou N, O'Sullivan J, Kent N, Proudfoot N, Mellor J.** 2003. Isw1 chromatin remodeling ATPase coordinates transcription elongation and termination by RNA polymerase II. Cell **115:**425-435.

98. **Vary JC, Jr., Gangaraju VK, Qin J, Landel CC, Kooperberg C, Bartholomew B, Tsukiyama T.** 2003. Yeast Isw1p forms two separable complexes in vivo. Mol Cell Biol **23:**80-91.

99. **Higgins VJ, Alic N, Thorpe GW, Breitenbach M, Larsson V, Dawes IW.** 2002. Phenotypic analysis of gene deletant strains for sensitivity to oxidative stress. Yeast **19:**203-214.

100. **Stephen DW, Rivers SL, Jamieson DJ.** 1995. The role of the YAP1 and YAP2 genes in the regulation of the adaptive oxidative stress responses of Saccharomyces cerevisiae. Mol Microbiol **16:**415-423.

101. **Reimand J, Vaquerizas JM, Todd AE, Vilo J, Luscombe NM.** 2010. Comprehensive reanalysis of transcription factor knockout expression data in Saccharomyces cerevisiae reveals many new targets. Nucleic Acids Res **38:**4768-4777.

102. **Attfield PV.** 1997. Stress tolerance: the key to effective strains of industrial baker's yeast. Nat Biotechnol **15:**1351-1357.

103. **Lindquist S.** 1992. Heat-shock proteins and stress tolerance in microorganisms. Curr Opin Genet Dev **2:**748-755.

104. **Li S, Chen X, Liu L, Chen J.** 2016. Pyruvate production in Candida glabrata: manipulation and optimization of physiological function. Crit Rev Biotechnol **36:**1-10.

105. **Caspeta L, Caro-Bermúdez MA, Ponce-Noyola T, Martinez A.** 2014. Enzymatic hydrolysis at high-solids loadings for the conversion of agave bagasse to fuel ethanol. Applied Energy **113:**277-286.

106. **Abdel-Banat BM, Hoshida H, Ano A, Nonklang S, Akada R.** 2010. High-temperature fermentation: how can processes for ethanol production at high temperatures become superior to the traditional process using mesophilic yeast? Appl Microbiol Biotechnol **85:**861-867.

107. **Kristensen JB, Felby C, Jorgensen H.** 2009. Yield-determining factors in high-solids enzymatic hydrolysis of lignocellulose. Biotechnol Biofuels **2:**11.

108. **Yamamoto N, Maeda Y, Ikeda A, Sakurai H.** 2008. Regulation of thermotolerance by stress-induced transcription factors in Saccharomyces cerevisiae. Eukaryot Cell **7:**783-790.

109. **Zahringer H, Thevelein JM, Nwaka S.** 2000. Induction of neutral trehalase Nth1 by heat and osmotic stress is controlled by STRE elements and Msn2/Msn4 transcription factors: variations of PKA effect during stress and growth. Mol Microbiol **35:**397-406.

110. **Gasch AP, Spellman PT, Kao CM, Carmel-Harel O, Eisen MB, Storz G, Botstein D, Brown PO.** 2000. Genomic expression programs in the response of yeast cells to environmental changes. Mol Biol Cell **11:**4241-4257.

111. **Leach MD, Cowen LE.** 2014. To sense or die: mechanisms of temperature sensing in fungal pathogens. Current Fungal Infection Reports **8:**185-191.

112. **Roe SM, Prodromou C, O'Brien R, Ladbury JE, Piper PW, Pearl LH.** 1999. Structural basis for inhibition of the Hsp90 molecular chaperone by the antitumor antibiotics radicicol and geldanamycin. J Med Chem **42:**260-266.

113. **Calcagno AM, Bignell E, Rogers TR, Jones MD, Muhlschlegel FA, Haynes K.** 2005. Candida glabrata Ste11 is involved in adaptation to hypertonic stress, maintenance of wild-type levels of filamentation and plays a role in virulence. Med Mycol **43:**355-364.

114. **Junttila MR, Li S-P, Westermarck J.** 2008. Phosphatase-mediated crosstalk between MAPK signaling pathways in the regulation of cell survival. The FASEB Journal **22:**954-965.

115. **Saito H.** 2010. Regulation of cross-talk in yeast MAPK signaling pathways. Curr Opin Microbiol **13:**677-683.

116. **Levin DE.** 2005. Cell wall integrity signaling in Saccharomyces cerevisiae. Microbiol Mol Biol Rev **69:**262-291.

117. **Leng G, Song K.** 2016. Direct interaction of Ste11 and Mkk1/2 through Nst1 integrates high-osmolarity glycerol and pheromone pathways to the cell wall integrity MAPK pathway. FEBS Lett **590:**148-160.

118. **Leach MD, Klipp E, Cowen LE, Brown AJ.** 2012. Fungal Hsp90: a biological transistor that tunes cellular outputs to thermal inputs. Nat Rev Microbiol **10:**693-704.

119. **Borkovich KA, Farrelly FW, Finkelstein DB, Taulien J, Lindquist S.** 1989. hsp82 is an essential protein that is required in higher concentrations for growth of cells at higher temperatures. Molecular and Cellular Biology **9:**3919-3930.

120. **Cowen LE, Lindquist S.** 2005. Hsp90 potentiates the rapid evolution of new traits: drug resistance in diverse fungi. Science **309:**2185-2189.

121. **Jarosz DF, Lindquist S.** 2010. Hsp90 and environmental stress transform the adaptive value of natural genetic variation. Science **330:**1820-1824.

122. **Rutherford SL, Lindquist S.** 1998. Hsp90 as a capacitor for morphological evolution. Nature **396:**336-342.

123. **Chen G, Bradford WD, Seidel CW, Li R.** 2012. Hsp90 stress potentiates rapid cellular adaptation through induction of aneuploidy. Nature **482:**246-250.

124. **Louvion J-F, Abbas-Terki T, Picard D.** 1998. Hsp90 Is Required for Pheromone Signaling in Yeast. Molecular Biology of the Cell **9:**3071-3083.

125. **Millson SH, Truman AW, Wolfram F, King V, Panaretou B, Prodromou C, Pearl LH, Piper PW.** 2004. Investigating the protein-protein interactions of the yeast Hsp90 chaperone system by two-hybrid analysis: potential uses and limitations of this approach. Cell Stress & Chaperones **9:**359-368.

126. **Mishra P, Flynn JM, Starr TN, Bolon DN.** 2016. Systematic Mutant Analyses Elucidate General and Client-Specific Aspects of Hsp90 Function. Cell Rep **15:**588-598.

127. **Mollapour M, Tsutsumi S, Donnelly AC, Beebe K, Tokita MJ, Lee MJ, Lee S, Morra G, Bourboulia D, Scroggins BT, Colombo G, Blagg BS, Panaretou B, Stetler-Stevenson WG, Trepel JB, Piper PW, Prodromou C, Pearl LH, Neckers L.** 2010. Swe1Wee1-dependent tyrosine phosphorylation of Hsp90 regulates distinct facets of chaperone function. Mol Cell **37:**333-343.

APPENDIX

Table A-1. The list of genes that are differentially regulated in adaptive mutants as compared to parental strains after exposure to 1 mM of H_2O_2 for 30 minutes

gene ID	H2-8Y	H2-11G	H2-18Y	H2-22Y	Ortholog[a]	Phenotype(Sc)[b]
CAGL0M04323g	Not found	Not found	UP	Not found	*ACE2*	NA
CAGL0D06424g	Not found	DOWN	Not found	Not found	*ACO1*	NA
CAGL0F02431g	Not found	Not found	UP	Not found	*ACO2*	NA
CAGL0B02717g	Not found	UP	UP	UP	*ACS2*	NA
CAGL0F08305g	DOWN	DOWN	DOWN	DOWN	*MTM1*	decreased when nullified: "Brown JA, et al. (2006)"
CAGL0K04499g	Not found	UP	Not found	Not found	*ADE6*	NA
CAGL0I07843g	DOWN	Not found	Not found	Not found	*ADH1*	NA
CAGL0J01441g	Not found	Not found	UP	Not found	*ADH3*	NA
CAGL0K11418g	Not found	UP	UP	Not found	*ADK1*	NA
CAGL0J09966g	UP	UP	UP	UP	*YDJ1*	decreased when nullified: "Outten CE, et al. (2005)"
CAGL0A03586g	DOWN	Not found	DOWN	Not found	*AFB1*	NA
CAGL0G09042g	Not found	DOWN	DOWN	DOWN	*AFT2*	NA
CAGL0G01122g	Not found	DOWN	DOWN	DOWN	*CIS1*	decreased when nullified: "Auesukaree C, et al. (2009)"
CAGL0H05995g	Not found	DOWN	DOWN	DOWN	*AIM2*	NA
CAGL0J01287g	Not found	UP	Not found	Not found	*AIP1*	NA
CAGL0L05500g	Not found	UP	Not found	UP	*ALB1*	NA
CAGL0J03212g	Not found	Not found	UP	Not found	*ALD5*	NA
CAGL0L12254g	Not found	Not found	UP	Not found	*ALT1*	NA
CAGL0L06578g	Not found	DOWN	DOWN	DOWN	*AMA1*	NA
CAGL0H07491g	Not found	DOWN	DOWN	Not found	*AMN1*	NA
CAGL0F05247g	Not found	DOWN	DOWN	Not found	*APD1*	NA
CAGL0K08536g	Not found	DOWN	DOWN	Not found	*APE1*	NA
CAGL0F04521g	Not found	DOWN	DOWN	DOWN	*ECM13*	decreased when nullified: "Brown JA, et al. (2006)"
CAGL0D00154g	Not found	DOWN	Not found	Not found	*AQY1*	NA
CAGL0C05115g	Not found	UP	UP	UP	*ARG1*	NA
CAGL0I08987g	Not found	Not found	UP	UP	*ARG4*	NA
CAGL0E04092g	Not found	DOWN	Not found	Not found	*ARN1*	NA
CAGL0A03102g	Not found	Not found	DOWN	DOWN	*ARO10*	NA
CAGL0H10142g	Not found	DOWN	Not found	Not found	*ARO3*	NA
CAGL0C01573g	Not found	Not found	UP	Not found	*ARO4*	NA

Table A-1. Continued

gene ID	H2-8Y	H2-11G	H2-18Y	H2-22Y	*Ortholog*[a]	Phenotype(Sc)[b]
CAGL0K04653g	Not found	UP	Not found	UP	*ART5*	NA
CAGL0C00231g	Not found	DOWN	DOWN	DOWN	*FCY21*	decreased when nullified: "Brown JA, et al. (2006)"
CAGL0F05709g	Not found	Not found	Not found	UP	*ATC1*	NA
CAGL0L06006g	Not found	DOWN	Not found	DOWN	*ATG1*	NA
CAGL0L05742g	Not found	DOWN	DOWN	DOWN	*MRS3*	decreased when nullified: "Brown JA, et al. (2006)"
CAGL0M07920g	UP	Not found	UP	UP	*PDC1*	decreased when nullified: "Brown JA, et al. (2006)"
CAGL0H00704g	Not found	DOWN	DOWN	DOWN	*ATG41*	NA
CAGL0H02101g	Not found	DOWN	DOWN	DOWN	*RTC3*	decreased when nullified: "Brown JA, et al. (2006)";
CAGL0M09581g	UP	Not found	UP	UP	*ATP1*	NA
CAGL0B03069g	Not found	UP	UP	UP	*TAL1*	decreased when nullified: "Ng CH, et al. (2008)";
CAGL0B02343g	Not found	Not found	DOWN	Not found	*ATR1*	NA
CAGL0D04686g	Not found	Not found	Not found	DOWN	*AXL1*	NA
CAGL0G06842g	UP	UP	Not found	Not found	*BBC1*	NA
CAGL0H00594g	Not found	UP	UP	Not found	*BBP1*	NA
CAGL0C02541g	UP	Not found	UP	Not found	*BDF1*	NA
CAGL0G00220g	UP	UP	UP	UP	*BGL2*	NA
CAGL0M09867g	DOWN	Not found	Not found	Not found	*BLS1*	NA
CAGL0I07975g	Not found	Not found	Not found	UP	*BRX1*	NA
CAGL0I03300g	Not found	DOWN	Not found	DOWN	*BUD16*	NA
CAGL0M07678g	Not found	UP	Not found	Not found	*BUD22*	NA
CAGL0F08041g	UP	UP	UP	Not found	*PFK1*	increased when nullified: "Brown JA, et al. (2006)"
CAGL0M03553g	UP	UP	Not found	Not found	*CAF40*	NA
CAGL0L00957g	Not found	Not found	Not found	DOWN	*CAJ1*	NA
CAGL0K12496g	DOWN	DOWN	DOWN	DOWN	*CAK1*	NA
CAGL0K05115g	Not found	UP	UP	Not found	*CCL1*	NA
CAGL0I04752g	Not found	UP	Not found	Not found	*CDS1*	NA
CAGL0B00286g	Not found	DOWN	Not found	Not found	*CHA1*	NA
CAGL0A03718g	Not found	UP	UP	Not found	*CHC1*	NA
CAGL0C03069g	Not found	UP	UP	Not found	*CHO1*	NA
CAGL0L10626g	UP	Not found	Not found	Not found	*CIK1*	NA
CAGL0G06402g	Not found	Not found	UP	Not found	*CIR2*	NA
CAGL0K12276g	Not found	UP	UP	UP	*PHO88*	increased when nullified: "Brown JA, et al. (2006)"
CAGL0G02035g	Not found	Not found	UP	Not found	*CKA2*	NA

Table A-1. Continued

gene ID	H2-8Y	H2-11G	H2-18Y	H2-22Y	*Ortholog*[a]	Phenotype(Sc)[b]
CAGL0M04367g	Not found	UP	UP	Not found	*CKI1*	NA
CAGL0M11044g	Not found	Not found	DOWN	Not found	*CLB1*	NA
CAGL0M11990g	Not found	Not found	Not found	UP	*CLN3*	NA
CAGL0M01870g	Not found	Not found	Not found	DOWN	*CMR3*	NA
CAGL0H07425g	Not found	UP	Not found	Not found	*CNS1*	NA
CaglfMp03	UP	Not found	Not found	Not found	*COB*	NA
CAGL0G01298g	DOWN	Not found	Not found	Not found	*COG5*	NA
CAGL0L06072g	UP	UP	Not found	Not found	*COM2*	NA
CAGL0D00528g	Not found	UP	UP	UP	*FAS1*	increased when nullified: "Matias AC, et al. (2007)"
CaglfMp04	Not found	DOWN	Not found	DOWN	*COX1*	NA
CAGL0E03245g	Not found	UP	Not found	UP	*NSR1*	decreased when nullified: "Ando A, et al. (2007)"
CAGL0L02299g	UP	UP	Not found	Not found	*VPS1*	decreased when nullified: "Auesukaree C, et al. (2009)"
CAGL0I09592g	Not found	UP	UP	UP	*CPA1*	NA
CAGL0C04917g	Not found	Not found	UP	UP	*CPA2*	NA
CAGL0I01782g	Not found	Not found	Not found	DOWN	*CRM1*	NA
CAGL0F06149g	UP	Not found	Not found	Not found	*CSM3*	NA
CAGL0H05005g	Not found	UP	UP	Not found	*CSR1*	NA
CAGL0C02629g	DOWN	Not found	Not found	Not found	*CST9*	NA
CAGL0D04268g	UP	Not found	Not found	Not found	*CTF18*	NA
CAGL0B03531g	Not found	DOWN	DOWN	Not found	*CTO1*	NA
CAGL0E03025g	Not found	UP	UP	Not found	*ECL1*	decreased when nullified: "Azuma K, et al. (2009)"; increased when over-expressed: "Azuma K, et al. (2009)"
CAGL0L09933g	UP	UP	Not found	Not found	*CUE5*	NA
CAGL0K10736g	Not found	DOWN	Not found	Not found	*CYB2*	NA
CAGL0H06545g	Not found	UP	UP	Not found	*ATG32*	decreased when nullified: "Brown JA, et al. (2006)"
CAGL0H06369g	UP	UP	UP	UP	*CYS3*	NA
CAGL0E03157g	UP	Not found	Not found	UP	*CYS4*	NA
CAGL0L05280g	Not found	DOWN	DOWN	Not found	*CYT2*	NA
CAGL0I06028g	Not found	Not found	Not found	UP	*DAS1*	NA
CAGL0G03047g	Not found	Not found	Not found	DOWN	*DBF2*	NA
CAGL0L03846g	Not found	UP	Not found	Not found	*DBP2*	NA

Table A-1. Continued

gene ID	H2-8Y	H2-11G	H2-18Y	H2-22Y	*Ortholog*[a]	Phenotype(Sc)[b]
CAGL0M02915g	Not found	Not found	DOWN	DOWN	*ATG36*	decreased when nullified: "Brown JA, et al. (2006)"
CAGL0L02915g	Not found	UP	UP	Not found	*DED1*	NA
CAGL0H08129g	Not found	DOWN	DOWN	Not found	*DFG16*	NA
CAGL0I09812g	Not found	UP	UP	Not found	*DGK1*	NA
CAGL0M00902g	Not found	Not found	UP	Not found	*DIF1*	NA
CAGL0L07678g	Not found	Not found	Not found	UP	*DIM1*	NA
CAGL0F02607g	Not found	Not found	DOWN	DOWN	*DIT2*	NA
CAGL0I05148g	Not found	DOWN	DOWN	Not found	*DLD1*	NA
CAGL0B04675g	Not found	Not found	Not found	DOWN	*DOM34*	NA
CAGL0G09955g	Not found	Not found	UP	Not found	*DPM1*	NA
CAGL0D06556g	Not found	Not found	UP	Not found	*DPS1*	NA
CAGL0K02475g	Not found	UP	UP	Not found	*DSS4*	NA
CAGL0J11484g	Not found	DOWN	DOWN	Not found	*DUG3*	NA
CAGL0A04675g	Not found	DOWN	Not found	DOWN	*ATG8*	decreased when nullified: "Brown JA, et al. (2006)"
CAGL0L00341g	Not found	UP	Not found	UP	*EBP2*	NA
CAGL0D05632g	DOWN	Not found	Not found	DOWN	*COX17*	decreased when nullified: "Brown JA, et al. (2006)"
CAGL0L08184g	Not found	UP	UP	Not found	*ELO2*	decreased when nullified: "Brown JA, et al. (2006)"
CAGL0I06050g	Not found	UP	UP	Not found	*INO1*	decreased when nullified: "Brown JA, et al. (2006)"
CAGL0L03696g	Not found	Not found	DOWN	Not found	*ECM3*	NA
CAGL0M01826g	UP	UP	UP	UP	*ECM33*	NA
CAGL0L02255g	DOWN	Not found	Not found	Not found	*ECM9*	NA
CAGL0K00583g	Not found	UP	UP	Not found	*ELO1*	NA
CAGL0B03817g	Not found	DOWN	Not found	DOWN	*MHO1*	decreased when nullified: "Brown JA, et al. (2006)"
CAGL0G04851g	Not found	UP	Not found	Not found	*ELO3*	NA
CAGL0F08261g	Not found	DOWN	DOWN	Not found	*ENO1*	NA
CAGL0L12364g	Not found	UP	UP	Not found	*ERG10*	NA
CAGL0E04334g	Not found	Not found	Not found	UP	*ERG11*	NA
CAGL0K04477g	Not found	Not found	UP	UP	*ERG25*	NA
CAGL0F01793g	Not found	Not found	Not found	UP	*ERG3*	NA
CAGL0M11946g	UP	Not found	Not found	Not found	*ERV46*	NA
CAGL0I09108g	Not found	DOWN	DOWN	Not found	*ESBP6*	NA
CAGL0F04631g	Not found	Not found	DOWN	DOWN	*MOH1*	decreased when nullified: "Brown JA, et al. (2006)"

Table A-1. Continued

gene ID	H2-8Y	H2-11G	H2-18Y	H2-22Y	*Ortholog*[a]	Phenotype(Sc)[b]
CAGL0G08492g	Not found	DOWN	Not found	Not found	*EST1*	NA
CAGL0K10384g	Not found	UP	UP	Not found	*FAB1*	NA
CAGL0F00363g	Not found	UP	UP	Not found	*OPI3*	decreased when nullified: "Brown JA, et al. (2006)"
CAGL0E06138g	Not found	UP	UP	UP	*FAS2*	NA
CAGL0L02497g	Not found	Not found	UP	Not found	*FBA1*	NA
CAGL0I04048g	Not found	Not found	Not found	DOWN	*FBP1*	NA
CAGL0I05082g	Not found	DOWN	DOWN	Not found	*PIN4*	decreased when nullified: "Brown JA, et al. (2006)"
CAGL0F00187g	Not found	DOWN	DOWN	Not found	*FET4*	NA
CAGL0I04664g	DOWN	Not found	DOWN	Not found	*FIG1*	NA
CAGL0M13827g	DOWN	Not found	Not found	Not found	*FKS3*	NA
CAGL0D06732g	UP	Not found	Not found	Not found	*FLO1*	NA
CAGL0E06666g	Not found	Not found	DOWN	DOWN	*FLO1*	NA
CAGL0I10362g	Not found	UP	Not found	Not found	*FLO5*	NA
CAGL0E00275g	Not found	Not found	DOWN	Not found	*FLO5*	NA
CAGL0M14069g	UP	Not found	Not found	Not found	*FLO9*	NA
CAGL0L13299g	Not found	Not found	DOWN	DOWN	*FLO9*	NA
CAGL0H06017g	DOWN	DOWN	DOWN	DOWN	*FLR1*	NA
CAGL0G05269g	Not found	DOWN	DOWN	DOWN	*FMP16*	NA
CAGL0H09966g	Not found	DOWN	DOWN	DOWN	*FMP23*	NA
CAGL0K03553g	Not found	Not found	DOWN	DOWN	*FOL3*	NA
CAGL0L11484g	Not found	Not found	UP	UP	*FPR3*	NA
CAGL0L01177g	Not found	Not found	DOWN	Not found	*FRD1*	NA
CAGL0L10912g	Not found	UP	UP	Not found	*TPO4*	decreased when nullified: "Brown JA, et al. (2006)"
CAGL0F01705g	Not found	UP	Not found	Not found	*FRS1*	NA
CAGL0F04499g	Not found	Not found	Not found	UP	*FUI1*	NA
CAGL0M12144g	Not found	UP	Not found	Not found	*FUN12*	NA
CAGL0M04917g	Not found	DOWN	Not found	Not found	*FUS2*	NA
CAGL0J04290g	Not found	Not found	Not found	DOWN	*FUS3*	NA
CAGL0H04037g	Not found	Not found	UP	Not found	*GAC1*	NA
CAGL0L03267g	Not found	DOWN	Not found	Not found	*GAP1*	NA
CAGL0H02057g	Not found	UP	UP	Not found	*GAR1*	NA
CAGL0J07172g	Not found	Not found	DOWN	DOWN	*SCP1*	decreased when nullified: "Brown JA, et al. (2006)"; increased when nullified: "Gourlay CW, et al. (2004)"
CAGL0F01287g	Not found	Not found	UP	UP	*GAS5*	NA

Table A-1. Continued

gene ID	H2-8Y	H2-11G	H2-18Y	H2-22Y	*Ortholog*[a]	Phenotype(Sc)[b]
CAGL0K07634g	Not found	DOWN	DOWN	DOWN	*GAT1*	NA
CAGL0I08327g	Not found	UP	UP	UP	*GCD11*	NA
CAGL0J09790g	Not found	Not found	UP	Not found	*GGC1*	NA
CAGL0F01683g	Not found	UP	Not found	UP	*RPL22A*	decreased when nullified: "Chan CT, et al. (2012)";
CAGL0J10978g	Not found	Not found	Not found	UP	*GIC2*	NA
CAGL0G08107g	DOWN	Not found	Not found	Not found	*GIS1*	NA
CAGL0I06006g	Not found	UP	Not found	UP	*RPA34*	decreased when nullified: "Higgins VJ, et al. (2002)"; increased when nullified: "Brown JA, et al. (2006)"
CAGL0L01089g	Not found	Not found	UP	Not found	*GLT1*	NA
CAGL0F06677g	Not found	DOWN	DOWN	DOWN	*GPA1*	NA
CAGL0K01683g	Not found	Not found	UP	Not found	*GPD1*	NA
CAGL0F07117g	Not found	DOWN	Not found	Not found	*GPG1*	NA
CAGL0G08294g	Not found	UP	Not found	Not found	*GPN3*	NA
CAGL0E05984g	DOWN	DOWN	DOWN	DOWN	*GRE1*	NA
CAGL0D01298g	Not found	UP	UP	Not found	*TKL1*	decreased when nullified: "Ng CH, et al. (2008)";
CAGL0G01364g	Not found	UP	Not found	Not found	*GRS1*	NA
CAGL0F01045g	Not found	Not found	UP	UP	*RPS15*	decreased when nullified: "Okada N, et al. (2014)";
CAGL0F03927g	Not found	UP	UP	UP	*GUA1*	NA
CAGL0C05555g	Not found	DOWN	Not found	Not found	*GUD1*	NA
CAGL0K12100g	Not found	Not found	UP	Not found	*HEM13*	NA
CAGL0D06138g	Not found	DOWN	Not found	Not found	*HEM2*	NA
CAGL0H10538g	DOWN	Not found	Not found	Not found	*HEM25*	NA
CAGL0L10780g	Not found	UP	UP	UP	*HFA1*	NA
CAGL0H07601g	Not found	Not found	Not found	DOWN	*HFM1*	NA
CAGL0C01595g	Not found	Not found	DOWN	DOWN	*HIS7*	NA
CAGL0D01364g	Not found	UP	Not found	UP	*CYC8*	decreased when nullified: "Outten CE, et al. (2005)"
CAGL0I04730g	Not found	UP	UP	Not found	*HMT1*	NA
CAGL0L11990g	Not found	DOWN	Not found	DOWN	*GRX4*	decreased when nullified: "Pujol-Carrion N and de la Torre-Ruiz MA (2010)"; increased when nullified: "Pujol-Carrion N and de la Torre-Ruiz MA (2010)"

Table A-1. Continued

gene ID	H2-8Y	H2-11G	H2-18Y	H2-22Y	*Ortholog*[a]	Phenotype(Sc)[b]
CAGL0K05973g	Not found	Not found	Not found	UP	*HSP60*	NA
CAGL0A01804g	Not found	DOWN	Not found	Not found	*HXT1*	NA
CAGL0M04103g	Not found	Not found	DOWN	Not found	*HXT14*	NA
CAGL0I00286g	Not found	DOWN	Not found	Not found	*HXT2*	NA
CAGL0A01826g	Not found	Not found	Not found	DOWN	*HXT3*	NA
CAGL0A02321g	Not found	Not found	UP	Not found	*HXT5*	NA
CAGL0A02211g	DOWN	Not found	Not found	Not found	*HXT7*	NA
CAGL0J03058g	UP	Not found	Not found	Not found	*ICL1*	NA
CAGL0H07469g	Not found	DOWN	DOWN	DOWN	*ICS2*	NA
CAGL0M11462g	Not found	Not found	UP	Not found	*ICT1*	NA
CAGL0G02673g	Not found	DOWN	DOWN	Not found	*IDH1*	NA
CAGL0K09944g	Not found	DOWN	Not found	DOWN	*PDE2*	decreased when nullified: "Wilson D, et al. (2010)";
CAGL0L01199g	Not found	DOWN	DOWN	Not found	*IES6*	NA
CAGL0C00759g	Not found	UP	Not found	Not found	*IFH1*	NA
CAGL0K10428g	Not found	Not found	DOWN	DOWN	*IGD1*	NA
CAGL0K03465g	UP	Not found	UP	Not found	*ILV2*	NA
CAGL0B03993g	Not found	Not found	UP	Not found	*ILV3*	NA
CAGL0M09042g	Not found	Not found	DOWN	Not found	*IME1*	NA
CAGL0G04455g	Not found	Not found	DOWN	DOWN	*IME2*	NA
CAGL0C04983g	Not found	UP	UP	Not found	*ADO1*	increased when nullified: "Brown JA, et al. (2006)"
CAGL0J10252g	Not found	Not found	Not found	UP	*IMP4*	NA
CAGL0J10494g	Not found	Not found	DOWN	DOWN	*APT2*	increased when nullified: "Brown JA, et al. (2006)"
CAGL0B01947g	Not found	UP	UP	Not found	*INO2*	NA
CAGL0I07359g	Not found	UP	UP	Not found	*INO4*	NA
CAGL0H09878g	Not found	Not found	Not found	UP	*IPP1*	NA
CAGL0K03069g	Not found	DOWN	DOWN	Not found	*IRC21*	NA
CAGL0G03905g	Not found	DOWN	Not found	Not found	*ISA1*	NA
CAGL0J04048g	Not found	DOWN	DOWN	DOWN	*ISU2*	NA
CAGL0I07447g	Not found	UP	UP	Not found	*ITR2*	NA
CAGL0D02090g	Not found	Not found	UP	UP	*ASC1*	increased when nullified: "Brown JA, et al. (2006)"
CAGL0D02948g	Not found	Not found	Not found	UP	*KAR2*	NA
CAGL0B00462g	DOWN	Not found	Not found	Not found	*KAR4*	NA
CAGL0F06589g	Not found	DOWN	Not found	DOWN	*KAR5*	NA
CAGL0M02431g	Not found	Not found	UP	Not found	*KES1*	NA
CAGL0K09614g	Not found	UP	Not found	Not found	*KRE33*	NA

Table A-1. Continued

gene ID	H2-8Y	H2-11G	H2-18Y	H2-22Y	*Ortholog*[a]	Phenotype(Sc)[b]
CAGL0K12012g	Not found	UP	UP	Not found	*KRS1*	NA
CAGL0K12760g	DOWN	Not found	Not found	Not found	*LAM5*	NA
CAGL0K02211g	Not found	Not found	Not found	UP	*LCP5*	NA
CAGL0M07359g	Not found	Not found	DOWN	Not found	*LEE1*	NA
CAGL0H00396g	Not found	DOWN	DOWN	DOWN	*LEU3*	NA
CAGL0H03377g	Not found	UP	UP	Not found	*DBP3*	increased when nullified: "Brown JA, et al. (2006)"
CAGL0H07975g	Not found	UP	Not found	UP	*LHP1*	NA
CAGL0H03113g	Not found	DOWN	Not found	Not found	*LIF1*	NA
CAGL0J05412g	Not found	UP	Not found	Not found	*LSG1*	NA
CAGL0G06798g	Not found	DOWN	DOWN	Not found	*LSO1*	NA
CAGL0J00891g	Not found	UP	Not found	Not found	*LTV1*	NA
CAGL0F02563g	Not found	UP	Not found	UP	*HPT1*	increased when nullified: "Brown JA, et al. (2006)"
CAGL0K10978g	Not found	Not found	UP	Not found	*LYS4*	NA
CAGL0C03443g	UP	Not found	UP	UP	*LYS9*	NA
CAGL0F00715g	Not found	DOWN	Not found	Not found	*MAK16*	NA
CAGL0J00671g	Not found	DOWN	DOWN	Not found	*MAS2*	NA
CAGL0I07227g	Not found	DOWN	DOWN	Not found	*IDH2*	increased when nullified: "Brown JA, et al. (2006)"
CAGL0I09724g	Not found	DOWN	Not found	Not found	*MCH5*	NA
CAGL0I09702g	Not found	DOWN	DOWN	DOWN	*MCH5*	NA
CAGL0F00935g	Not found	DOWN	DOWN	Not found	*PEX15*	increased when nullified: "Brown JA, et al. (2006)"
CAGL0E01705g	UP	Not found	Not found	Not found	*MDH2*	NA
CAGL0J06028g	Not found	DOWN	Not found	Not found	*MEP2*	NA
CAGL0J08316g	Not found	Not found	Not found	UP	*MET2*	NA
CAGL0K08668g	Not found	Not found	Not found	UP	*MET28*	NA
CAGL0B02651g	Not found	DOWN	Not found	Not found	*MET32*	NA
CAGL0I04994g	Not found	Not found	Not found	UP	*MET6*	NA
CAGL0K06677g	DOWN	DOWN	DOWN	Not found	*MET8*	NA
CAGL0C01919g	DOWN	Not found	DOWN	DOWN	*MFA2*	NA
CAGL0C05467g	Not found	Not found	DOWN	Not found	*MFG1*	NA
CAGL0F08195g	Not found	Not found	DOWN	Not found	*MGA1*	NA
CAGL0F03817g	Not found	Not found	UP	Not found	*MGL2*	NA
CAGL0J10164g	Not found	UP	UP	Not found	*RPL16B*	increased when nullified: "Brown JA, et al. (2006)"
CAGL0A01628g	Not found	UP	Not found	Not found	*MIG1*	NA
CAGL0C03740g	Not found	Not found	Not found	DOWN	*MIT1*	NA

Table A-1. Continued

gene ID	H2-8Y	H2-11G	H2-18Y	H2-22Y	*Ortholog*[a]	Phenotype(Sc)[b]
CAGL0E06006g	Not found	DOWN	Not found	DOWN	*MMT2*	NA
CAGL0C03982g	Not found	DOWN	DOWN	DOWN	*MNT3*	NA
CAGL0C03960g	Not found	Not found	DOWN	Not found	*MNT3*	NA
CAGL0C03938g	Not found	Not found	Not found	DOWN	*MNT3*	NA
CAGL0A03278g	Not found	Not found	UP	UP	*RPL19A*	increased when nullified: "Brown JA, et al. (2006)"
CAGL0A00341g	Not found	DOWN	DOWN	DOWN	*MPO1*	NA
CAGL0K11880g	UP	UP	UP	Not found	*MRH1*	NA
CAGL0B02497g	Not found	UP	UP	Not found	*TUB3*	increased when nullified: "Brown JA, et al. (2006)"
CAGL0G09559g	Not found	Not found	UP	Not found	*MSB1*	NA
CAGL0F08833g	Not found	UP	UP	UP	*MSB2*	NA
CAGL0L03289g	Not found	UP	UP	Not found	*UTH1*	increased when nullified: "Brown JA, et al. (2006)"
CAGL0M08624g	UP	Not found	Not found	Not found	*MSW1*	NA
CAGL0J05060g	UP	Not found	Not found	Not found	*ZAP1*	decreased when nullified; "Higgins VJ, et al. (2002) "
CAGL0K04367g	Not found	Not found	DOWN	Not found	*MUP1*	NA
CAGL0E04004g	Not found	DOWN	Not found	Not found	*MUP3*	NA
CAGL0J01727g	UP	Not found	Not found	Not found	NA	NA
CAGL0I11011g	UP	Not found	Not found	Not found	NA	NA
CAGL0M14091g	Not found	DOWN	DOWN	Not found	NA	NA
CAGL0I08151g	Not found	DOWN	DOWN	DOWN	NA	NA
CAGL0B01743g	Not found	DOWN	DOWN	Not found	NA	NA
CAGL0K00110g	Not found	Not found	DOWN	Not found	NA	NA
CAGL0J11990g	Not found	Not found	Not found	DOWN	NA	NA
CAGL0B02365g	UP	Not found	Not found	Not found	*NAB6*	NA
CAGL0C03762g	Not found	DOWN	DOWN	DOWN	*NAS2*	NA
CAGL0C05313g	Not found	UP	UP	Not found	*NAT1*	NA
CAGL0G00286g	Not found	Not found	Not found	UP	*GAS1*	decreased when nullified: "Ando A, et al. (2007)"
CAGL0E00737g	Not found	Not found	UP	Not found	*HMO1*	decreased when nullified: "Ando A, et al. (2007)"
CAGL0D04114g	Not found	Not found	UP	Not found	*NCP1*	NA
CAGL0B02431g	Not found	Not found	UP	Not found	*NDI1*	NA
CAGL0K02959g	Not found	UP	UP	Not found	*NEM1*	NA
CAGL0H02783g	UP	Not found	Not found	Not found	*NET1*	NA
CAGL0K12628g	Not found	Not found	Not found	UP	*RPO41*	decreased when nullified: "Bonawitz ND, et al. (2006)";

Table A-1. Continued

gene ID	H2-8Y	H2-11G	H2-18Y	H2-22Y	*Ortholog*[a]	Phenotype(Sc)[b]
CAGL0H03817g	Not found	DOWN	DOWN	Not found	*NFS1*	NA
CAGL0L01859g	Not found	DOWN	DOWN	Not found	*NFU1*	NA
CAGL0K06655g	Not found	UP	Not found	Not found	*NGR1*	NA
CAGL0I02398g	Not found	UP	UP	UP	*NMD3*	NA
CAGL0G05357g	Not found	Not found	Not found	DOWN	*NNR1*	NA
CAGL0E06380g	Not found	Not found	Not found	DOWN	*NNR2*	NA
CAGL0L04832g	DOWN	Not found	DOWN	Not found	none	NA
CAGL0J02552g	DOWN	Not found	Not found	Not found	none	NA
CAGL0H04059g	DOWN	DOWN	Not found	Not found	none	NA
CAGL0D02750g	DOWN	Not found	Not found	Not found	none	NA
CAGL0C00781g	DOWN	Not found	DOWN	Not found	none	NA
CAGL0G00836g	UP	Not found	Not found	Not found	none	NA
CAGL0C01133g	UP	Not found	Not found	Not found	none	NA
CAGL0C00968g	UP	Not found	Not found	Not found	none	NA
CAGL0B00110g	UP	DOWN	DOWN	Not found	none	NA
CAGL0M12793g	Not found	DOWN	Not found	Not found	none	NA
CAGL0K13024g	Not found	DOWN	Not found	Not found	none	NA
CAGL0K11946g	Not found	DOWN	Not found	Not found	none	NA
CAGL0K07678g	Not found	DOWN	DOWN	Not found	none	NA
CAGL0K07359g	Not found	DOWN	DOWN	Not found	none	NA
CAGL0K07205g	Not found	DOWN	DOWN	DOWN	none	NA
CAGL0H07337g	Not found	DOWN	DOWN	DOWN	none	NA
CAGL0H02277g	Not found	DOWN	Not found	Not found	none	NA
CAGL0F09273g	Not found	DOWN	Not found	Not found	none	NA
CAGL0D05654g	Not found	DOWN	DOWN	Not found	none	NA
CAGL0C02365g	Not found	DOWN	DOWN	DOWN	none	NA
CAGL0B01595g	Not found	DOWN	DOWN	DOWN	none	NA
CAGL0A03410g	Not found	DOWN	DOWN	DOWN	none	NA
CAGL0A01892g	Not found	UP	Not found	Not found	none	NA
CAGL0E01661g	Not found	Not found	DOWN	DOWN	none	NA
CAGL0G07645g	Not found	Not found	DOWN	DOWN	none	NA
CAGL0J11616g	Not found	Not found	DOWN	Not found	none	NA
CAGL0G03993g	Not found	Not found	DOWN	Not found	none	NA
CAGL0G06710g	Not found	Not found	DOWN	Not found	none	NA
CAGL0A04873g	Not found	Not found	DOWN	Not found	none	NA
CAGL0L07194g	Not found	Not found	DOWN	Not found	none	NA
CAGL0L08536g	Not found	Not found	DOWN	Not found	none	NA
CAGL0B04235g	Not found	Not found	DOWN	Not found	none	NA
CAGL0I02596g	Not found	Not found	DOWN	DOWN	none	NA

Table A-1. Continued

gene ID	H2-8Y	H2-11G	H2-18Y	H2-22Y	*Ortholog*[a]	Phenotype(Sc)[b]
CAGL0E06094g	Not found	Not found	UP	Not found	none	NA
CAGL0L03388g	Not found	Not found	Not found	DOWN	none	NA
CAGL0D06534g	Not found	Not found	Not found	DOWN	none	NA
CAGL0L10092g	Not found	Not found	Not found	DOWN	none	NA
CAGL0J01800g	Not found	Not found	Not found	DOWN	none	NA
CAGL0M08096g	Not found	Not found	Not found	DOWN	none	NA
CAGL0J11374g	Not found	Not found	Not found	DOWN	none	NA
CAGL0C01617g	Not found	Not found	Not found	DOWN	none	NA
CAGL0L12496g	Not found	Not found	Not found	DOWN	none	NA
CAGL0A01650g	Not found	Not found	Not found	DOWN	none	NA
CAGL0A00649g	Not found	Not found	Not found	DOWN	none	NA
CAGL0K01859g	Not found	UP	Not found	UP	*NOP1*	NA
CAGL0L09713g	DOWN	Not found	Not found	Not found	*ATP7*	decreased when nullified: "Brown JA, et al. (2006)"
CAGL0L03806g	Not found	UP	Not found	Not found	*NOP15*	NA
CAGL0J10032g	UP	UP	Not found	Not found	*NOP2*	NA
CAGL0I09790g	Not found	UP	Not found	UP	*NOP58*	NA
CAGL0G07843g	Not found	Not found	Not found	UP	*NOP7*	NA
CAGL0M06105g	Not found	UP	UP	Not found	*NPL4*	NA
CAGL0L07480g	Not found	Not found	UP	Not found	*NRG2*	NA
CAGL0K02233g	Not found	Not found	Not found	UP	*NSA2*	NA
CAGL0E06182g	UP	Not found	Not found	Not found	*NSL1*	NA
CAGL0C04257g	DOWN	Not found	Not found	Not found	*COQ1*	decreased when nullified: "Brown JA, et al. (2006)"
CAGL0H09724g	Not found	UP	Not found	UP	*NUG1*	NA
CAGL0D04708g	Not found	Not found	Not found	DOWN	*CTR1*	decreased when nullified: "Brown JA, et al. (2006)"
CAGL0C03333g	Not found	DOWN	Not found	Not found	*FRE6*	decreased when nullified: "Brown JA, et al. (2006)"
CAGL0C00429g	DOWN	Not found	Not found	Not found	*NYV1*	NA
CAGL0E03784g	Not found	Not found	UP	Not found	*OCA5*	NA
CAGL0K03267g	Not found	UP	Not found	Not found	*OPI1*	NA
CAGL0D03762g	Not found	Not found	DOWN	Not found	*GIC1*	decreased when nullified: "Brown JA, et al. (2006)"
CAGL0K04147g	Not found	UP	UP	UP	*ORM1*	NA
CAGL0K10362g	Not found	Not found	Not found	UP	*ORT1*	NA
CAGL0L09537g	Not found	DOWN	DOWN	Not found	*OYE2*	NA
CAGL0K10890g	Not found	DOWN	Not found	DOWN	*OYE2*	NA
CAGL0J01892g	Not found	Not found	UP	Not found	*PAN1*	NA

Table A-1. Continued

gene ID	H2-8Y	H2-11G	H2-18Y	H2-22Y	*Ortholog*[a]	Phenotype(Sc)[b]
CAGL0H08503g	UP	Not found	Not found	Not found	*PBY1*	NA
CAGL0G02535g	UP	Not found	Not found	Not found	*PCC1*	NA
CAGL0J10846g	Not found	DOWN	DOWN	DOWN	*PCL5*	NA
CAGL0B00726g	Not found	Not found	Not found	DOWN	*GLK1*	decreased when nullified: "Brown JA, et al. (2006)"
CAGL0F05951g	Not found	DOWN	Not found	Not found	*IMP2*	decreased when nullified: "Brown JA, et al. (2006)"
CAGL0L09108g	Not found	DOWN	DOWN	Not found	*PDH1*	NA
CAGL0M00154g	Not found	Not found	DOWN	Not found	*LYP1*	decreased when nullified: "Brown JA, et al. (2006)"
CAGL0J04136g	Not found	DOWN	Not found	Not found	*MCT1*	decreased when nullified: "Brown JA, et al. (2006)"
CAGL0I08943g	UP	Not found	Not found	Not found	*PES4*	NA
CAGL0M07469g	Not found	Not found	Not found	DOWN	*PEX12*	NA
CAGL0K01991g	Not found	UP	Not found	Not found	*NCL1*	decreased when nullified: "Brown JA, et al. (2006)"
CAGL0I06292g	Not found	DOWN	DOWN	DOWN	*PEX2*	NA
CAGL0A00957g	Not found	UP	Not found	Not found	*PEX30*	NA
CAGL0J09570g	Not found	UP	Not found	Not found	*PEX5*	NA
CAGL0A01870g	Not found	DOWN	Not found	Not found	*PEP1*	decreased when nullified: "Brown JA, et al. (2006)"
CAGL0L10758g	Not found	UP	UP	Not found	*PFK2*	NA
CAGL0M13387g	Not found	Not found	DOWN	Not found	*PFS1*	NA
CAGL0E05654g	Not found	UP	Not found	Not found	*PGC1*	NA
CAGL0L07722g	Not found	Not found	UP	Not found	*PGK1*	NA
CAGL0K03421g	Not found	Not found	Not found	DOWN	*PGM2*	NA
CAGL0C02321g	Not found	DOWN	DOWN	DOWN	*PHM8*	NA
CAGL0B02475g	Not found	Not found	Not found	DOWN	*PHO84*	NA
CAGL0A04213g	Not found	UP	Not found	Not found	*PIN4*	decreased when nullified: "Brown JA, et al. (2006)"
CAGL0A02970g	Not found	Not found	DOWN	Not found	*PHO92*	NA
CAGL0F04103g	DOWN	Not found	Not found	Not found	*YBL028C*	decreased when nullified: "Brown JA, et al. (2006)"
CAGL0A03883g	Not found	Not found	Not found	DOWN	*QRI5*	decreased when nullified: "Brown JA, et al. (2006)";
CAGL0M08492g	Not found	Not found	UP	UP	*PIR1*	NA
CAGL0M08514g	UP	Not found	UP	Not found	*PIR3*	NA
CAGL0F07007g	Not found	DOWN	Not found	DOWN	*PKP2*	NA
CAGL0L11066g	Not found	UP	UP	Not found	*PLP2*	NA

Table A-1. Continued

gene ID	H2-8Y	H2-11G	H2-18Y	H2-22Y	*Ortholog*[a]	Phenotype(Sc)[b]
CAGL0A00495g	Not found	UP	UP	Not found	*PMA1*	NA
CAGL0K09460g	Not found	UP	Not found	UP	*PNO1*	NA
CAGL0L04378g	Not found	DOWN	Not found	Not found	*PNS1*	NA
CAGL0B03553g	Not found	UP	Not found	Not found	*POL5*	NA
CAGL0A03905g	DOWN	Not found	Not found	Not found	*HMX1*	decreased when nullified: "Collinson EJ, et al. (2011)"; increased when nullified: "Collinson EJ, et al. (2011)"
CAGL0D05060g	Not found	UP	Not found	Not found	*PPT1*	NA
CAGL0J08371g	Not found	Not found	DOWN	Not found	*PRM1*	NA
CAGL0I05500g	Not found	Not found	Not found	UP	*PRS2*	NA
CAGL0G07667g	Not found	Not found	UP	Not found	*PRY1*	NA
CAGL0D01034g	Not found	Not found	Not found	UP	*PSA1*	NA
CAGL0E04620g	Not found	Not found	UP	UP	*PST1*	NA
CAGL0G02453g	Not found	DOWN	DOWN	Not found	*PTR2*	NA
CAGL0I09130g	Not found	DOWN	DOWN	Not found	*PTR3*	NA
CAGL0A04037g	Not found	UP	Not found	Not found	*PWP1*	NA
CAGL0M03245g	Not found	DOWN	Not found	Not found	*PXP1*	NA
CAGL0C04873g	Not found	Not found	UP	Not found	*PXP2*	NA
CAGL0G08624g	Not found	DOWN	DOWN	DOWN	*QDR1*	NA
CAGL0G01540g	Not found	Not found	UP	Not found	*NCE103*	decreased when nullified: "Gotz R, et al. (1999)"
CAGL0H00803g	Not found	UP	UP	UP	*RBD2*	NA
CAGL0E05280g	Not found	Not found	DOWN	Not found	*GRE2*	decreased when nullified: "Higgins VJ, et al. (2002)"
CAGL0F05929g	Not found	DOWN	DOWN	Not found	*RCH1*	NA
CAGL0F00649g	Not found	Not found	DOWN	Not found	*RCK2*	NA
CAGL0E02343g	Not found	Not found	Not found	UP	*RCL1*	NA
CAGL0J04158g	DOWN	Not found	Not found	Not found	*RCN2*	NA
CAGL0G00792g	Not found	Not found	Not found	DOWN	*REC102*	NA
CAGL0C01837g	Not found	DOWN	Not found	Not found	*RER1*	NA
CAGL0H03751g	Not found	Not found	DOWN	DOWN	*RFX1*	NA
CAGL0B04213g	Not found	Not found	Not found	DOWN	*RGC1*	NA
CAGL0E03762g	Not found	DOWN	Not found	Not found	*RIM101*	NA
CAGL0E03630g	Not found	Not found	DOWN	Not found	*RIM4*	NA
CAGL0E05698g	Not found	Not found	DOWN	Not found	*RKM1*	NA
CAGL0G08041g	Not found	UP	Not found	Not found	*RLI1*	NA
CAGL0K04257g	Not found	Not found	Not found	DOWN	*RME1*	NA
CAGL0F00561g	Not found	Not found	Not found	UP	*RPA12*	NA

Table A-1. Continued

gene ID	H2-8Y	H2-11G	H2-18Y	H2-22Y	*Ortholog*[a]	Phenotype(Sc)[b]
CAGL0E05500g	Not found	Not found	Not found	UP	*RPA190*	NA
CAGL0M10549g	Not found	Not found	UP	Not found	*RCF2*	decreased when nullified: "Higgins VJ, et al. (2002)"
CAGL0E01485g	UP	Not found	Not found	Not found	*RTC1*	decreased when nullified: "Higgins VJ, et al. (2002)"
CAGL0J07766g	Not found	Not found	Not found	UP	*RPA49*	NA
CAGL0L03872g	Not found	Not found	Not found	UP	*RPC19*	NA
CAGL0J05698g	Not found	Not found	Not found	UP	*RPC31*	NA
CAGL0B04125g	Not found	UP	Not found	UP	*RPC40*	NA
CAGL0G10109g	Not found	Not found	Not found	UP	*RPC82*	NA
CAGL0K00781g	Not found	Not found	Not found	UP	*YGR210C*	decreased when nullified: "Higgins VJ, et al. (2002)"
CAGL0M10241g	Not found	UP	UP	Not found	*RPL14A*	NA
CaglfMp11	Not found	DOWN	Not found	Not found	*COX2*	decreased when nullified: "Khalimonchuk O, et al. (2007)"
CAGL0J07612g	Not found	Not found	UP	Not found	*ZWF1*	decreased when nullified: "Larochelle M, et al. (2006)";
CAGL0G04741g	Not found	DOWN	Not found	Not found	*LEU4*	decreased when nullified: "Martinez-Pastor M, et al. (2010)"
CAGL0H04521g	Not found	UP	Not found	UP	*RPL32*	NA
CAGL0I03828g	DOWN	Not found	UP	Not found	*RPO21*	NA
CAGL0M12496g	Not found	UP	Not found	Not found	*VHR1*	decreased when nullified: "Michel S, et al. (2015)"
CAGL0G00990g	Not found	UP	UP	UP	*RPP0*	NA
CAGL0M04873g	Not found	UP	UP	UP	*RPS10A*	NA
CAGL0J07238g	Not found	UP	UP	Not found	*RPS12*	NA
CAGL0L06864g	Not found	Not found	Not found	DOWN	*SIP5*	NA
CAGL0M03971g	Not found	DOWN	Not found	DOWN	*SKP2*	NA
CAGL0K01529g	Not found	Not found	Not found	UP	*SLM3*	NA
CAGL0L11286g	DOWN	Not found	Not found	Not found	*SMA2*	NA
CAGL0K01287g	DOWN	Not found	Not found	Not found	*SMD1*	NA
CAGL0A03476g	DOWN	Not found	Not found	Not found	*SMF3*	NA
CAGL0M06325g	UP	Not found	Not found	Not found	*SMP1*	NA
CAGL0F05687g	Not found	Not found	Not found	DOWN	*SND1*	NA
CAGL0L02123g	Not found	UP	Not found	Not found	*SNF5*	NA
CAGL0G01848g	Not found	Not found	Not found	UP	*SNT309*	NA
CAGL0G06424g	Not found	UP	Not found	Not found	*SNX3*	NA

Table A-1. Continued

gene ID	H2-8Y	H2-11G	H2-18Y	H2-22Y	*Ortholog*[a]	Phenotype(Sc)[b]
CAGL0B00484g	Not found	Not found	UP	Not found	*SPB1*	NA
CAGL0L08976g	Not found	Not found	Not found	UP	*SPB4*	NA
CAGL0F07953g	Not found	DOWN	DOWN	DOWN	*SPG1*	NA
CAGL0I06644g	Not found	DOWN	Not found	Not found	*SPI1*	NA
CAGL0L05830g	Not found	Not found	Not found	DOWN	*SPO74*	NA
CAGL0D05720g	Not found	Not found	Not found	DOWN	*SPO75*	NA
CAGL0K04455g	Not found	Not found	DOWN	DOWN	*SPR3*	NA
CAGL0L11704g	Not found	Not found	DOWN	Not found	*SPT2*	NA
CAGL0H04697g	Not found	Not found	UP	Not found	*SPT5*	NA
CAGL0L09647g	Not found	UP	UP	UP	*SQT1*	NA
CAGL0L07018g	Not found	Not found	Not found	DOWN	*SRL4*	NA
CAGL0J09900g	Not found	Not found	UP	Not found	*POR1*	decreased when nullified: "Pereira C, et al. (2007)"
CAGL0B00792g	Not found	UP	Not found	Not found	*SRO9*	NA
CAGL0G03795g	Not found	UP	UP	UP	*SSA2*	NA
CAGL0M06083g	UP	UP	Not found	UP	*SSE2*	NA
CAGL0M00990g	UP	Not found	Not found	Not found	*SEN1*	decreased when nullified: "Sariki SK, et al. (2016)";
CAGL0H00374g	DOWN	Not found	Not found	Not found	*SST2*	NA
CAGL0L10560g	Not found	UP	UP	Not found	*SSZ1*	NA
CAGL0K12430g	Not found	DOWN	Not found	Not found	*STE2*	NA
CAGL0M08184g	Not found	DOWN	DOWN	DOWN	*STE3*	NA
CAGL0L02761g	Not found	DOWN	Not found	Not found	*STE4*	NA
CAGL0L06336g	Not found	DOWN	Not found	Not found	*STE5*	NA
CAGL0K00363g	Not found	DOWN	Not found	Not found	*STE6*	NA
CAGL0J09262g	Not found	DOWN	Not found	DOWN	*STF1*	NA
CAGL0E00869g	Not found	UP	UP	Not found	*STM1*	NA
CAGL0L06094g	Not found	DOWN	DOWN	DOWN	*STR3*	NA
CAGL0L09625g	DOWN	Not found	Not found	Not found	*STS1*	NA
CAGL0L08426g	Not found	DOWN	DOWN	DOWN	*SUE1*	NA
CAGL0H00957g	Not found	UP	Not found	Not found	*SUI3*	NA
CAGL0M07315g	Not found	UP	UP	Not found	*SUR1*	NA
CAGL0I04246g	Not found	DOWN	Not found	Not found	*SUT1*	NA
CAGL0M05335g	DOWN	Not found	Not found	Not found	*TAF5*	NA
CAGL0F03069g	UP	Not found	Not found	Not found	*CAD1*	decreased when nullified: "Stephen DW, et al. (1995)"
CAGL0J00451g	DOWN	DOWN	DOWN	DOWN	*TDH3*	NA
CAGL0L04180g	Not found	DOWN	Not found	Not found	*TEP1*	NA
CAGL0D02266g	DOWN	Not found	Not found	Not found	*TFB6*	NA

Table A-1. Continued

gene ID	H2-8Y	H2-11G	H2-18Y	H2-22Y	*Ortholog*[a]	Phenotype(Sc)[b]
CAGL0E04708g	Not found	Not found	Not found	DOWN	*TGL2*	NA
CAGL0I04356g	Not found	UP	UP	Not found	*TIF2*	NA
CAGL0I08393g	Not found	UP	UP	Not found	*TIF3*	NA
CAGL0E03289g	Not found	UP	Not found	Not found	*TIF4631*	NA
CAGL0D03718g	Not found	UP	Not found	UP	*TIF5*	NA
CAGL0L07502g	Not found	Not found	UP	Not found	*TIP1*	NA
CAGL0M13717g	Not found	Not found	DOWN	Not found	*ADE4*	increased when nullified: "Brown JA, et al. (2006)"
CAGL0K09042g	Not found	UP	Not found	Not found	*TMA16*	NA
CAGL0M05599g	Not found	Not found	UP	Not found	*TOS1*	NA
CAGL0M03773g	UP	Not found	UP	UP	*TOS6*	NA
CAGL0H04235g	Not found	Not found	Not found	UP	*DUS1*	increased when nullified: "Brown JA, et al. (2006)"
CAGL0K08360g	Not found	UP	Not found	Not found	*TRM2*	NA
CAGL0J09746g	Not found	Not found	Not found	UP	*TRM8*	NA
CAGL0E00583g	Not found	UP	UP	Not found	*TRX3*	NA
CAGL0D00880g	Not found	UP	Not found	UP	*TSR1*	NA
CAGL0D00220g	Not found	UP	Not found	Not found	*ECM1*	increased when nullified: "Brown JA, et al. (2006)"
CAGL0M12100g	Not found	Not found	DOWN	DOWN	*TYE7*	NA
CAGL0E00671g	DOWN	Not found	Not found	Not found	*UBC1*	NA
CAGL0G02563g	Not found	Not found	Not found	DOWN	*UBP11*	NA
CAGL0D03344g	UP	Not found	Not found	Not found	*UBR2*	NA
CAGL0C03784g	Not found	Not found	DOWN	Not found	*URM1*	NA
CAGL0G03443g	Not found	UP	Not found	Not found	*KAP123*	increased when nullified: "Brown JA, et al. (2006)"
CAGL0J01265g	Not found	UP	Not found	Not found	*UTP15*	NA
CAGL0M09845g	Not found	UP	Not found	Not found	*UTP21*	NA
CAGL0C02211g	Not found	Not found	Not found	UP	*UTR2*	NA
CAGL0L01287g	DOWN	Not found	Not found	Not found	*UTR4*	NA
CAGL0D03674g	Not found	UP	Not found	Not found	*NEW1*	increased when nullified: "Brown JA, et al. (2006)"
CAGL0K12254g	Not found	DOWN	DOWN	DOWN	*VID24*	NA
CAGL0J01265g	Not found	UP	Not found	Not found	*UTP15*	NA
CAGL0M09845g	Not found	UP	Not found	Not found	*UTP21*	NA
CAGL0M01430g	Not found	Not found	Not found	UP	*UTP4*	NA
CAGL0C02211g	Not found	Not found	Not found	UP	*UTR2*	NA
CAGL0L01287g	DOWN	Not found	Not found	Not found	*UTR4*	NA

Table A-1. Continued

gene ID	H2-8Y	H2-11G	H2-18Y	H2-22Y	*Ortholog*[a]	Phenotype(Sc)[b]
CAGL0D03674g	Not found	UP	Not found	Not found	*NEW1*	increased when nullified: "Brown JA, et al. (2006)"
CAGL0K12254g	Not found	DOWN	DOWN	DOWN	*VID24*	NA
CAGL0F01023g	Not found	Not found	Not found	UP	*NOP12*	increased when nullified: "Brown JA, et al. (2006)"
CAGL0J03960g	Not found	DOWN	Not found	Not found	*WTM2*	NA
CAGL0H00660g	Not found	DOWN	DOWN	DOWN	*YAH1*	NA
CAGL0K08756g	Not found	DOWN	Not found	DOWN	*YAP5*	NA
CAGL0K01771g	Not found	DOWN	Not found	Not found	*YAT1*	NA
CAGL0L04928g	Not found	UP	Not found	Not found	*NUP100*	increased when nullified: "Brown JA, et al. (2006)"
CAGL0H10054g	Not found	UP	UP	Not found	*YBR053C*	NA
CAGL0M05401g	Not found	Not found	Not found	DOWN	*YBR201C-A*	NA
CAGL0C01771g	Not found	DOWN	Not found	Not found	*YBR241C*	NA
CAGL0C03289g	Not found	DOWN	Not found	Not found	*YBT1*	NA
CAGL0L06886g	Not found	Not found	UP	Not found	*RPL13A*	increased when nullified: "Brown JA, et al. (2006)"
CAGL0D00990g	Not found	DOWN	Not found	Not found	*YDL057W*	NA
CAGL0J09284g	Not found	DOWN	DOWN	DOWN	*YDL129W*	NA
CAGL0G08019g	Not found	DOWN	DOWN	Not found	*YDR090C*	NA
CAGL0H01111g	Not found	UP	Not found	Not found	*YDR286C*	NA
CAGL0B03487g	UP	UP	UP	Not found	*YEF3*	NA
CAGL0I00792g	Not found	Not found	UP	Not found	*RPS16A*	increased when nullified: "Brown JA, et al. (2006)"
CAGL0H03311g	Not found	DOWN	Not found	DOWN	*YGL081W*	NA
CAGL0F07293g	Not found	DOWN	DOWN	DOWN	*YGL114W*	NA
CAGL0F07359g	DOWN	DOWN	DOWN	DOWN	*YGL117W*	NA
CAGL0L06116g	Not found	DOWN	Not found	Not found	*YGL185C*	NA
CAGL0J06050g	Not found	Not found	UP	Not found	*YGP1*	NA
CAGL0E01991g	Not found	Not found	UP	Not found	*RPS19A*	increased when nullified: "Brown JA, et al. (2006)"
CAGL0I01276g	Not found	DOWN	Not found	Not found	*YHR112C*	NA
CAGL0I08547g	Not found	Not found	Not found	UP	*YER156C*	increased when nullified: "Brown JA, et al. (2006)"
CAGL0D02134g	Not found	DOWN	Not found	Not found	*YKL133C*	increased when nullified: "Brown JA, et al. (2006)"
CAGL0H02541g	Not found	Not found	UP	Not found	*YMR252C*	NA
CAGL0K02629g	DOWN	Not found	Not found	Not found	*YNL134C*	NA
CAGL0J11462g	Not found	UP	UP	Not found	*YNL190W*	NA

Table A-1. Continued

gene ID	H2-8Y	H2-11G	H2-18Y	H2-22Y	*Ortholog*[a]	Phenotype(Sc)[b]
CAGL0J11550g	Not found	Not found	DOWN	Not found	*YNL195C*	NA
CAGL0I05610g	Not found	Not found	Not found	DOWN	*YNR014W*	NA
CAGL0A02002g	DOWN	Not found	Not found	DOWN	*YOL024W*	NA
CAGL0K05203g	Not found	DOWN	Not found	Not found	*YOP1*	NA
CAGL0L10362g	Not found	DOWN	DOWN	DOWN	*YOR062C*	NA
CAGL0I02794g	Not found	DOWN	Not found	Not found	*YOR114W*	NA
CAGL0I07315g	Not found	DOWN	Not found	DOWN	*YOR131C*	NA
CAGL0L11088g	Not found	UP	UP	Not found	*YOR283W*	NA
CAGL0H05225g	Not found	DOWN	Not found	Not found	*YPL067C*	NA
CAGL0G09108g	Not found	Not found	DOWN	Not found	*YPL199C*	NA
CAGL0E01727g	DOWN	DOWN	Not found	DOWN	*YPS1*	NA
CAGL0E01749g	Not found	Not found	Not found	DOWN	*YPS1*	NA
CAGL0I01144g	Not found	Not found	Not found	DOWN	*YPT35*	NA
CAGL0H10076g	Not found	UP	UP	Not found	*YRO2*	NA
CAGL0E02651g	Not found	DOWN	Not found	DOWN	*YSP3*	NA
CAGL0M05593g	DOWN	Not found	Not found	Not found	*YSY6*	NA
CAGL0L10890g	Not found	Not found	Not found	UP	*YTM1*	NA
CAGL0K05863g	Not found	Not found	Not found	DOWN	*AIM14*	increased when nullified: "Rinnerthaler M, et al. (2012)"
CAGL0H07645g	DOWN	Not found	Not found	Not found	*ZIP2*	NA
CAGL0E01353g	Not found	Not found	Not found	UP	*ZRT2*	NA
CAGL0G09064g	Not found	Not found	DOWN	Not found	*YIG1*	increased when nullified: "Wei M, et al. (2009)"

a. *S. cerevisiae* orthologs of *C. glabrata* genes are given based on the sequence similarities according to the CGD;
b. phenotypes relevant to the H_2O_2 resistance for *S. cerevisiae* ortholog from SGD with literature source;

Table A-2. The list of putative transcription factors whose targets are significantly enriched in the group of differentially regulated genes in adaptive mutants

SID	Transcription Factor	p-value	Gene	Ortholog[a]	Phenotype(Sc)[b]
H2-8Y	Zap1p	0.014594	CAGL0J05060g	*YJL056C*	decreased when nullified; "Higgins VJ, et al. (2002)"
H2-8Y	YPR022C	0.026584	CAGL0K02343g	*YPR022C*	NA
H2-8Y	YER130C	0.03422	CAGL0L06072g	*YER130C*	NA
H2-8Y	Smp1p	0.100796	CAGL0M06325g	*YBR182C*	NA
H2-8Y	Kar4p	0.139106	CAGL0B00462g	*YCL055W*	NA
H2-8Y	Gis1p	0.145057	CAGL0G08107g	*YDR096W*	NA
H2-8Y	Cad1p	0.681985	CAGL0F03069g	*YDR423C*	decreased when nullified; "Stephen DW, et al. (1995)"
H2-8Y	Isw1p	0.073937	CAGL0C01683g	*YBR245C*	NA
H2-11G	Sfp1p	0	CAGL0D00682g	*YLR403W*	NA
H2-11G	Sin3p	1.42E-09	CAGL0E02475g	*YOL004W*	NA
H2-11G	Snf5p	2.56E-09	CAGL0L02123g	*YBR289W*	NA
H2-11G	Mga2p	6.67E-09	CAGL0F06831g	*YIR033W*	increased when nullified; "Brown JA, et al. (2006)"
H2-11G	Opi1p	3.24E-08	CAGL0K03267g	*YHL020C*	NA
H2-11G	Ino4p	1.94E-05	CAGL0I07359g	*YOL108C*	NA
H2-11G	Met32p	0.000145	CAGL0B02651g	*YDR253C*	NA
H2-11G	Ino2p	0.000435	CAGL0B01947g	*YDR123C*	NA
H2-11G	Mig1p	0.000893	CAGL0A01628g	*YGL035C*	NA
H2-11G	Cyc8p	0.001721	CAGL0D01364g	*YBR112C*	decreased when nullified; "Outten CE, et al. (2005)"
H2-11G	Ifh1p	0.008537	CAGL0C00759g	*YLR223C*	NA
H2-11G	Leu3p	0.025661	CAGL0H00396g	*YLR451W*	NA
H2-11G	Rim101p	0.038835	CAGL0E03762g	*YHL027W*	NA
H2-11G	Gat1p	0.061423	CAGL0K07634g	*YFL021W*	NA
H2-11G	Sut1p	0.098679	CAGL0I04246g	*YGL162W*	NA
H2-11G	Yap5p	0.173185	CAGL0K08756g	*YIR018W*	NA
H2-11G	Wtm2p	0.263787	CAGL0J03960g	*YOR229W*	NA
H2-11G	YER130C	0.43651	CAGL0L06072g	*YER130C*	NA
H2-11G	Aft2p	0.458859	CAGL0G09042g	*YPL202C*	NA
H2-18Y	Sin3p	0	CAGL0E02475g	*YOL004W*	NA
H2-18Y	Ace2p	0	CAGL0M04323g	*YLR131C*	NA
H2-18Y	Hmo1p	7.00E-15	CAGL0E00737g	*YDR174W*	decreased when nullified; "Ando A, et al. (2007)"
H2-18Y	Mga1p	4.18E-08	CAGL0F08195g	*YGR249W*	NA
H2-18Y	Tye7p	3.87E-06	CAGL0M12100g	*YOR344C*	NA
H2-18Y	Tis11p	1.65E-05	CAGL0E01243g	*YLR136C*	NA
H2-18Y	Ino2p	0.000114	CAGL0B01947g	*YDR123C*	NA
H2-18Y	Rfx1p	0.000158	CAGL0H03751g	*YLR176C*	NA
H2-18Y	Leu3p	0.000698	CAGL0H00396g	*YLR451W*	NA

Table A-2. Continued

SID	Transcription Factor	p-value	Gene	Ortholog[a]	Phenotype(Sc)[b]
H2-18Y	Nrg2p	0.002145	CAGL0L07480g	*YBR066C*	NA
H2-18Y	Ino4p	0.003157	CAGL0I07359g	*YOL108C*	NA
H2-18Y	Ime1p	0.036737	CAGL0M09042g	*YJR094C*	NA
H2-18Y	Aft2p	0.189644	CAGL0G09042g	*YPL202C*	NA
H2-18Y	Spt2p	0.262999	CAGL0L11704g	*YER161C*	NA
H2-18Y	Gat1p	0.269699	CAGL0K07634g	*YFL021W*	NA
H2-22Y	Sfp1p	0	CAGL0M09955g	*YLR403W*	NA
H2-22Y	Msn4p	1.86E-05	CAGL0M13189g	*YKL062W*	decreased when nullified; "Okada N, et al. (2014)"; increased when nullified; "Brown JA, et al. (2006)"
H2-22Y	Rme1p	0.000422	CAGL0K04257g	*YGR044C*	NA
H2-22Y	Tye7p	0.003755	CAGL0M12100g	*YOR344C*	NA
H2-22Y	Met28p	0.004657	CAGL0K08668g	*YIR017C*	NA
H2-22Y	Rfx1p	0.005114	CAGL0H03751g	*YLR176C*	NA
H2-22Y	Leu3p	0.007114	CAGL0H00396g	*YLR451W*	NA
H2-22Y	Ssn3p	0.017495	CAGL0L12650g	*YPL042C*	increased when nullified; "Brown JA, et al. (2006)"
H2-22Y	Gat1p	0.032651	CAGL0K07634g	*YFL021W*	NA
H2-22Y	Aft2p	0.112828	CAGL0G09042g	*YPL202C*	NA
H2-22Y	Yap5p	0.124861	CAGL0K08756g	*YIR018W*	NA

a. *S. cerevisiae* orthologs of *C. glabrata* genes are given based on the sequence similarities according to the CGD;
b. phenotypes relevant to the H_2O_2 resistance for *S. cerevisiae* ortholog from SGD with literature source;